IOAN DRAGAN

Lecturer at the Politechnical Institute of Cluj Rumania

Visiting Research Fellow 1963/64 sponsored by British Council

AN INVESTIGATION OF THE HOT TORSION TEST USED IN STUDIES OF HOT WORKABILITY

Work carried out in the Department of Metallurgy
at Birmingham College of Advanced Technology in 1964,
and submitted for the M.Sc Degree of
The University of Aston in Birmingham, in 1966

ACKNOWLEDGEMENTS

Thanks are due to British Council, Rumanian Ministry of Education and Professor Domsa Alexandru, Rector of the Politechnical Institute of Cluj who gave me the opportunity of going to England and specialising in my profession in the Department of Metallurgy of Birmingham College of Advanced Technology. I heartily thank Professor I.G. Slater, Head of Department who very kindly provided facilities for studying and working in laboratories, and who generously showed interest and encouragement for my work. I greatly thank Mr. K.A. Reynolds who as supervisor helped me in many ways all the time of my stay in England, and who by useful discussions contributed largely to a fruitful experience and to support it in the best and happiest way. I wish to record thanks also to Mr. R. Lyndon for help in making the testing machine; Mr. H. Martin for help in manufacturing the heating equipment; Mr. J. Fuggle for the microanalysis studies; Mr. N. Shirley for photographic services; secretaries for kindly help in many things and typing this work; and all members of the department who in one way or another contributed to a pleasant time at the College and generally in England.

I also thank Round Oak Steelworks who provided the necessary cast steel for experiments; Walter Somers Limited forge where some of the experimental material was forged, and The British Cast Iron Research Association for providing spheroidal graphite cast iron.

The way I was helped in the Department, and the visits I made in England will cause me to remember with great pleasure the College of Advanced Technology, and those members of the College with whom I came into contact, during the time I spent in England.

SUMMARY

The use of as-cast and wrought metals for the manufacture of various shapes by forging requires a knowledge of the ductility of metals and alloys at high temperatures. A review of literature reveals that each type of test used for hot workability measurement has some characteristic that usually gives different results than those obtained by using one of the other tests. For this reason, to enable a better assessment of the hot workability of materials to be made, a correction formula is proposed. Hot workability measurement by means of the torsion test is of considerable interest and the main factors which characterise this type of testing are discussed in detail.

It was found that the axial force which appears during twisting is closely connected with deformation behaviour and is not significantly affected by fibre structure or crystal lattice. Compressive force is suggested to be due to grain deformation and tensile force to grain boundary sliding. These phenomena can be connected by a formula which allows axial force in the torsion test to be used for studying a material's behaviour from the point of view of grain boundary sliding in a very easy way. Phase transformations and recrystallisation may also be studied by measuring the variation of axial force with time at various temperatures.

It was also found that the generally accepted plasticity equations cannot be used in a simple way for studying the axial stress distribution across the specimen cross section, on account

of the factors which give rise to the force. A formula is proposed for taking account of the influence of axial force on the hot ductility measurement by torsion test, thus allowing a better comparison between the ductilities of various metals and alloys to be made.

Studies of the manner of fracture revealed that cracks which first form within the specimen at elevated temperature in the steels used originated at inclusions along the fibre structure. Although axial tensile stresses markedly influence the appearance of these cracks they are not the main cause. Factors connected with specimen dimensions which may affect the ductility were also studied, and revealed that specimen diameter seems to affect the ductility more than its length.

Experiments on as-cast mild steel showed that different results are obtained on specimens taken from different parts of the ingot and that wrought material has generally better ductility than cast.

Nodular cast iron has some ductility and can be deformed in the temperature range of 850 - 1000°C in the cast state, and 720 - 1020°C after annealing. Ductility was slightly less than half that of specimens cut from mild steel ingots.

AN INVESTIGATION OF THE HOT TORSION TEST USED IN STUDIES OF HOT WORKABILITY

CHAPTER 1

INTRODUCTION

Many components have a form such that they are best manufactured either by forging or by casting. It is often difficult to decide which method to use for making a particular item and it is not unusual to find similar engineering components forged by one manufacturer and cast by another. Casting is usually more economical than forging but substitution of a casting for a forging is sometimes limited by the mechanical properties which are required since the mechanical properties of wrought materials are usually better than of cast ones (1,2).

The significance of the above statement may be better realised by considering not just a specimen cut from one of the sound regions of an item but by taking the entire piece as a specimen. For instance, if a casting has the shape shown in Fig. 1.1 and specimens from 3 sides have a tensile strength of 48 kg/mm^2 and from one side of 40 kg/mm^2 (which may contain porosity or other defects) it may be stated that the strength of the material is 48 kg/mm^2 but the strength of the whole piece is only 40 kg/mm^2. Supposing that such a piece were to be forged from the same material and the strength thereby increased to 50 kg/mm^2 on all sides; it could be concluded that the strength of the material increased by about 4% but the strength of the piece by 25%. These aspects are more significant for components manufactured from steels and other alloys which cannot be cast easily without developing unsoundness.

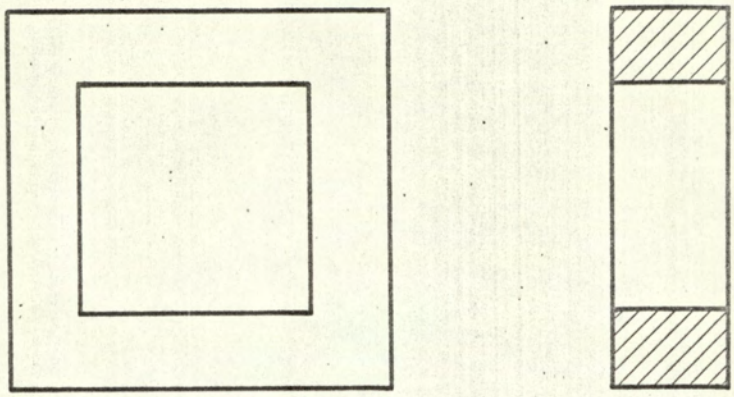

Fig. 1.1. Piece in the form of frame.

The above example illustrates the tendency for components to be manufactured by deformation. For complicated shapes however much time and energy is required in preparing a semifinished product prior to the final shaping operation. The quantity of the material which is lost by flash in the final stage also depends on the way the semifinished product is produced and this may appreciably affect the cost of the forging. Using casting for the production of semifinished products followed by forging as a final operation could produce some items with better mechanical properties, surface quality and higher dimensional accuracy than by casting alone and cheaper than by forging alone. Balahanov (3) and Lane (4) showed some interest in using this combined method. The latter showed that material and time may be saved with such a technique but very few data have as yet been established.

For the development of this type of processing it is necessary to know the hot working characteristics of a material both in the as-cast and wrought conditions.

One of the author's main interests is the study of some of the deformation problems associated with cast pre-forms. Experimental work on a few materials has already been carried out at the Politechnical Institute of Cluj from where he was supported as an exchange Fellowship by the British Council and Rumanian Educational Ministry during the period October 1963 - October 1964. During the Fellowship, held at the Birmingham College of Advanced Technology, his interest was followed up by the work described in this thesis.

Work at Birmingham was in progress to study the hot workability of metals and had reached the stage where a hot torsion testing machine

was to be built. This test has already been used by several workers to study metallurgical variables involved in metal deformation at high temperatures, but the test itself was not well understood. Accordingly the present programme of working was undertaken with the objects of:

(1) Constructing a hot torsion testing machine in which compression and tension could be superimposed on torsion, so that the nature of the deformation might be explained.

(2) Studying some problems associated with the torsion test such as axial force appearance during twisting and its effect on hot workability measurement, the nature of the fracture of the specimens and the effect of specimen size and geometry.

(3) Using the hot torsion test to study the effect of prior deformation on the hot workability of cast metals.

(4) Using the hot torsion test to determine the hot workability of spheroidal graphite cast iron (which could be considered a possible material for cast pre-forms).

Accordingly, this thesis begins with a survey of methods for assessing hot workability in which the reasons for selecting the hot torsion test are discussed and then continues by describing the experimental work carried out during the year

1964 when the aspects listed overleaf were studied.

HOT WORKABILITY AND HOT WORKABILITY TESTING.

Chapter 2. INTRODUCTION.

2.1.

Before starting to discuss methods for hot workability measurement it is appropriate to deal with some general aspects connected with this form of testing.

Henning and Boulger (5) said that pure metals having F.C.C., B.C.C. or H.C.P. structures generally exhibit decreasing workability in this order. But when they are alloyed, the classical division is not so distinct because so many new factors appear such as composition, number of phases and grain size. Although workability usually increases with rise in temperature, they gave eight distinct workability behaviours exhibited by various alloy systems such as in Fig. 2.1. Pure metals and single phase alloys exhibit increasing workability with increasing temperature (type 1). However, grain growth causes a reduction in workability at high temperature (type 11). Alloys containing elements which form insoluble compounds exhibit fracture at forging temperature (type 111) but if those compounds dissolve with rise in temperature an improvement in workability will occur too (type 1V). Alloys undergoing phase transformations generally change their workability when the phase change occurs (type V - V111). However they also remarked that above the recrystallisation temperature workability is affected by strain rate. Indeed, metal deformation at temperatures where work hardening recovery or recrystalization, grain

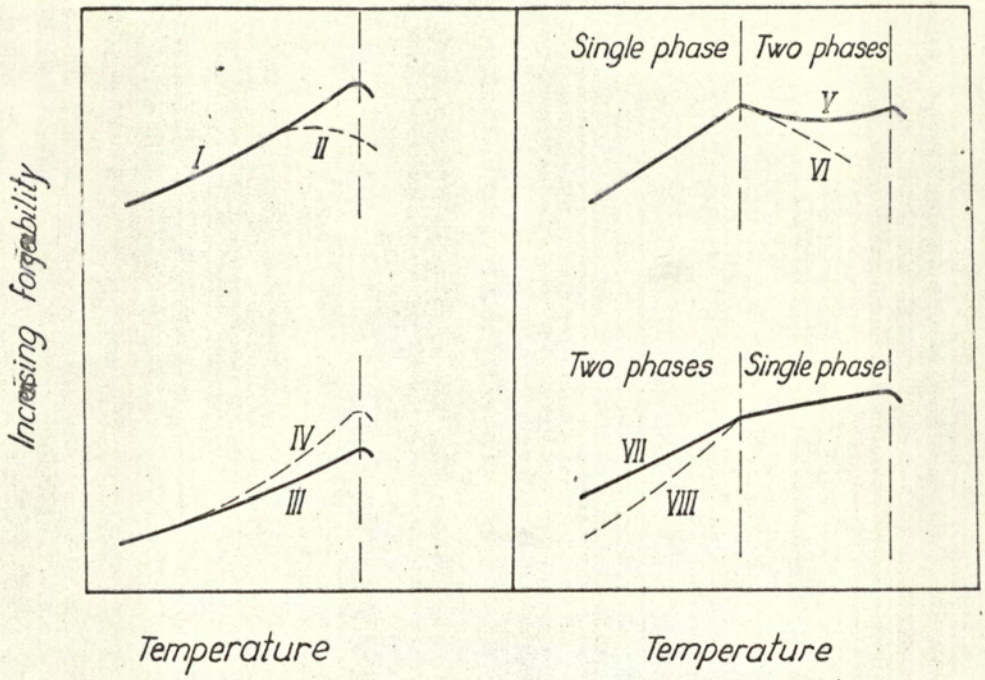

Fig.2.1. Scheme of the forgeability variation with temperature [5].

boundary sliding etc. proceed simultaneously and where deformation is affected by strain rate in different ways is a very complicated phenomenon. Therefore, it is not easy to take all these factors into consideration and give a complete and clear definition for hot workability. It can only be defined that "hot workability is the capacity of metals and alloys for supporting permanent deformation at high temperature under various conditions of stress and strain rate".

In the above definition the terms "high temperature" and "hot workability" have been used, and it is necessary to qualify these statements by further definition: that a metal or alloy is hot worked if examined at room temperature after deformation it shows no work hardening (i.e. it is fully annealed).

We know that for many metals and alloys recovery commences at about 0.3Tm and recrystallization at about $0.4T_m$ (T_n being the melting temperature in degrees Kelvin) (6). We also know that for some metals recrystallization occurs at the same time as recovery. Both recovery and recrystallization commence at lower temperature if the degree of deformation rises, as shown in Fig. 2.2. (7) . Because recovery and recrystallization require a certain time for completion, in defining hot working range it is necessary to take account of the rate of cooling after deformation as well as the rate of deformation. If the speed of cooling is slow the lower limit of temperature range for hot working may be lower than if the speed of cooling is greater. For this reason there is no absolute temperature range over which a

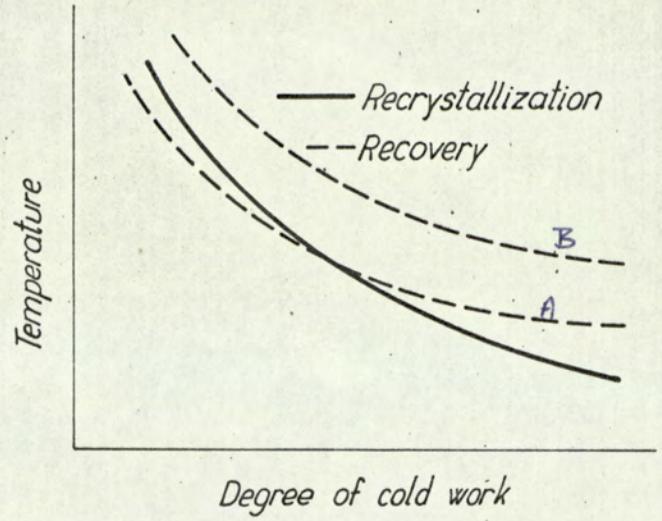

Fig.2.2. Effect of degree of cold work on recovery and recrystallization temperature for different types of metals [7].

A-with high stacking fault energy; B-with low stacking fault energy.

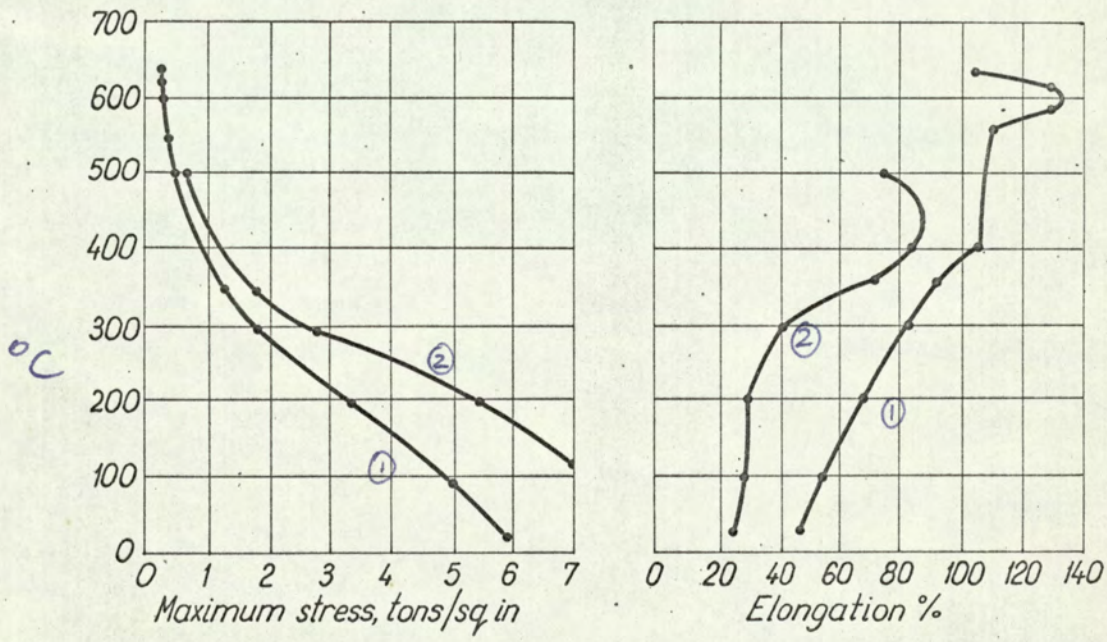

Fig.2.3. Variation of strengths and ductility with temperature for aluminium [9].
1- Fully annealed; 2-cold worked.

metal or alloy can be hot worked but it can be defined as a function of the way recovery and recrystallization occur. On this basis Kirk (8) used the following definitions:

- Hot working range is where after deformation the specimen is fully annealed.

- Cold range is where after deformation the specimen is work hardened and no restoration occurs or is so small that it can be neglected.

- Intermediate range where the specimen after deformation is only partially restored.

Later Gubkin (6) arrived at almost the same conclusions that hot working range is usually over 0.7Tm, cold working under 0.3Tm and intermediate range between these two.

From the point of view of hot workability, interest centres on the dynamic balance between work hardening, recovery and recrystallization. Dynamic restoration for a particular material depends first on temperature and second on the degree of deformation. The degree of work hardening, for a given material and temperature is dependent on strain rate. Strain rate also affects not only work hardening but also the temperature rise within the specimen, grain boundary sliding etc. There are still many unsolved problems associated with these effects during deformation at high temperatures.

If it is not easy to give a complete definition for hot workability then it is much more difficult to measure it. Several tests have been proposed and used by different

investigators, each claiming some degree of success in the application of data to plant problems, the main forms of testing being the following:

1) Tensile test which measures the hot workability (and the ductility in general) by ratio $\frac{\Delta l}{l_o}$, $\frac{\Delta A}{A_o}$ etc. (where l_o is initial length, A_o initial area, Δl total elongation, and ΔA total reduction in area).

2) Compression test which measures the hot workability by ratio $\frac{\Delta h}{h_o}$, $\frac{\Delta f}{A_o}$ etc. (where h_o is initial height of the specimen, A_o initial area, Δf area after deforming, Δh reduction in height).

3) Torsion test which measures the hot workability by the number of revolutions to failure of the specimen.

4) Impact bending which measures indirectly the ductility by the energy necessary to break the specimen or by the degree of bending before fracture.

With such a wide range of tests, it is difficult to decide which is best for hot workability measurement and to discover whether there exists any connection between their results. If we consider that one particular parameter will be used for hot workability measurement for a material, for some condition of testing, where hot workability corresponds to x units and compare this value with $\Delta A/A_o$ (from tensile test), with $\Delta f/A_o$ (from compression test), with the number of revolutions to failure n (from torsion test) with the energy required to failure K (by impact bending) etc. they may be equated using coefficients in the form: -

$$\chi = C_1 \frac{\Delta A}{A_0} = C_2 \frac{Af}{A_0} = C_3 n = C_4 k$$

It would seem that the coeficients used will not have the same values for all conditions of testing, and the best method for hot workability measurement would be that which maintains its coefficient as constant as possible by varying one parameter of deformation. But without a value or units in which to measure it is not possible to make this comparison. However, it is possible to discover whether there is a change in the manner of deformation by maintaining conditions as constant as possible and varying one vector at a time. For a better appreciation of this aspect it is necessary to review the work already carried out on hot workability tests.

2.2.

REVIEW OF LITERATURE

Most of the investigations carried out deal with two main problems:

1) The effect of strain rate and temperature on the resistance to deformation.

2) The effect of strain rate and temperature on the hot ductility.

Each will be discussed in the light of the different tests used.

2.2.1.

Tensile Test

Martin (9) was one of the earliest investigators of a

material's behaviour at high temperatures using the tensile test. Using aluminium he observed that the ductility increased and the strength decreased somewhat up to 325°C, then above this, a marked increase in ductility occurred. He attributed this increase to a sudden rise in the rate of recrystallization. He found some differences in behaviour at high temperatures between previously cold-worked material and fully annealed. For cold worked material the resistance to deformation was greater and the ductility less than for fully annealed. The differences lessened when the temperature was increased, more for strength and less for ductility (Fig.2.3). He studied also the influence of strain rate (using the terms "slow" and "fast") on the resistance to deformation and ductility.

Portevin and Bastien (10) who used various types of test for hot workability carried out tensile tests on light alloys and measured the elongation, reduction in area and the energy required for fracture. The variation of these parameters against temperature for two materials is shown in Fig. 2.4, from which it can be seen that although the elongation reduction in area and the energy required for fracture sppear to vary in different ways they have maxima at about the same temperature, for an Al-3% Mg alloy. This does not happen in Al-6% Mg where the energy required for deformation showed no change at temperatures where an increase in ductility occurred

Clark and Datwyler (11) using both slow and impact

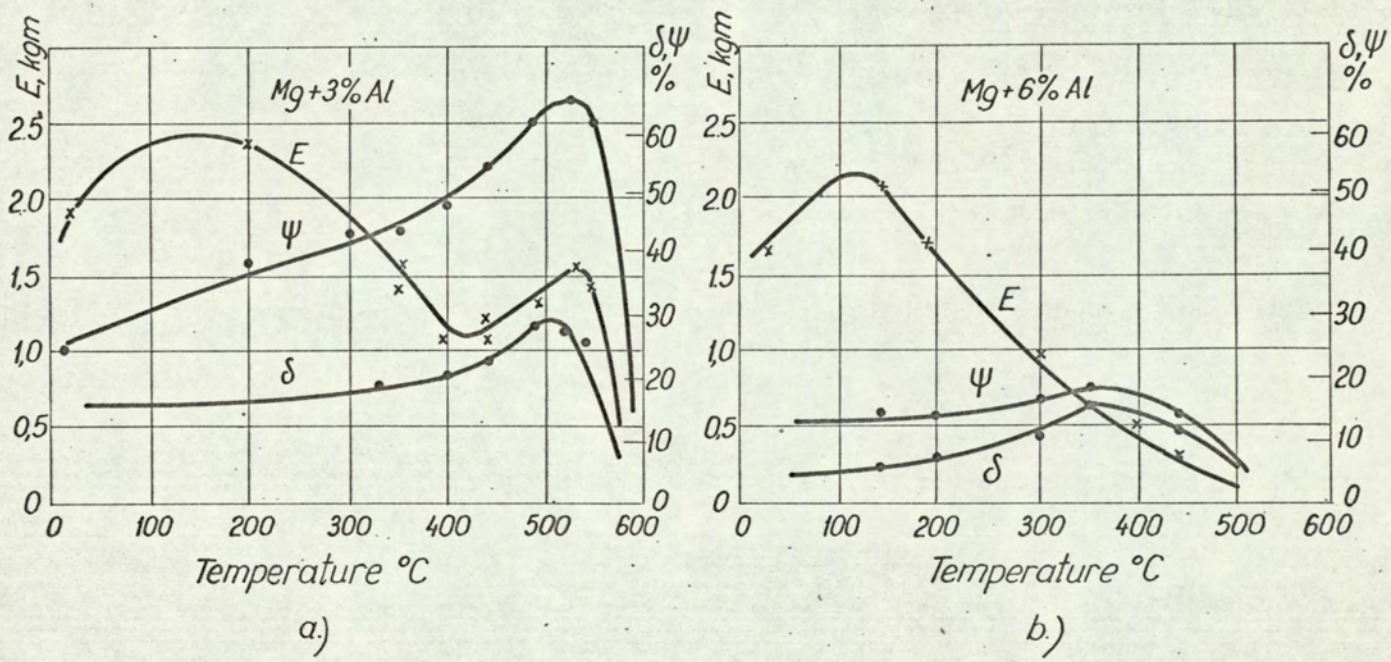

Fig.2.4. Variation of elongation δ, reduction in area ψ and energy required for fracture E against temperature for two alloys [10].

Table 2.1

Material	Yield Point	Maximum Load	Elongat - ion	Reduction of area	Energy to Fracture
SAE 6140	-	1.020	2.205	2.940	2.865
SAE 1015	1.328	1.285	1.418	1.055	1.376
SAE 1018	1.995	1.397	0.992	0.946	0.964
18.8 alloy	1.224	1.212	0.682	0.782	0.600
Duraluminium 17S-T	1.294	1.094	1.000	1.035	0.885
Brass	1.387	1.142	1.163	1.136	1.203
Aluminium	1.52 2	1.323	1.628	1.093	1.627
Copper	1.433	1.390	1.527	0.986	1.597

tensile test at room temperature determined force/elongation curves for a number of metals and alloys. They observed that strain rate affects yield stress, maximum stress, elongation, reduction in area and the energy required for fracture, but not all in the same way. Using the ratio of dynamic average to static average values they noticed a variation over wide limits for different materials. From table 2.1 it can be seen that this ratio is higher for yield stress and for maximum stress for all materials The ratios for elongation, reduction in area and the energy required for fracture differ from metal to metal in the proportion of about 3.2 for elongation, 3.7 for reduction in area and 4.7 for energy to fracture. (This difference is much smaller for yield stress (about 1.6) and for maximum stress (about 1.3). However, there is clearly some connection between the variation of ratios of elongation, reduction in area and the energy to fracture which has a value approaching either elongation ratio or reduction in area ratio.

Mann (12) studied the strain rate influence on the energy required for impact tensile fracture, measuring at the same time the elongation and reduction in area. The experiments were made at room temperature but he used more values for strain rate than the two reported by Clark and Datwyler. Making tests on rolled manganese and silicon bronze he observed that at a certain value of strain rate a steep fall in energy occurred which was not the same for both materials (Fig. 2.5a). It is

significant that at the point where a drop in energy occurred an increase in elongation and reduction in area takes place (Fig.2.5b). He called this point "transition velocity". Alteration of the condition of the material causes the transition velocity to change its position (Fig.2.6a). Changing the specimen size produced no change in transition velocity (Fig. 2.6b). From these results he concluded: -

1) For each metal and alloy there is a transition velocity where the energy required for rupture falls, which does not depend on specimen size but only on the condition of the material.

2) When the energy drops the elongation and reduction in area usually increase.

McGregor (13) analysed data obtained by many investigators and showed that the effect of strain rate on the resistance to deformation obeys a logarithmic law of the form:

2.2.

$$S = S_1 + S_2 \log \frac{V}{V_1} \qquad (2.2)$$

where S is the resistance to deformation for a speed V

S_1 is the resistance to deformation for a speed V_1

S_2 is constant.

In his analyses he also used results obtained at low temperatures.

Manjoine and Nadai (14,15) using a high speed testing machine carried out experiments on copper, aluminium

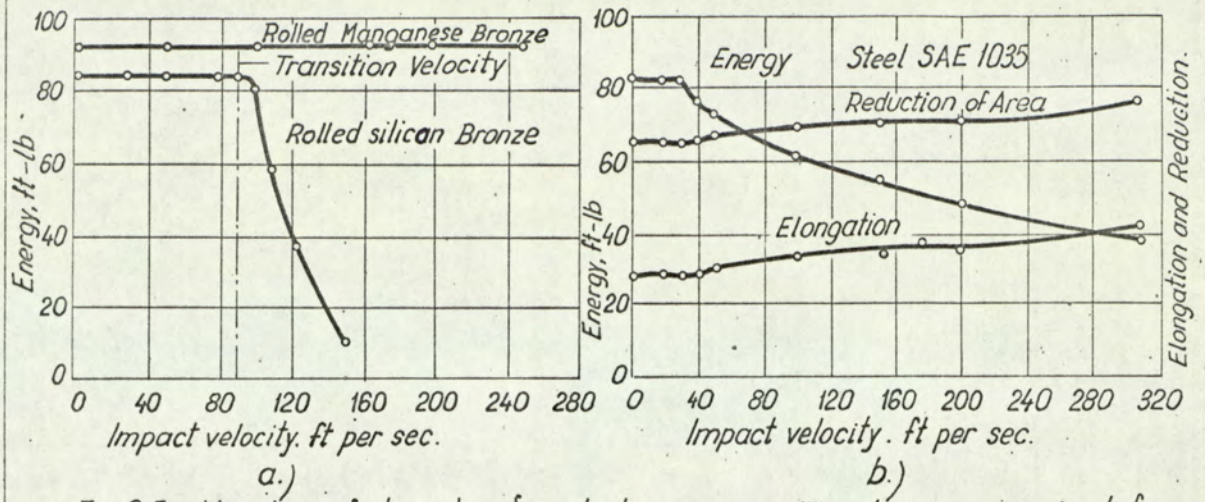

Fig. 2.5. Variation of elongation δ, reduction in area Ψ and energy required for fracture E against impact velocity [12].

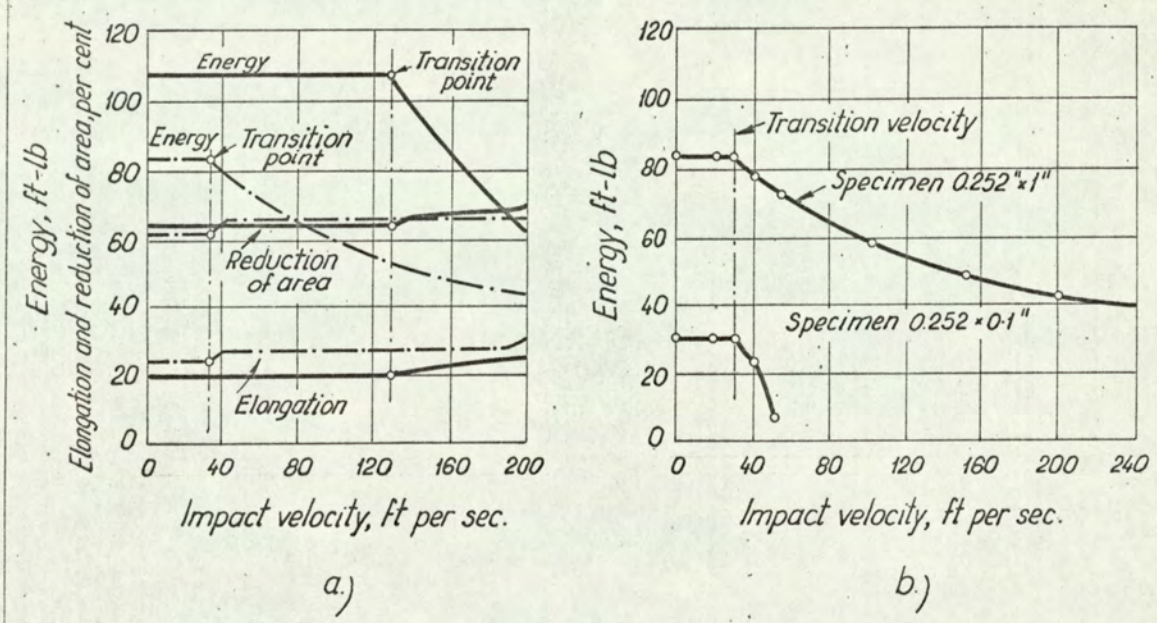

Fig. 2.6. Variation of elongation δ, reduction in area Ψ and energy E required for fracture against impact velocity for steel SAE 1035 [12].

—— Quenched quickly; —·— Annealed.

and steel to determine the influence of the temperature and strain rate on the resistance to deformation. Their results are summarised in Fig. 2.7. They also show the fractures of specimens broken under various conditions of testing. From their results it is important to notice the following:

1) Strain rate has a smaller effect on resistance to deformation at lower temperatures than at higher temperatures. For a strain rate of 1000/sec the resistance of aluminium at 600°C, of copper at 1000°C and of steel at 1200°C, is between 1/3 and 1/4 of their respective values at room temperature. On this basis it would be anticipated that by increasing the strain rate further the resistance to deformation at elevated temperatures could approach values at room temperatures, provided no restoration had time to occur.

2) Strain rate has a smaller effect on the elongation at lower temperatures than at higher temperatures. For instance the elongation of copper at 500°C is about the same for the three speeds (135, 450 and 900/sec). At 800°C the elongation is about the same for 135 and 450/sec but much smaller for 900/sec . The elongation of aluminium at 600°C deformed with a strain rate of 1000/sec is greater than when deformed with a strain rate of 8.5 10^{-4}/ sec

It is apparent that while the resistance to deformation is affected by strain rate in about the same manner for all materials, the deformation process is different for those metals. Furthermore, the elongation is not a linear variation with strain rate since, with

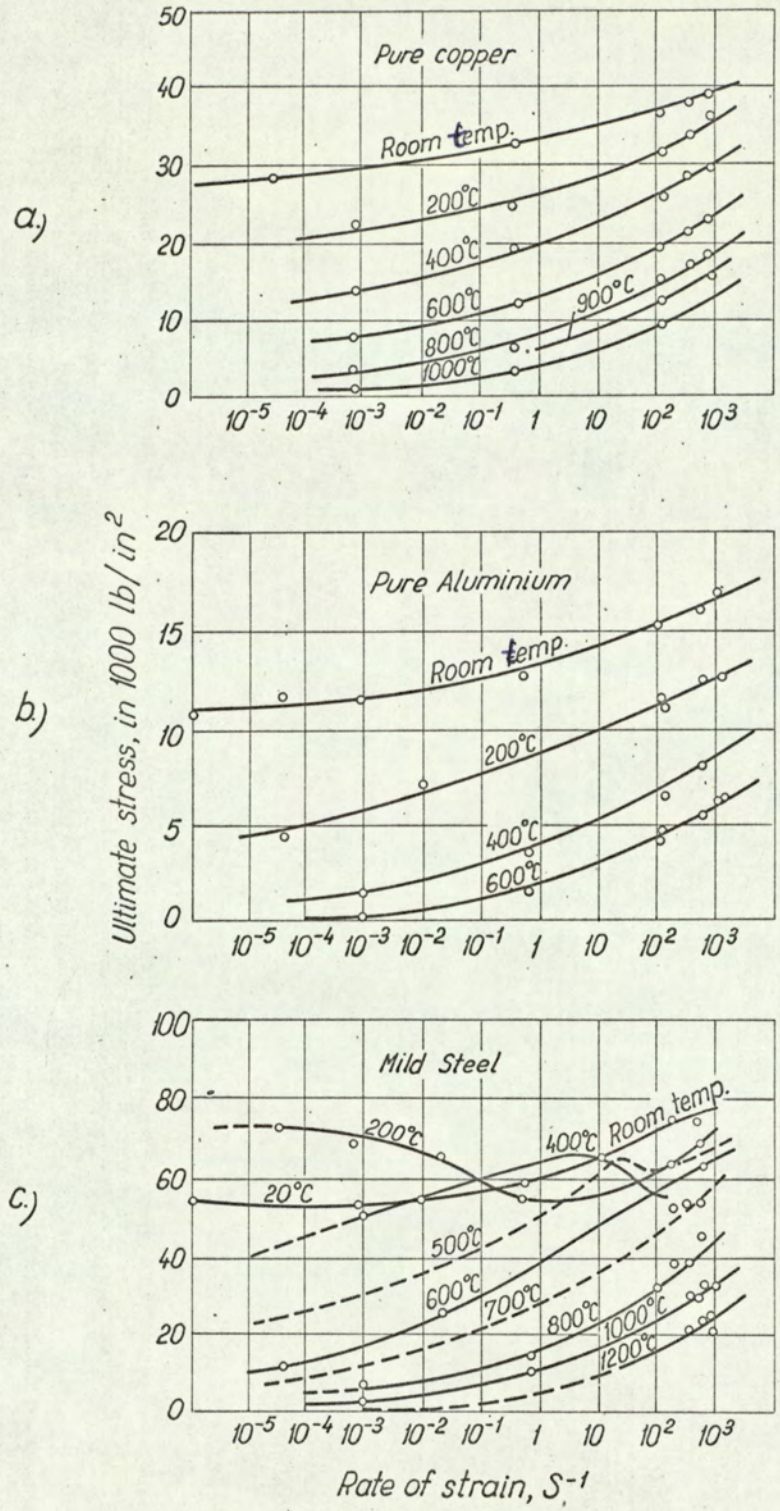

Fig.2.7. Variation of ultimate stress for various temperatures and strain rates of copper, aluminium and mild steel [14,15].

copper no change in elongation occurred passing from 135 to 450/sec (at 600 and 800°C) but from 450 to 900/sec the elongation fell steeply.

Greenwood, Miller and Suiter (16) making tests on copper and brass at temperatures up to 600°C using strain rates of 0.2, 40 and 1000%/hour observed that by increasing the strain rate the ductility increased as shown in Fig. 2.8 Intergranular cavities were observed after deformation at high temperatures, their extent increasing with rise in temperature and decreasing at high strain rates.

Nordheim, King and Grant (17) investigated the influence of strain rate on the hot ductility and fracture characteristics of three irons with low carbon content and various levels of phosphorus and oxygen. Using strain rates of between 0.001 to 50%/sec the variation of elongation and reduction in area for two irons are shown in Fig. 2.9. No marked difference in ductility occurred with either iron at 1600 and 2200°F but at 1800°F the ductility was smaller for strain rates of 0.001 and 50%/sec and greater at 0.1% They also studied microstructures and found that for specimens deformed at 1800°F with low strain rates the fracture was intergranular, for intermediate rates transgranular and for high rates transgranular, although some intergranular cracks were observed near the fracture. They arrived at the following conclusions:

1) Up to 0.09% phosphorus has no effect on ductility and fracture characteristics;

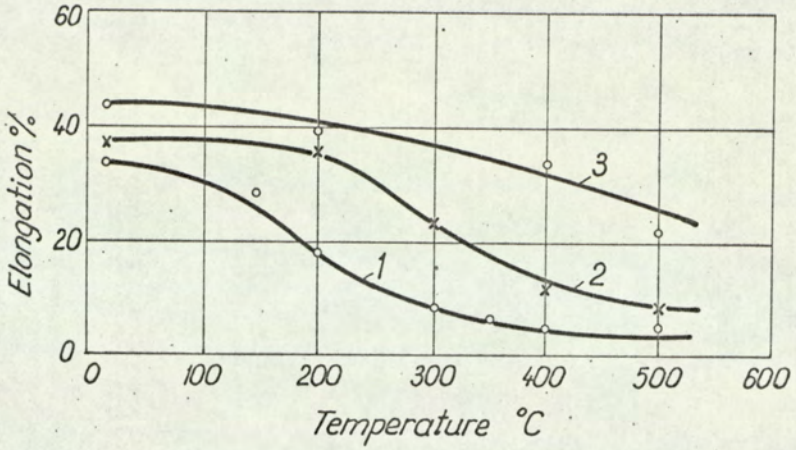

Fig.28. Variation of elongation against temperature for copper with various strain rates [16].
1- 0·2% h^{-1}; 2-40% h^{-1}; 3-1000% h^{-1}.

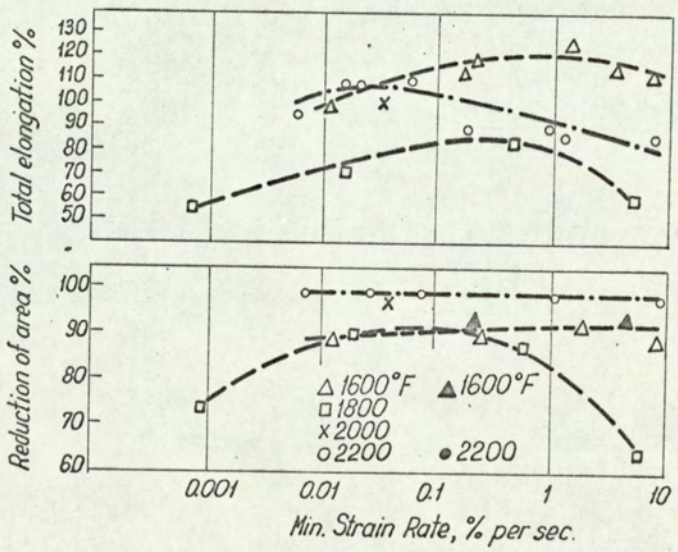

Fig.2.9. Variation of elongation and reduction of area against temperature for two irons [17].
△ □ x ○ Heat R1, 0.059% P; ▲ ● Heat R2, 0.089% P.

2) Strain rate has very little effect on ductility in the range of temperature which was studied except at 1800°F where it was slightly reduced.

Castro and Poussardin (18) investigated the effect of strain rate on the ductility of some steels. Their results for a mild steel deformed with a strain rate of 5/sec and 400/sec are shown in Fig. 2.10. It will be seen that the ductility at 400/sec is higher up to 1200°C than for 5/sec and above this temperature range they change their relative positions. These investigators also postulated that at low temperature the ductility is reduced at low strain rates by the production of precipitates, which have insufficient time to form at high strain rates. At high temperatures they assumed that the slow strain rate permits recrystallization and this accounts for the ductility being greater.

Leech, Gregory and Eborall (19) carried out experiments for hot workability measurement using a device adqpted to an Izod impact machine. The strain rate used was about 260 /sec . They measured the elongation, reduction in area and the energy required for fracture at various temperatures, using brass and bronze. Variation of these characteristics against temperature are shown in Fig. 2.11 and 2.12. They compared results with those of Voce and Hallowes who used a notched bar test (Tab. 2.II). They also used a rolling test and measured reduction in height at which edge cracking appeared.

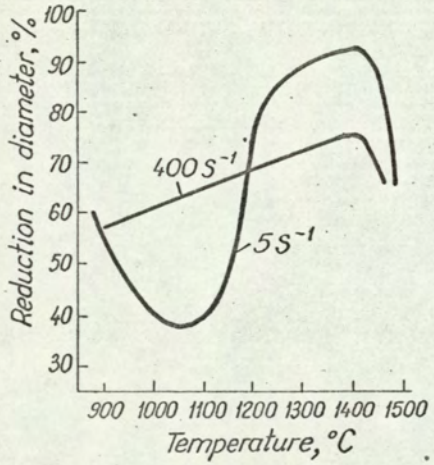

Fig. 2.10. Variation of ductility against temperature for mild steel. [18].

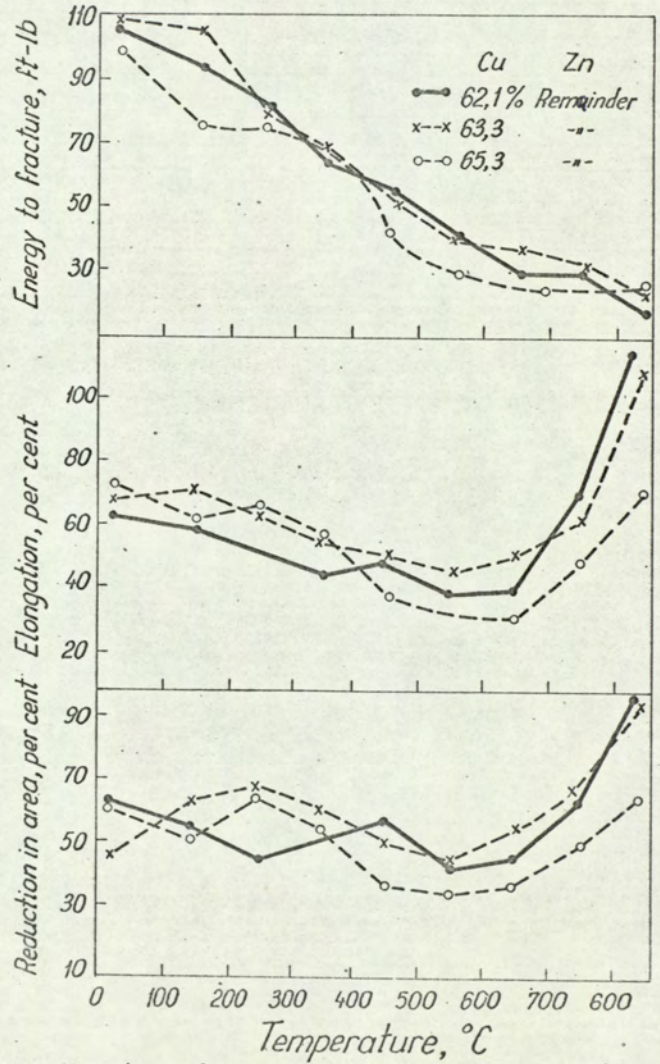

Fig. 2.11. Variation of elongation, reduction in area and energy required for fracture against temperature for Cu-Zn alloys [19].

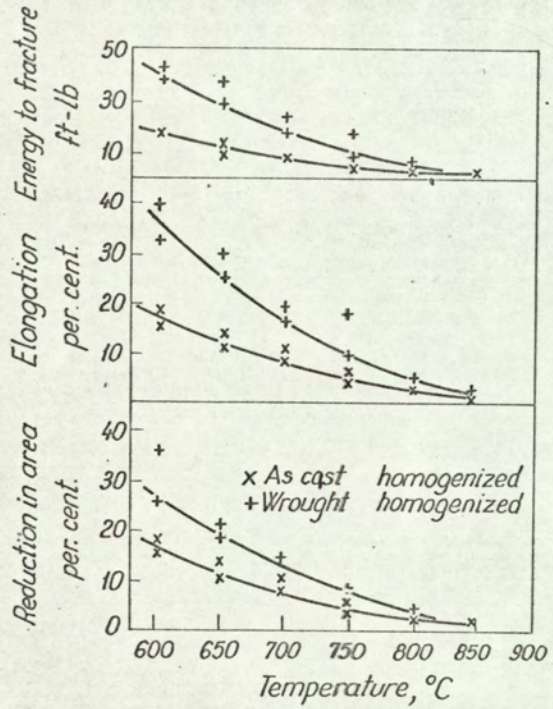

Fig. 2.12. Variation of elongation, reduction in area and energy required for fracture against temperature for bronze [19].

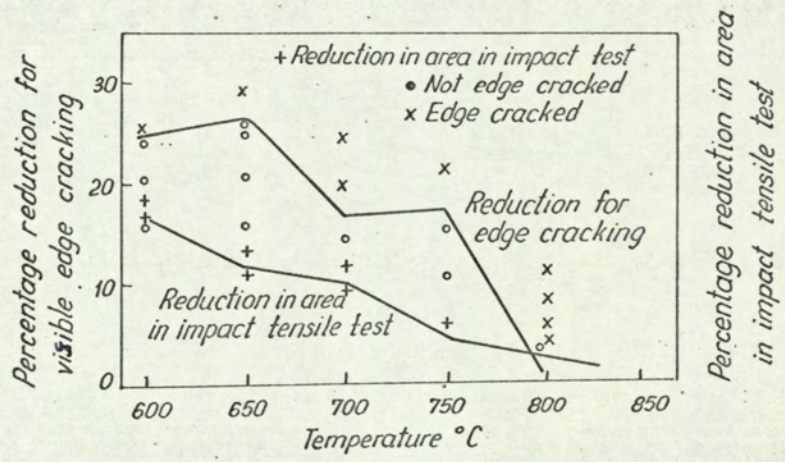

Fig. 2.13. Reduction of area by tensile test and reduction in height by rolling at which cracks first appeared, against temperature [19]

Table 2.2

Material		Energy to fracture ft - lb	Elongation %	Notched bar impact value ft - lb
KAV 95	a	58	70	68
	b	59	70	-
KAV 75	a	53	58	-
	b	53	60	33
	c	52	58	-
	d	51-5	60	-
KAV 91	a	15	14	-
	b	14	14	5
	c	12	12	-

*

As reported by Voce and Hallowes.

Reduction in area by impact tensile test and reduction in height by rolling at which the cracks appeared are shown in Fig. 2.13. Because the reduction in area is generally below the reduction in height they came to the conclusion that the impact tensile test is suitable for hot workability measurement. From their results may be concluded: -

1) There is no direct relationship between the energy required for fracture and elongation and reduction in area;

2) There is no proportional relationship between elongation, reduction in area, impact strength and reduction in height by rolling.

Bridgman (20) studied the tensile test from the point of stress distribution in the necked region and, Using an approximation, he found the following equations for stresses:

$$\sigma_s = \sigma_\theta = Y \cdot \ln \frac{a^2 + 2aR - r^2}{2aR} \qquad 2.3$$

$$\sigma_z = Y \left[1 + \ln \frac{a^2 + 2aR - r^2}{2aR} \right] \qquad 2.4$$

Where σ_z is axial, σ_s radial and σ_θ circumferential stress in the necked region;

Y = yield stress;

a = radius of specimen in the necked region (Fig.2.14a).

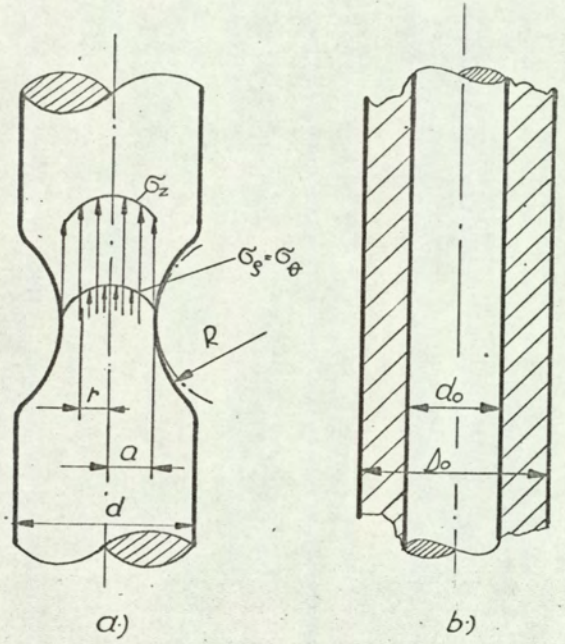

Fig. 2.14. Scheme of specimen deformed by tensile testing.
a- necked region; b-special specimen.

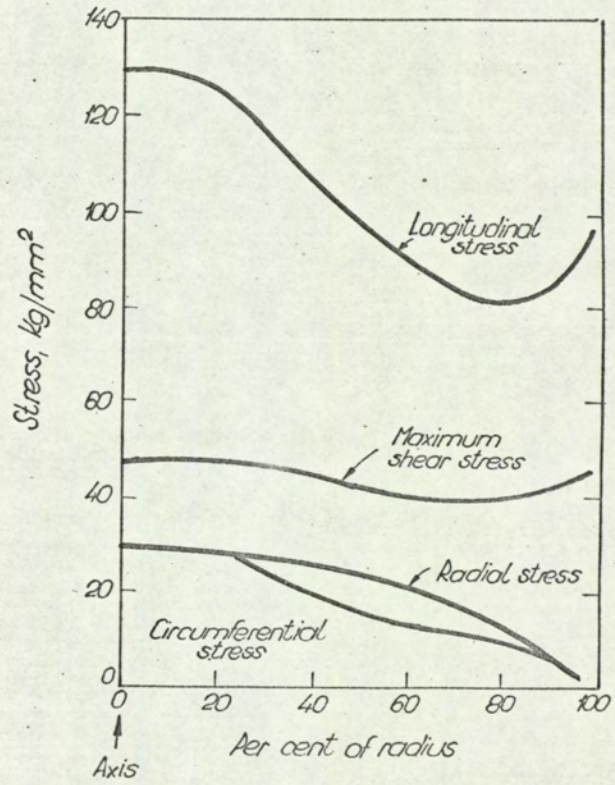

Fig. 2.15. Variation of stress across the specimen section in a tensile test (22)

R = the curvature of specimen in the necked region;

γ = radius inside of specimen $(0 < \gamma < a)$

Using hollow specimens containing a solid core (Fig. 2.14b) he showed that deformation across the neck is quite uniform. For instance, for specimens which before deformation had the ratio $D_o/d = 1.95$ after a reduction in area of 92% rose to 2.09. However, it seems that at the middle of specimens the deformation was slightly higher.

Davidenkov and Spiridonova (21) who also studied stress distribution in the necked region gave the following equations for calculating the stresses:

$$\sigma_{min} = \frac{\sigma_m}{1 + 0.25\, a/R} \qquad 2.5$$

$$\sigma_{max} = \sigma_m \left(\frac{R + 0.5a}{R + 0.25a} \right) \qquad 2.6$$

Where $\sigma_{min} = \sigma_Z$ for $\gamma = a$ (Fig. 2.14a)

$\sigma_{max} = \sigma_Z$ for $\gamma = 0$;

σ_m is medium value of σ_Z ($\sigma_m = \frac{P}{\pi a^2}$, P being axial force).

Parker, Davis & Flanigan (22) studied the stress distribution in tensile specimen experimentally, using solid and hollow specimens. The variation of the stresses across specimen section is shown in Fig. 2.15.

Puttick (23) studying tensile test fractures observed that the fracture started from the axis, and developed towards outside.

Comparing both theoretical and experimental stress distribution and also the point of initiation of fracture, nonuniformity in stress distribution across specimen section is evident and the fracture starts from that place where axial stress has maximum value, i.e. from the axis.

If we take into consideration the equations 2.3 - 2.6, for γ = constant, we can write a function of the form:

$$\sigma_z = f\left(\frac{a}{R}\right) \qquad 2.7$$

Bridgeman, studying the variation of the ratio $\frac{a}{R}$ observed that it is not constant during deformation but increases if the strain is raised, such as in Fig. 2.16. He studied also the influence of hydrostatic pressure on deformation, and observed that it has a significant effect on flow stress and ductility. The variation of the ductility at fracture against pressure of pulling for a few materials is shown in Fig. 2.17.

Investigations were also made on the influence of specimen size on ductility. Williams and Hall (24) studied this aspect at low temperature. They found that reduction in area is not affected by specimen size at 20°C when the ratio l/d was constant (l being specimen gauge length and d its diameter), but at lower temperatures it is affected (Fig.2.18). Shahanian and Lane (25) studied this aspect in creep. Using a wide range of specimen sizes and ratios of l/d they came to the conclusion that increasing the ratio l/d results in

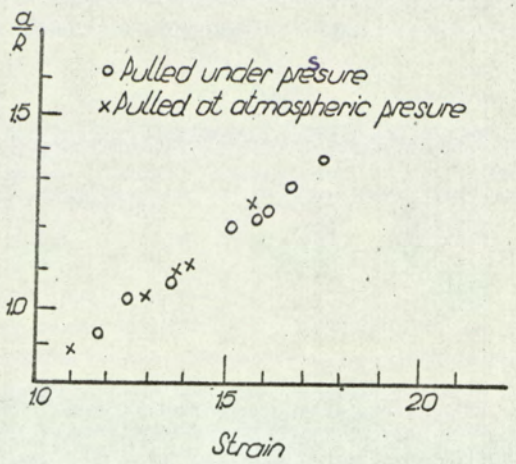

Fig. 2.16. Variation of the ratio $\frac{a}{p}$ against strain [20].

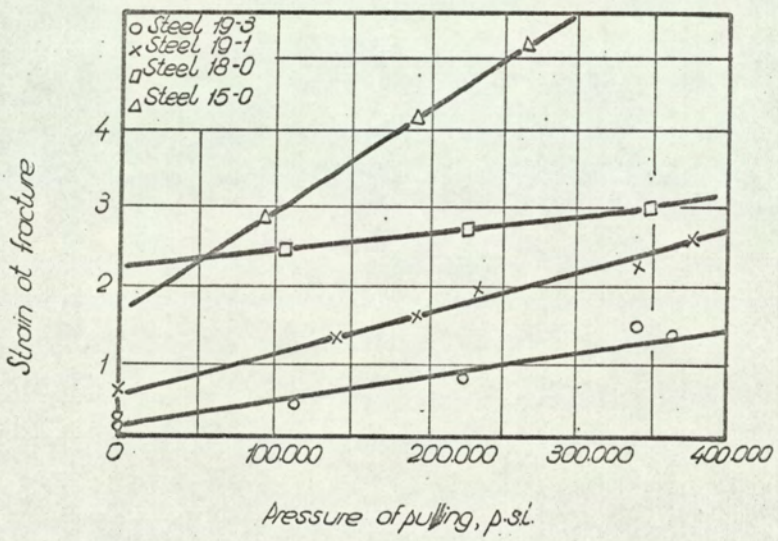

Fig. 2.17. Variation of strain to fracture against pressure of pulling. [20].

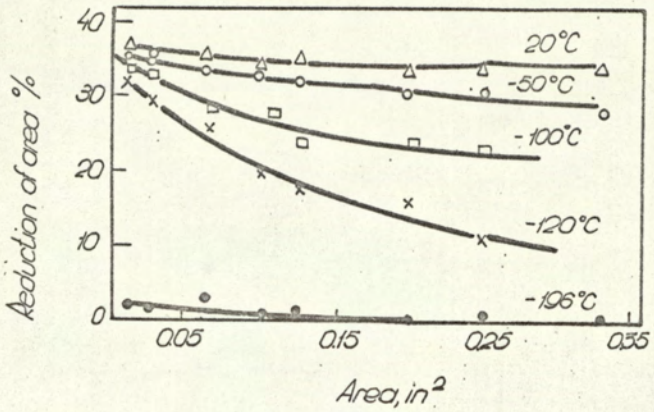

Fig. 2.18. Variation of reduction in area against the specimen area [24].

decreases in rupture time and total elongation. However, a change in diameter has little effect on ductility if the ratio $\frac{l}{d}$ is kept constant.

CONCLUSIONS.

1) The strength of metals is affected by strain rate less at low temperatures than at higher temperatures. For a given temperature it is possible to relate stress and strain rate in a form of logarithmic law which gives satisfactory results for many metals and alloys.

2) Elongation and reduction in area are affected by strain rate in a much more complex manner than stress. Although the conditions of testing were quite different, comparing the results obtained on copper by Nadai and Manjoine with those of Greenwood, Miller and Suiter it can be readily seen that at 600°C the ductility rose by increasing strain rate from 0.4/hr(0.00011/s) to 1000/hr(0.28 sec^{-1}) but no change in ductility occurred by increasing strain rate from 135/sec to 450/sec, and the ductility decreased by increasing the strain rate from 450/ sec to 900/sec^{-1}. From the results of Nordheim, King and Grant and those of Castro and Poussardin on mild steel the curve of ductility as a function of strain rate would have at least two maxima at a temperature of 1800°C.

3) There is no close connection between elongation and reduction in area and the energy required for fracture. By varying the temperature and strain rate each behaves in a

different manner characteristic of each material.

4) Stress distribution across the specimen section in the necked region is not uniform, but depends on the form of the neck. The necking is influenced by temperature and strain rate so it follows that stress distribution in the necked region is also affected by these factors. However, by increasing strain rate at higher temperature it seems that this ratio does not change so much as at lower temperatures. Hence, at higher temperatures a rise in strain rate produces a more uniform stress distribution in the necked region and more uniform deformation along the specimen gauge.

5) The ductility is affected by hydrostatic pressure and by stress level at a given temperature. Because strain rate affects the form of the neck it may affect the ductility in a complex way.

6) The ductility is partly dependent on specimen geometry but if the ratio $\frac{l}{d}$ is kept constant the specimen dimensions seem to have little influence on ductility.

1.2.2. Compression test

Because this type of testing closely resembles several kinds of hot-working operations (forging, rolling, stamping etc.) it has been often studied particularly from the point of view of stress distribution as a function of specimen size and friction between test piece and platens.

It is well known that due to friction between specimen and platens phenomena occur which give rise to very complicated stress systems. A great number of works

have been published, and for solving problems many approximations have been made and many types of equations have been obtained. The usual approximations relate to the values of shear stress and how it varies on the contact surface between specimen and platens. In most cases the following have been accepted (6.26):

$$\tau = 2\mu k; \quad \tau = k, \quad \tau = \mu \sigma_z, \quad \tau = k \frac{x_c}{l_c} \qquad 2.8$$

where τ is shear stress on the contact surface between specimen and platens;

k - maximum shear stress;

σ_z - normal stress on the contact surface;

μ - frictional coefficient between specimen and platens;

l_c - portion over which it is assumed that τ varies linearly from zero to k;

x_c - a random value between o and lc .

For any conditions of testing and value of τ, the value of σ_z on the contact surface is giving by a function of the form:

$$\sigma_z = f\left(k, \frac{d}{h}, \mu\right) \qquad 2.9$$

By increasing the ratio $\frac{d}{h}$ (for a given value of k and μ) σ_z increases at the specimen axis. On the other hand by decreasing the friction coefficient μ the variation of σ_z along the specimen diameter is smaller and its maximum value is less for a given ratio $\frac{d}{h}$. As a general rule at the outside of the specimen $\sigma_z = 2k$ and at the specimen axis $\sigma_z = \sigma_z$ max, and radial stress σ_s outside is zero and at the specimen axis is maximum.

Robin (27) was one of the earliest investigators to use the compression test to determine various characteristics of materials at different temperatures. He showed that the higher the carbon content in steels the higher is its resistance to deformation or lower its forgeability. He also showed that some elements act favourably in decreasing the resistance at high temperatures (e.g. chromium) and others unfavourably (e.g. nickel).

Ellis (28), using impact compression, showed the influence of the transformation point in iron on its working properties. He pointed out that the atomic rearrangement which occurs at the Ac3 point seems to increase resistance to deformation.

Kent (29), using a drop-stamp, deformed specimens made from tin, lead, zinc, aluminium, copper and brass. Measuring the reduction in height at various temperatures, he observed that the resistance to deformation at high temperature is not as low as reported by other investigators using data from tensile tests with lower strain rates. In this way he pointed out the strain rate influence on the deformation behaviour

Cook and Larke (30) investigated the influence of friction and specimen size on the resistance to deformation of copper and copper alloys at room temperature. They varied the specimen diameter from 0.5 to 1 in. and the height from 0.2 to 1.5 inc. the ratio $\frac{do}{ho}$ being from 0.4 to 4. By deforming these specimens they drew a set of

curves of the form:

$$P = f\left(\frac{d_o}{h_o}, \frac{\Delta h}{h_o}\right) \qquad (2.10)$$

where p is medium normal stress required to produce deforming;

d_o - specimen diameter and ho-its height;

Δh - reduction in height.

At the same time the value of yield stress for various reduction in height were determined, as are shown in Fig. 2.19.

Alder and Philips (31) studied the effect of strain rate and temperature on the resistance to deformation of aluminium, copper and steel. Using a plastometer machine which provided a constant strain rate, they eliminated the friction between platens and specimen surfaces by lubrication. From their results they observed the following aspects:

1) The effect of strain rate on the stress of a given temperature and strain could be expressed with a reasonable approximation either by semilogaritmic formula written in the form:

$$\sigma = A \ln \bar{\epsilon} + \sigma_o \qquad (2.11)$$

or by a power lqw in the form

$$\sigma = \sigma_o \bar{\epsilon}^{\,n} \qquad (2.12)$$

where σ is the resistance to deformation for a given condition;

σ_o - stress value for unit strain rate;

$\bar{\epsilon}$ - true strain rate;

A and n - constants.

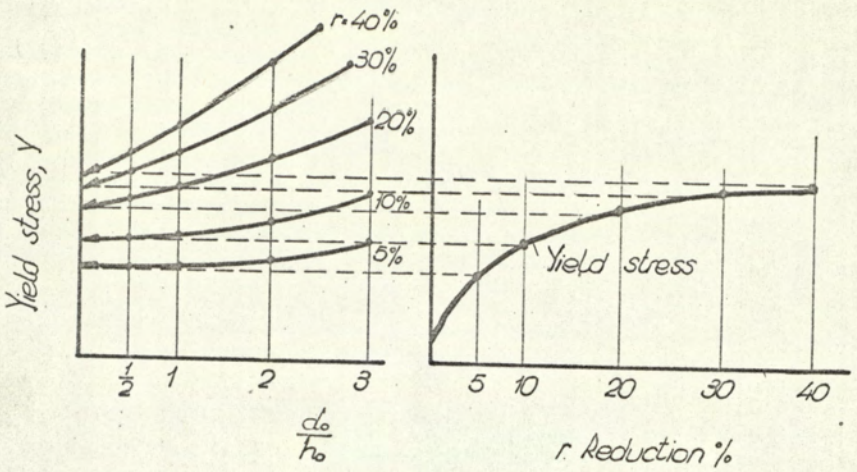

Fig. 2.19. The value of yield stress as a function of the ratio $\frac{d_0}{h_0}$ and reduction in height [30].

Fig. 2.20 illustrates the agreement between stress and strain using the equations 2.11 and 2.12. However, the authors came to the conclusion that equation 2.12 gives better results for high temperatures.

2) For copper and steel at high temperatures and strain (over 40%) a reduction in stress occurs. No reduction was found with aluminium alloy at any temperature and strain. Therefore, they came to the conclusion that no general relationship between stress and strain can be valied for all materials. They were particularly concerned with the equation : -

$$T_m = T\left(1 + k \ln \frac{\bar{\epsilon}}{\bar{\epsilon}_0}\right) \qquad (2.13)$$

where T_m is relative temperature;

T - absolute temperature;

k - coefficient;

$\bar{\epsilon}$ - true strain rate;

$\bar{\epsilon}_0$ - unit strain rate (which was taken 10^{-3} sec^{-1}).

The above equation was suggested by McGregor and Fisher (32) who considered that resistance to deformation is affected in the same way by an increase in strain rate as by a decrease in temperature.

3) The stress for a given strain and strain rate varies with temperature in a complex way for materials which were studied, and accepting the equation 2.12 they determined the values for $\bar{\sigma}_0$ and n at various temperatures and strains which are given in tables 2.III and 2.IV.

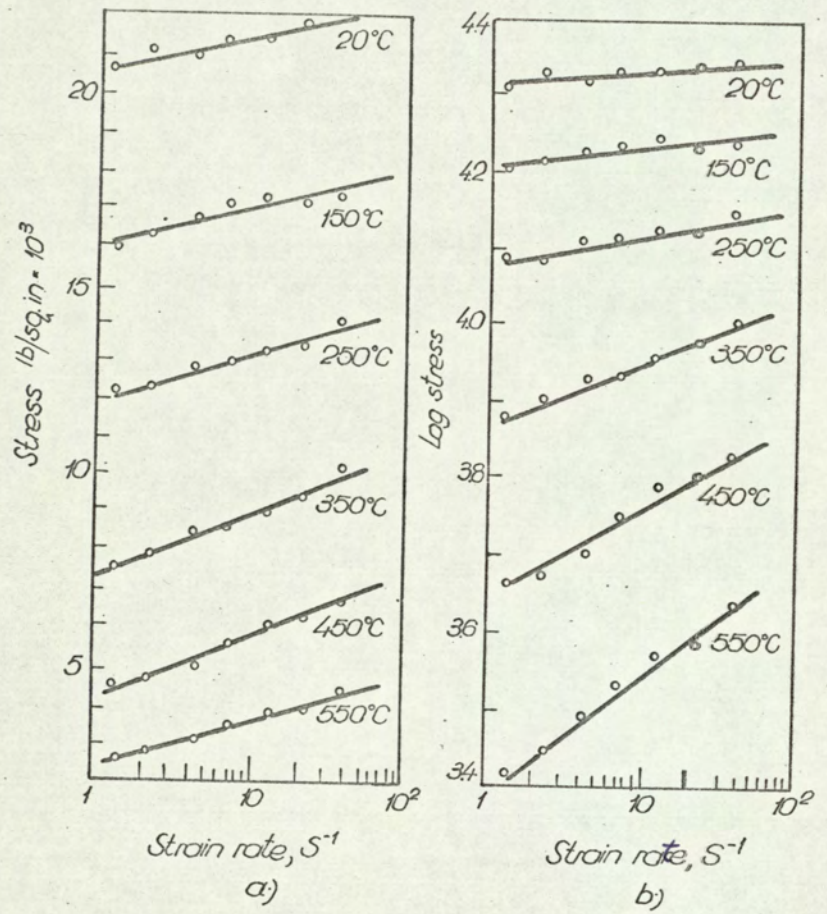

Fig. 2.20. Variation of stress against strain rate for various temperatures [31]. a - formula (2.11); b - formula (2.12)

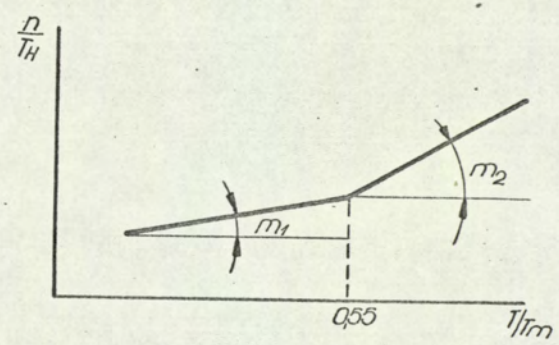

Fig. 2.21. Variation of the ratio n/T_H against the ratio T_H [31].

Table 2.III. The value of n for various materials, tamperatures and strain (31)

Metal	Temp. °C.	Value of n for a compression of				
		10%	20%	30%	40%	50%
Al	18	0.013	0.018	0.018	0.018	0.020
	150	0.022	0.022	0.021	0.024	0.026
	25C	0.026	0.031	0.035	0.041	0.041
	350	0.055	0.061	0.073	0.084	0.088
	450	0.100	0.098	0.100	0.116	0.130
Cu	18	0.010	0.001	0.002	0.006	0.010
	250	0.014	0.015	0.020	0.023	0.026
	300	0.016	0.018	0.017	0.025	0.024
	450	0.010	0.004	0.041	0.055	0.078
	750	0.096	0.097	0.128	0.186	0.182
	900	0.134	0.110	0.154	0.195	0.190
Fe	930	0.088	0.084	0.094	0.099	0.105
	1000	0.108	0.100	0.090	0.093	0.122
	1060	0.112	0.107	0.117	0.127	0.150
	1135	0.123	0.129	0.138	0.159	0.198
	1200	0.116	0.122	0.141	0.173	0.196

Table 2.IV. The value of σ_o for various materials, temperatures and strain (31)

Metal	Temp. °C.	Value of σ_o for a compression of				
		10%	20%	30%	40%	50%
Al	18	14.6	17.1	18.9	20.6	22.0
	150	11.4	13.5	15.0	16.1	17.0
	250	9.1	10.5	11.4	11.9	12.3
	350	6.3	6.9	7.2	7.3	7.4
	450	3.9	4.3	4.5	4.4	4.3
	550	2.2	2.4	2.5	2.4	2.4
Cu	18	26.3	40.3	49.0	54.1	55.7
	250	23.1	32.4	37.8	41.5	43.5
	300	20.2	26.5	30.2	32.2	34.4
	450	17.0	22.5	25.1	26.6	26.8
	750	7.6	9.7	10.0	8.5	8.2
	900	4.7	6.3	6.1	5.5	5.2
Fe	930	16.3	19.4	20.4	20.9	20.9
	1000	13.0	15.6	17.3	18.0	16.9
	1060	10.9	12.9	14.0	14.4	13.6
	1135	9.1	10.5	11.2	11.0	9.9
	1200	7.6	8.6	8.8	8.3	7.6

What is important from these data is that using the ratio:

$$T_H = \frac{T}{T_m} \qquad 2.14$$

where T is testing temperature in ^{o}K;

T_m - melting temperature in ^{o}K,

the variation of n with temperature is not great up to $T_H = 0.55$, but above this n increases steeply. Fig. 2.21 shows the variation of the ratio $\frac{n}{T_H}$ against ratio T_H and the values of m_1 and m_2 are given in table 2.V.

Table 2.V.

Values for m_1 and m_2 for various values of strain (31)

Compression %	10	20	30	40	50
m_1	0.045	0.050	0.055	0.060	0.065
m_2	0.36	0.38	0.41	0.46	0.52

Cook (33) carried out experiments on the strain rate and temperature effect on the resistance to deformation of more materials and some of his results are given in Fig. 2.22.. From this can be seen the complex effect of strain rate on the strength of materials at various temperatures and strain values.

Arnold and Parker (34) and Bailey and Singer (35) investigated the effect of strain, strain rate and

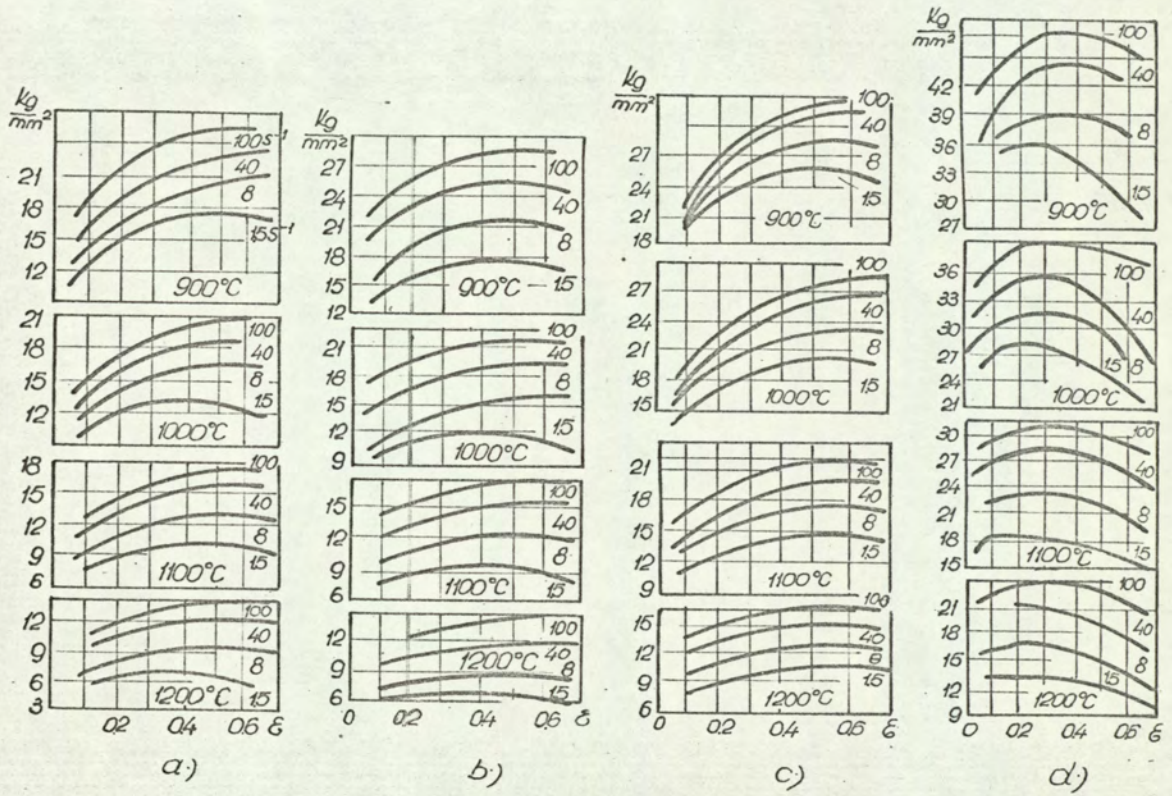

Fig 2.22. Variation of stress against strain at various temperatures and strain rates (35)
a - steel with 0,15 % C; b - steel with 0,56 % C; c - steel 1×18H8; d - steel 1F18×4B1

temperature on the resistance to deformation of aluminium and some aluminium alloys giving some results in curves of the form of those of Cook. However it is important to point out Bailey and Singer's conclusions which are:

1) Attempting to find an empirical formula relating yield stress to strain for various materials has little success. No relationship can be found to express correctly the shape of any stress-strain curves containing maximum and minimum strain.

2) For all materials tested the effect of strain rate on the yield stress at a given temperature and strain could be expressed by the power law. They also calculated the values of σ_0 and n for their materials and gave them as tables like those of Alder and Philips.

Discussion and conclusions on compression tests.

Because stress values depend largely on the friction coefficient μ and specimen size $\frac{do}{ho}$, by changing those values a change in the stress system occurs. As the specimen changes its dimensions during deformation and the ratio $\frac{d}{h}$ increases, implies that during deformation of the same specimen there is a change in stress system.

Stress values are affected by strain rate after a power law (for a given strain and temperature) but the relationship became much more complicated by changing the strain and temperature. For the latter no satisfactory equation could be given to fit various conditions of deformation

for a number of different materials.

It is necessary to point out that it is still not known how either the friction between specimen and platen or the specimen geometry as expressed by the diameter : height ratio affect hot-workability measurement at various temperatures and for different materials.

Bridgman (20) studying the influence of hydrostatic pressure on yield stress and ductility of some materials at room temperature observed that these properties improve when the pressure is increased. Specimens made from brittle material put into rings made from ductile material (Fig. 2.23), which created a hydrostatic pressure around them during deformation, could be deformed at appreciably high rates (6). Schroder (36) stated that the ductility of most materials is of a very high order under conditions where the strain is strictly compressive.

From the plasticity equation of the form:

$$(\sigma_z - \sigma_y)^2 + 3\tau_{zy}^2 = 3k^2 \qquad (2.15)$$

where σ_z is normal stress,

σ_y - radial stress,

τ - shear stress,

k - maximum shear stress,

it can be seen that by increasing σ_z σ_y will increase. Now σ_y may play the role of hydrostatic pressure, which implies that by increasing the ratio $\frac{d}{h}$ in the compression test ductility would be expected to improve.

As hot-workability measurement, using this test, is based on the appearance of cracks on the outside of the specimen where σ_3 seems to be zero it would appear that this stress has no effect, but the external surface cannot be considered separately from the interior, which is affected by σ_3 . Again friction between specimen and platens cannot be completely eliminated and due to the complex flow within the specimen, the deformation is not uniform and the specimen changes its shape. Furthermore, according to Sacks (37), as a cylindrical sample becomes barrel-shaped under upsetting operations tensile stresses come into play around the periphery (Fig. 2.24) which act as secondary stress restricting the amount of deformation, and causing cracks to develop. The nature of these tensile stresses is not yet understood.

Tomlinson and Stringer (38) investigating the closing of internal cavities in forging observed a very interesting phenomenon. Using block specimens 4" x 4" x 8" with an axial hole of $\frac{1}{4}$" dia they observed that in first stage of deformation (up to about $\frac{\Delta h}{h} = 0.36$) the diameter of the hole increased in the middle of specimen then above this value of $\frac{\Delta h}{h}$ it decreased, as shown in Fig. 2.25. From these results it can be seen that σ_3 at the middle height of the specimen varies in a complex manner during deformation and its value depends on the ratio $\frac{d}{h}$. It may be supposed that the tensile stress which appears in zone III will also

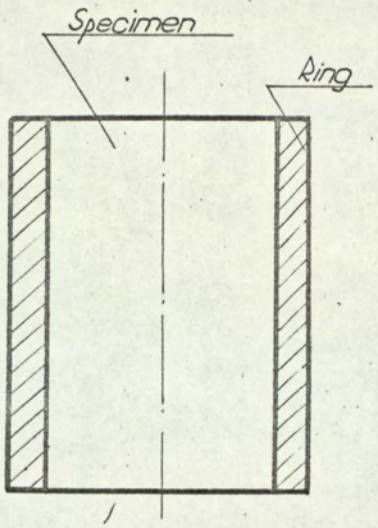

Fig. 2.23. Special specimen for compression test

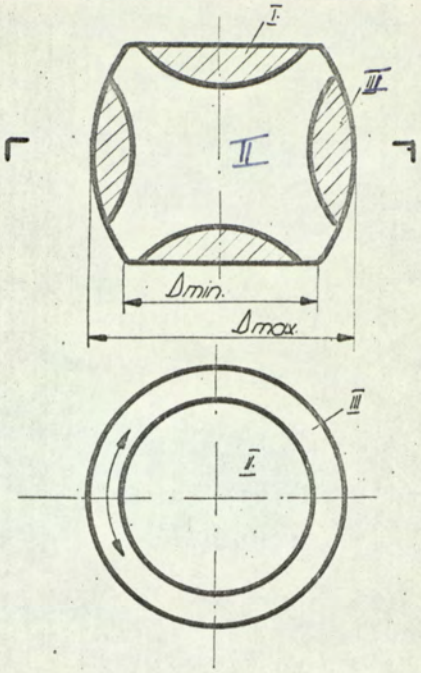

Fig. 2.24. Specimen deformed by compression test.

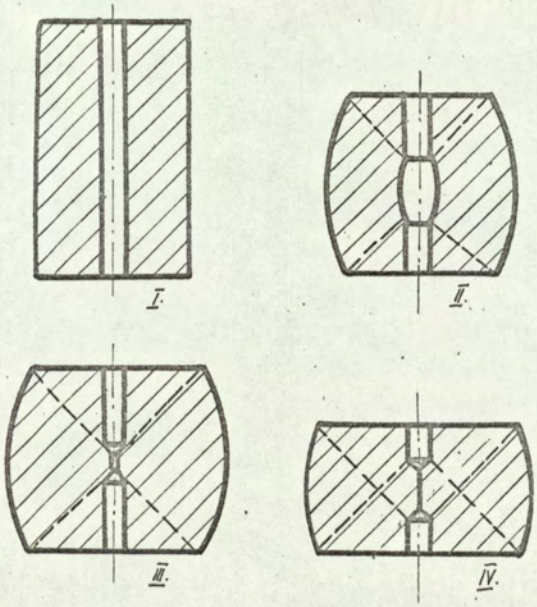

Fig. 2.25. Stages of deformation by upsetting. (38)

vary during deformation and will also depend on the ratio $\frac{Dmax}{Dmin}$. However, $\frac{Dmax}{Dmin}$ is affected by the frictional coefficient and lubrication has different effects on different materials. This can be seen from the results of Zeerleder et alia (39) who studied the influence of lubrication on conic punch penetration in specimens made from steel and aluminium (Fig. 2.26). Furthermore, the frictional coefficient is affected by temperature and speed of deformation (6). Thus from the foregoing it is clear that in compression tests many factors are involved during deformation which cannot easily be controlled, and these affect the ductility in a very complex way especially for materials which sustain big changes in the value of $\frac{d}{h}$ during deformation. For these reasons what is measured qunntitatively may not truly represent a quantitative measurement of the hot-workability characteristics.

2.2.3. Torsion Test.

Sauver (40) seems to be the first to use this type of testing for studying deformation at high temperatures. He twisted $\frac{1}{4}$ in. square bars of various plain carbon steels heated to temperatures between 600 and 1200°C. The deformation was not limited to any length and the temperature was not constant along the bar. Making tests in this way on steels with low carbon content he observed two portions which deformed more on the both sides of the centre region.

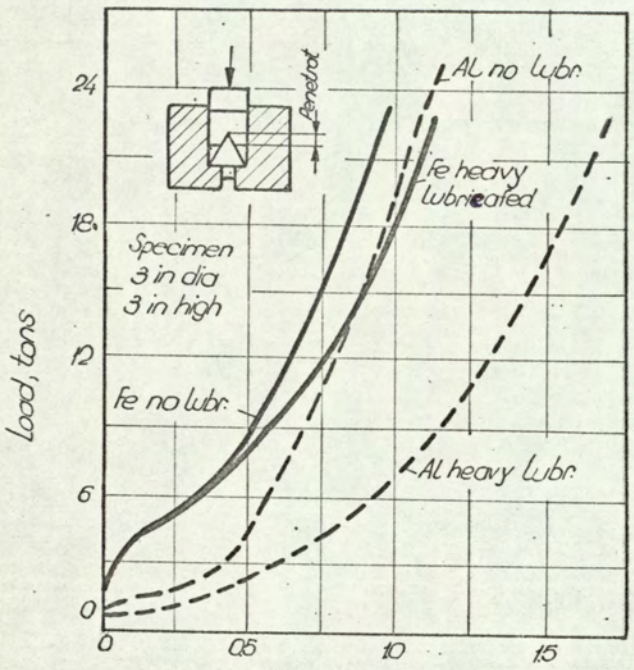

Fig. 2.26. Effect of lubrication on the penetration of conic punch for various values of load (39).

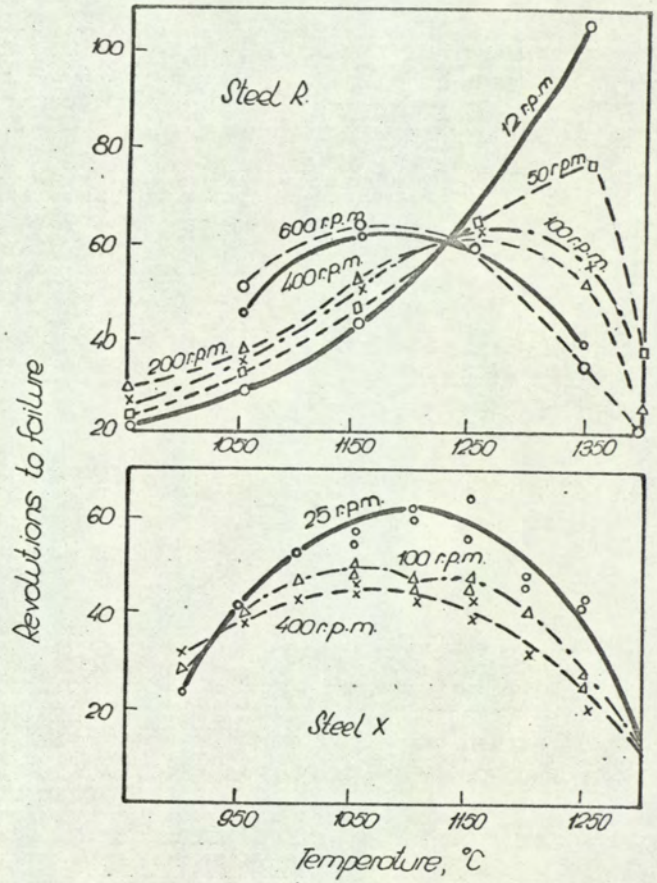

Fig. 2.27. Variation of number of revolution to failure against temperature for various strain rates (45).

He explained this by postulating that ferrite at its highest temperature is more ductile and has a lower strength than austenite at its lowest temperature.

Itihara (41) investigated the effect of impact torsion, using both static and dynamic methods. His device consisted essentially of a fly-wheel which, after acceleration, was coupled with the test specimen. He observed that metals behave differently under dynamic and static conditions, and it is not possible to use data obtained by static tests in characterising forging properties under dynamic conditions.

Ihring (42) using 5/16 in. dia bar specimens expressed the hot-workability as the number of revolutions to failure. Although he did not limit the length of bar, his results showed good correlation with practice.

Clark and Russ (43) employed a similar method of testing as Ihring and carried out experiments on steels in the temperature range 900 - 1400°C. They studied the form of fracture and concluded that the reduction in ductility above a certain temperature is associated with a change in the type of fracture from transcrystalline to intercrystalline.

Bloom, Clarke and Jennings (44) used a torsion test on 9/16" diameter bars for investigating the connection between ductility and structure for stainless steels in the temperature range 1040 - 1340°C. They found that on increasing the temperature the ductility increased and

as the ductility is strongly affected by structural transformation their results show that in the temperature ranges where more ferite is present the material is more ductile.

In all the above experiments no limitation in specimen length was used and specimens were deformed along a temperature gradient. Because the temperature varied along the specimen length the deformation was nomuniform. However, their results aroused great interest.

Hughes (45) seems to be first who used specimens with a restricted portion in the middle. Using an improved machine he recorded the torque and axial force which appeared during deformation. With his machine he could select deformation speeds from 12 to 600 rev/min. and he carried out experiments on steels in the temperature range 950 - 1350°C, using various specimen sizes and strain rates. From his experimental results the following aspects emerge: -

1) The ductility was affected by strain rate differently for various temperatures and materials. On increasing strain rate the ductility increased up to a particular temperature and then decreased, for one steel (R), and it decreased almost at every temperature for another steel (x) (Fig. 2.27). Furthermore, by increasing the strain rate the peak of ductility against temperature was moved towards lower temperature for steel R but remained at about the same temperature for steel x. Because the energy involved during

deformation appears as heat within the specimen and consequently the temperature increases more rapidly for higher speeds than for lower, Hughes concluded that temperature rise is the main factor influencing the ductility. It was a good explanation for steel R up to its peak, but this phenomenon seems to be more complicated at temperatures above the peak and for the alloy steel. (x).

2) By increasing the specimen diameter the ductility seems to increase (Fig. 2.28). However variation of diameter alters the strain rate at a given number of revolutions per minute. Thus the change in ductility is closely connected with the change in strain rate.

3) During deformation by torsion an axial force appeared which varied with the temperature.

4) Fracture started from the outside up to a temperature of about 1100°C, but above this temperature internal cracks appeared before the fracture occured in one of the steels (R). These cracks were orientated transversely at about the middle of the specimen radius. Hughes gave an explanation in terms of two factors:

a) The fibre structure, which before deformation was axially orientated, became radial during twisting. Thus, the cracks may form along the reorientated fibre structure.

b) Due to superimposition of axial and shear stresses, which according to Nadai (46) are distributed across the

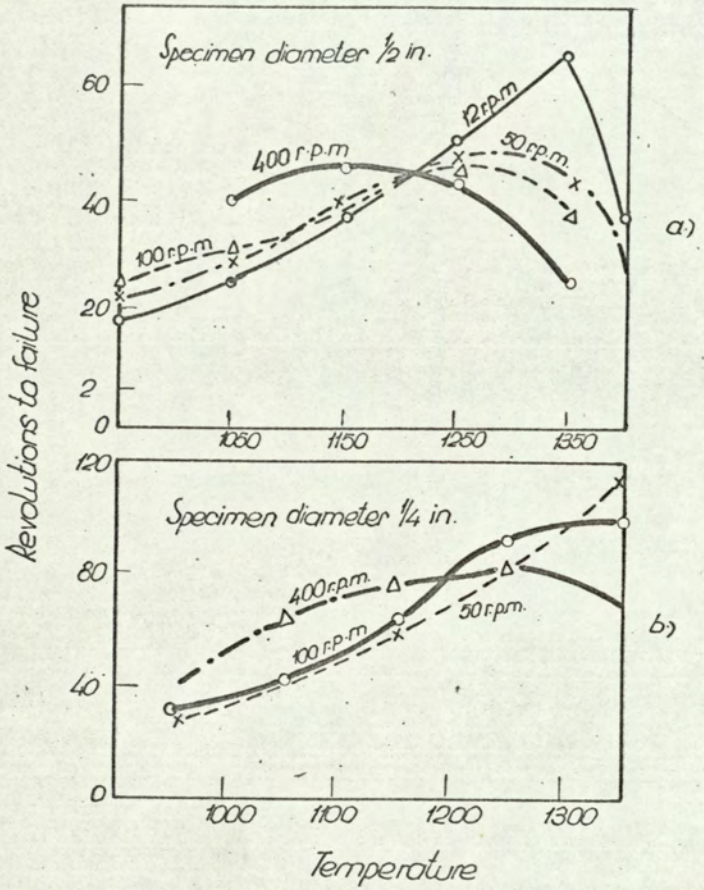

Fig. 2.28. Variation of number of revolutions to failure against temperature for specimens made from steel A (45).

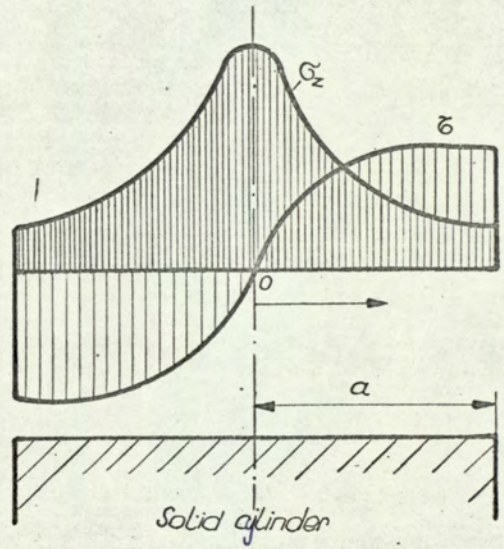

Fig. 2.29. Stress distribution in torsion test when an axial force is present (46).

specimen cross section as shown in Fig. 2.29. At the specimen axis shear stress is zero and axial stress has its maximum value. However, the cracks do not appear at the axis of th specimen but at the position where axial stress and shear stress have optimum values.

It is worthy of note that Hughes stated that the torsion test results showed a good correlation with the practice of rotary piercing, but it is not possible to assess hot-torsion test results with practical experience in other hot-working operations, the majority of which are less severe than rotary piercing.

Guenssier and Castro (47) employed this test for studying the hot-workability of a few alloy steels. They observed that if the specimens made from austenitic steel (18/8) were not restrained they became shorter during deformation whereas from 17% Cr ferritic steel they became longer. When the specimens were kept fixed an axial force appeared during deformation, tensile for the first steel and compressive for the second. They supposed that this complex stress system, different for various materials, may affect the ductility measurement as determined by the test.

Bastien and Portevin (48) investigated the speed of recrystallization of metals during deformation and showed that there is a critical speed which greatly influences the ductility at high temperatures. From their results for

a steel with 0.29% deformed at 1000°C, it can be seen that on increasing the number of revolutions per minute from 10 to 100 no sensible change in ductility occurred but from 100 to 400 the ductility increased markedly (Fig. 2.30).

Robbins, Cutter and Sherby (49) investigated the effect of structure on ductility of pure irons at elevated temperature. During testing the specimens were unrestrained and the strain rate was about 47% $sec.^{-1}$ Three irons were used: Armco iron (99.7%), Puron iron (99.95%) and vacuum melted iron (99.97%). From their results the following conclusions may be drawn: -

1) Pure iron had the highest ductility.

2) Ferrite is more ductile than austenite in the same range of temperature.

Studying the factors which affect the ductility, they said that the following would be expected to contribute to an increase in hot-workability :

a) Increase in number of slip mechanisms;

b) Increase of atomic selfdiffusion rate;

c) Increasing ease of twinning;

d) Increasing ease of grain boundary sliding;

e) Increasing ease of recrystallization.

They said that while the b.c.c. structure has 48 slip systems, f.c.c. has only 12. Furthermore, selfdiffusion takes place much more rapidly in b.c.c. than in f.c.c. hence b.c.c. is more ductile than f.c.c. at high

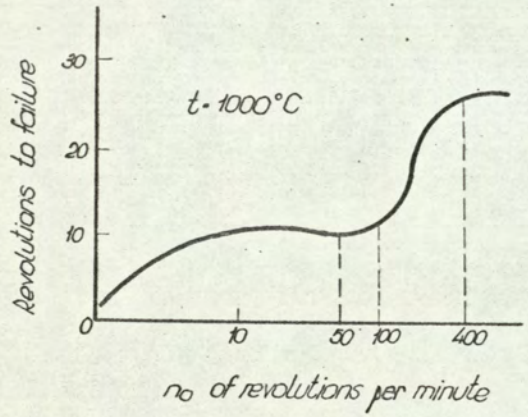

Fig. 2.30 Variation of number of revolution to failure against number of revolution per minute at 1000°C (48).

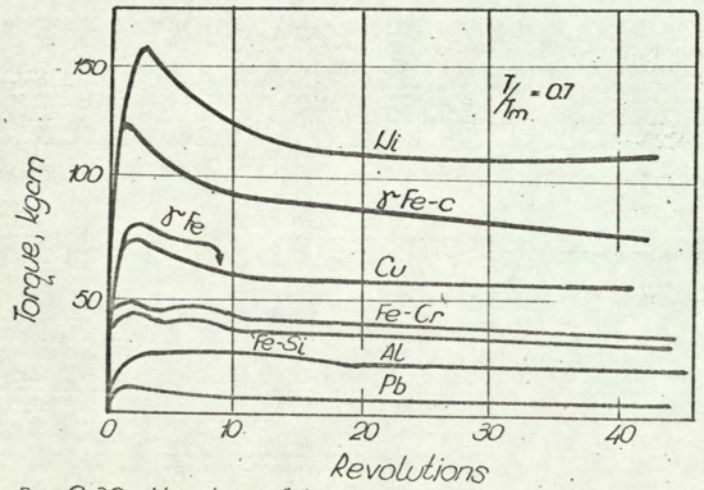

Fig. 2.32. Variation of torque against number of revolutions to failure at 0.7 Tm for more metals (51).

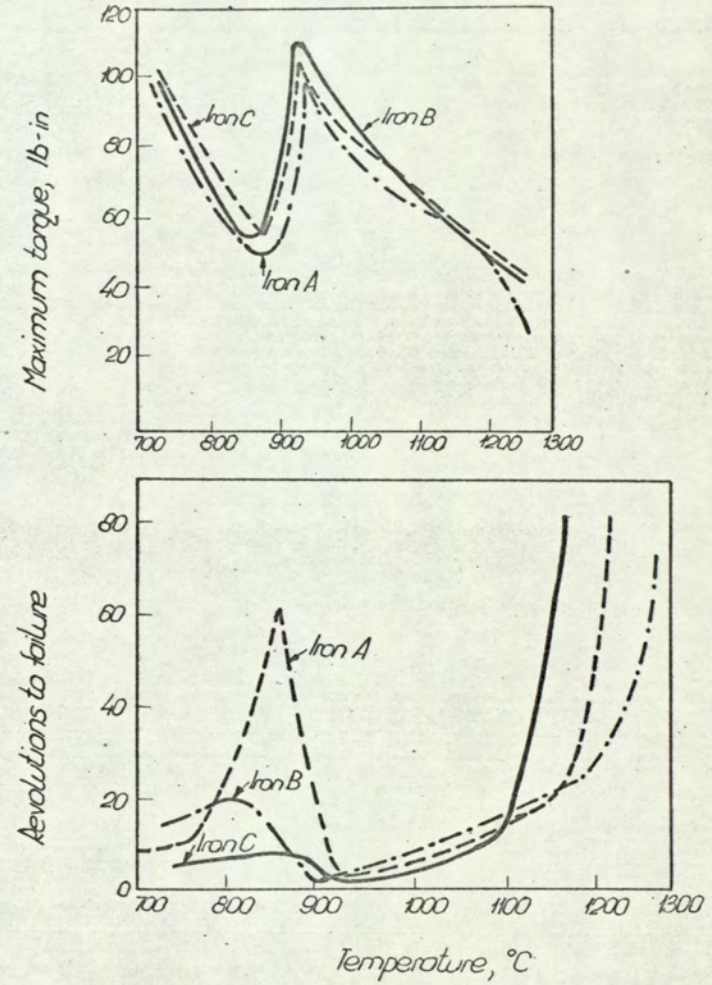

Fig. 2.31. Variation of torque and number of revolutions to failure against temperature for three pure irons (50).

temperatures. Giving a great importance to selfdiffusion in relation to its influence on ductility, they proposed the equation:

$$P = SD^{\frac{1}{2}}f(x). \qquad 2.16.$$

where P is the ductility of a given material;

D - selfdiffusibility corresponding to a given condition of deformation;

S - constant (approximately to the number of slip systems);

f (x) - a function which depends of other factors, not yet defined.

They suggested that steels with low content in carbon, because they have a quite good ductility and low strength, can be deformed in the ferritic condition, possibly more economically than in the austenitic condition.

Reynolds and Tegart (50) investigated the deformation behaviour of pure irons at elevated temperatures. In their work they used a high purity Swedish iron (A), a high oxygen Swedish iron (B) and Armco iron (C), which were deformed in the temperature range 700 - 1200°C. For deformation they used 66 rev/min. The curves of torque and number of revolutions to failure against temperature are given in Fig. 2.31. Both curves have about the same shape, but while there is no major difference in torque for the three irons, there is an appreciable difference in number of revolutions to failure.

The ductility curves were considered as divided into three regions:

1) ferrite region, where after deformation a marked substructure was present and the ductility was not so high. For iron A, when recrystallization was evident the ductility markedly increased.

2) The ferrite and austenite region, where the ductility fell to values less than either feritic or austenitic conditions.

3) The austenite region where the deformation was about the same as ferrite, particularly at the low temperatures, where an even substructure was observed.

One important aspect of their work is the fracture. In iron A at 750°C the cracks appeared on the surface. At 813°C external cracks were less, but internal cracks became more pronounced. At 850°C surface cracks disappeared and internal cracks were found in the centre of specimen, with severe cavitations near shoulder. These cracks were thought to be associated with $\alpha \rightarrow \gamma$ transformation. Making careful examination they observed at 863°C that the amount of γ was greatest at the middle of radius. At 973°C intercrystalline fracture was observed. At 1128°C the cracks were transverse to the axis and were most dense at about $\frac{3}{4}$ radius. At 1168°C cracking diminished and

voids appeared. At 1206°C large voids elongated transversely to the axis were present in a helical shell at mid-radius while voids were almost absent at the centre and surface.

On iron B the cracks and voids were about the same as in iron A. At 750°C many cracks were wholly or partially along grain boundaries except for a few associated with inclusions. Examination showed that the large holes in other regions were in boundaries and associated with some inclusions.

In Armco iron (C) at 936°C the cracks appeared at the surface. At 1206°C they disappeared from surface and appeared inside. At 1253°C large cracks appeared in the middle of specimen.

They concluded that severe cavitation which appears in γ range does not seem to be associated solely with inclusions because both irons A and C showed cavitation although they exhibited large differences in inclusion content. They concluded that further work is necessary to elucidate the mechanism of cavity appearance during hot-torsion testing.

Another very important aspect which they also investigated was the influence of specimen size on the number of revolutions to failure. They used specimens with various diameter keeping the ratio l/d constant, and with various ratio l/d keeping the diameter constant.

The results obtained on specimens with the ratio l/d variable for several temperatures are given in Table 2.VI and it can be seen that there is no clear relationship between the ratio l/d and the number of revolutions to failure.

Hardwick and Tegart (51, 52) studied the structural changes during deformation of copper, aluminium and nickel including dimensional changes during twisting and the connection between torque and structure. Making tests at 0.7 Tm they showed the variation of torque against the number of revolutions for more metals, illustrated in Fig. 2.32. From this figure can be seen the large differences in behaviour

Table 2.VI.

Number of revolutions to failure for various temperatures and ratios l/d (50)

Temperature °C	Relative size.		
	3	4	6
1050	2.8	3.4 (3.6)	10.0 (5.6)
1085	6.2	13.0 (9.3)	19.0 (12.4)
1150	30.2	39.0 (40)	45.5 (60)

The number from ( ) is proportional .

Studying the structure of specimens quenced at the peak of torque they found that aluminium showed a substructure formation starting from outside and going on towards inside. At the surface, grain boundaries became indistinct from subgrain boundaries. On the other hand copper showed at

the surface deformed grains and small recrystallised grains formed along grain boundaries and in the deformation bands. Nickel appeared to represent an intermediate behaviour between aluminium and copper, showing both subgrains and new recrystallised grains.

These phenomena were continuous during deformation and enlarged until the entire specimen section became similar to the outside.

Making tests at various temperatures they concluded that the structure changed in about the same manner as at 0.7 Tm, and torque had almost the same shape. For copper a pronounced peak appeared at low temperature, which decreased if the temperature was raised. The peak for aluminium was very small and a steady state was reached very rapidly. Nickel showed peaks at every temperature (Fig. 2.33). It was observed that the peak of torque was closely connected with the restoration processes, and its size is an indication of the ease with which restoration can occur. For aluminium where dislocation climb is rapid the initial work-hardened structure is already modified into an imperfect substructure by the time the maximum torque is reached. Since restoration is rapid, only a small peak is observed. With nickel, where dislocation climb is slower the initial work-hardening cannot be eliminated sufficiently rapidly by poly gonisation and enough energy is available to initiate recrystallization, which replaces the original polygonized grains by fine equiaxed ones. With copper

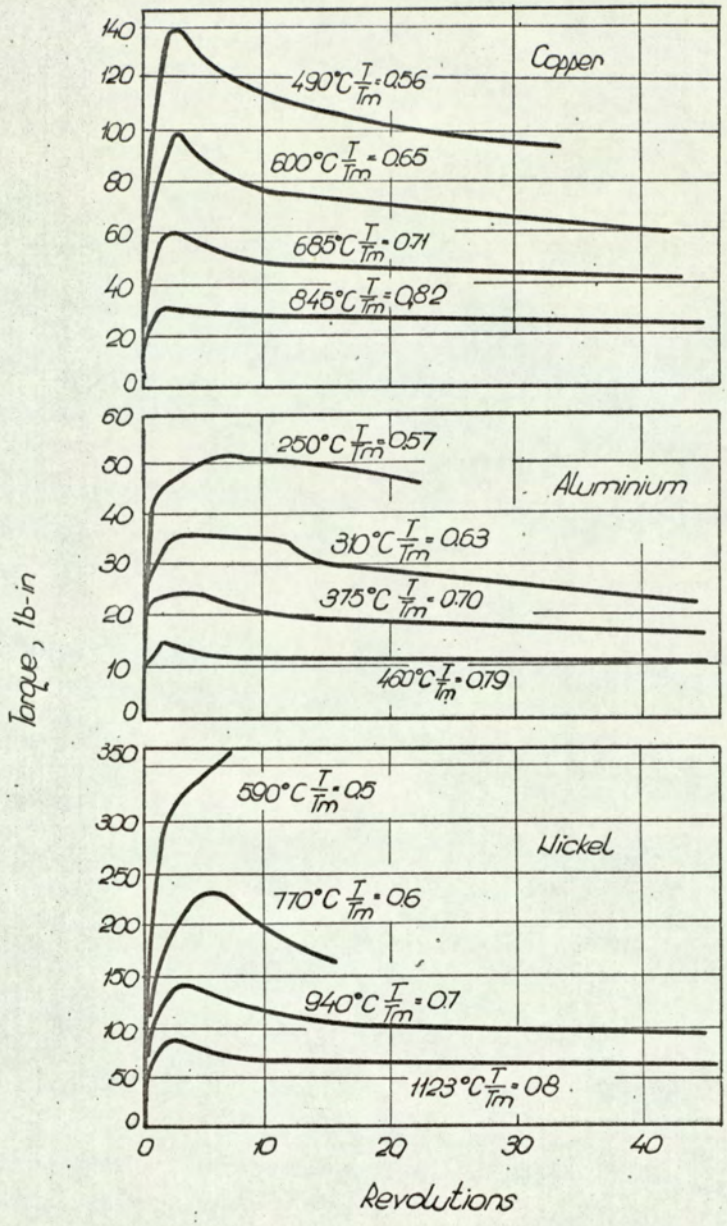

Fig. 2.33. Variation of torque against number of revolutions to failure at various temperatures (62)

dislocation climb is so slow that poligonization is not significant and recrystallization is operative immediately, hence both copper and nickel both show peaks in torque.

The same authors also dealt with changes in axial force during deformation. Axial force for 0.7 Tm and 66 rev/min, for various metals and alloys is shown in Fig. 2.34. For most materials axial force is compressive at the beginning of deformation and after a few turns if changes into tension, the most notable exception being aluminium for which axial force remains compressive throughout deformation. Deforming specimens freely resulted in change in length, in a linear manner with number of revolutions at a given temperature, as is shown in Fig. 2.35 for carbon steel. Conclusions reached were that axial force or change in specimen length is not due to geometric effects but is dependent upon material and temperature.

Rossard and Blain (53, 54) studied the influence of temperature and strain rate on the resistance to deformation by torsion. They used a machine capable of large variations of strain rate. In this way they obtained a series of curves torque-revolutions for various temperatures and strain rates. For a steel with 0.25% C deformed at 1200°C the curves torque-revolutions are shown in Fig. 2.36, where it may be seen that torque for 690 rev/min is about 5 times bigger than for 0.30 rev/min.

Starting from Nadai's equation of the form

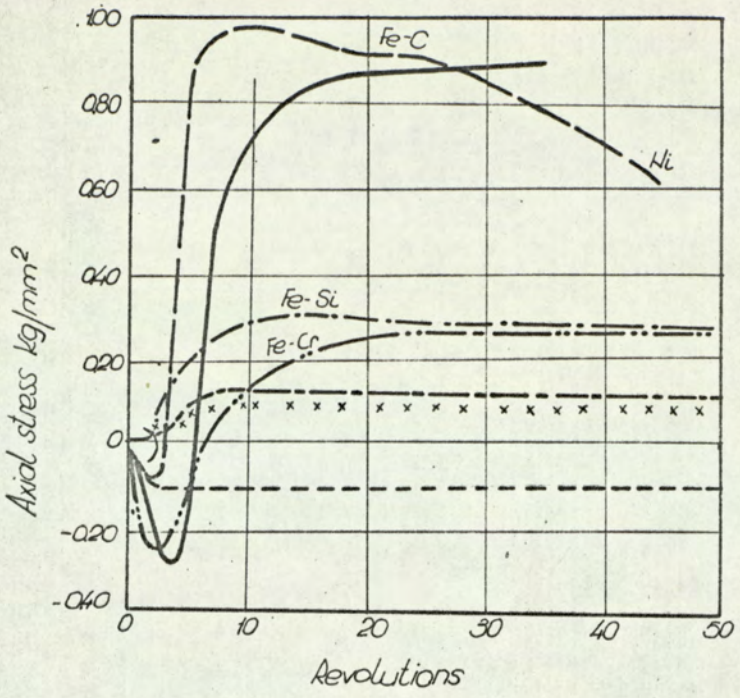

Fig. 2.34. Variation of axial force against number of revolutions to failure at 0.75 T_m (51).

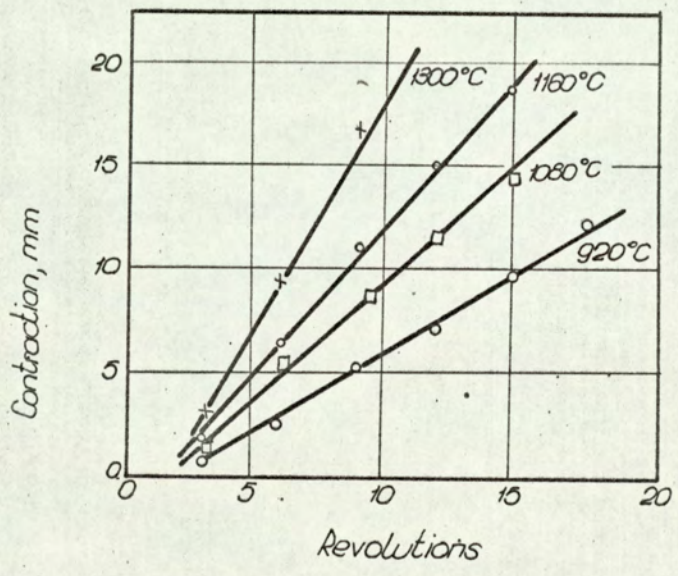

Fig. 2.35. Variation of specimen length against number of revolutions at various temperatures for carbon steel (51).

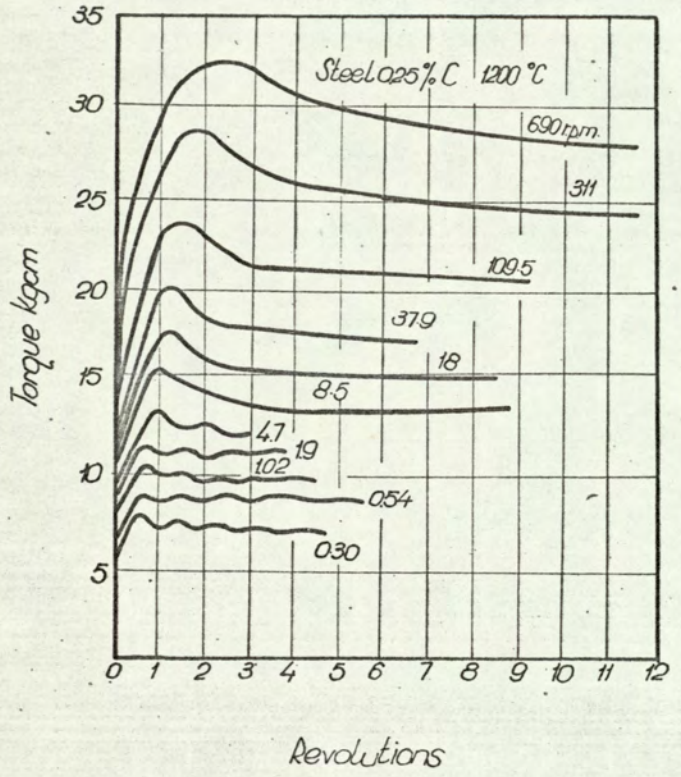

Fig. 2.36. Variation of torque against revolutions for various strain rates (53).

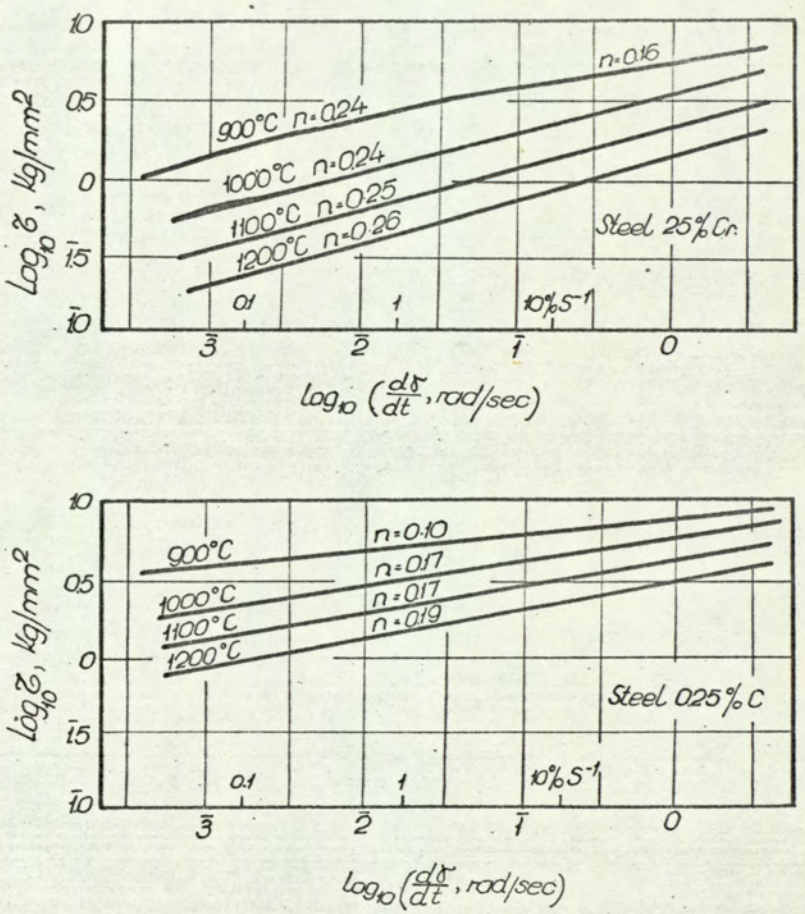

Fig. 2.37. Variation of shear stress with strain rates for two steels deformed at various temperatures (53).

$$\tau = \frac{1}{2\pi R^3}\left(\theta \cdot \frac{dT}{d\theta} + 3T\right)$$

2.17

where τ is shear stress;

R - specimen radius;

T - torque;

θ - angle of twisting,

and accepting that torque varies with strain rate after a power low of the form

$$T = To \left(\frac{d\theta}{dt}\right)^n \qquad 2.18,a$$

respective $\tau = \tau_o \left(\frac{d\gamma}{dt}\right)^n$ 2.18,b

where To and n are constants for a given temperature;

$\frac{d\Delta}{dt}$ - true strain rate by torsion, they gave an equation for calculated shear stress τ from torque T of the form

$$\tau = \frac{3+n}{2\pi R^3} T. \qquad (2.19)$$

Plotting curves of log τ against log $\frac{d\gamma}{dt}$ for a few steels they found an almost linear relation. For a steel with 0.25% C and for another with 25% Cr these curves are shown in Fig. 2.37. While n is constant for the carbon steel at a given strain rate at each temperature, for the chromium steel n is constant only at temperatures of 1000 - 1200°C; at 900°C it changes its value between 1 and 10% sec^{-1}. Another important aspect is shear

stress variation against temperature for three steels deformed with two different strain rates (Fig. 2.38)

These authors also studied structural changes during deformation by torsion and showed that the structure is affected by strain rate and temperature in opposite ways. The lower the temperature and the greater the strain rate the smaller are the resulting grain sizes.

Ormerod and Tegart (55) taking Rossard and Blain's equation (2.19) calculated the value of n for superpure aluminium using a speed of 66 rev/min. They compared their results obtained by torsion with those of Alder and Phillips obtained by compression, which are in quite good agreement as shown in Table 2.VII.

Table 2.VII. Values of n derived from torsion and compression tests for aluminium (55)

Temperature oC	Torsion	Compression
195	0.02	0.03
280	0.07	0.06
390	0.10	0.10
450	0.13	0.125
480	0.17	0.14
550	0.18	0.155

Conclusions

1) In the torsion test when the specimen is kept fixed its dimensions remain about the same throughout deformation, hence, for a given specimen size and number of revolutions per minute the deformation occurs

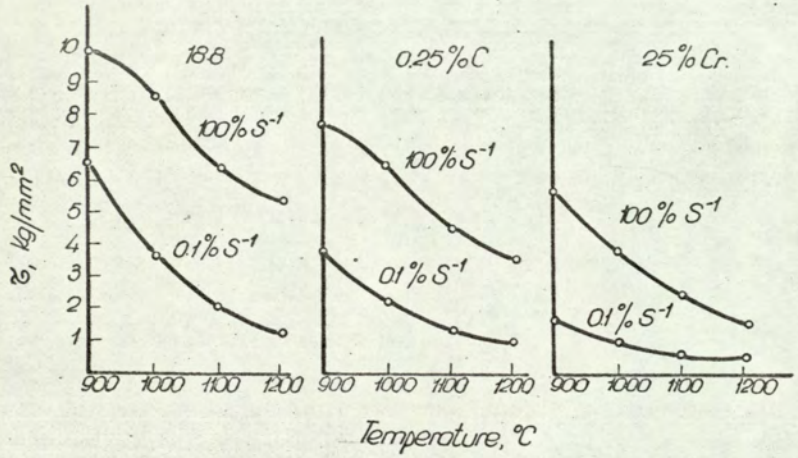

Fig. 238. Variation of shear stress with temperature for three steels deformed with two strain rates (54).

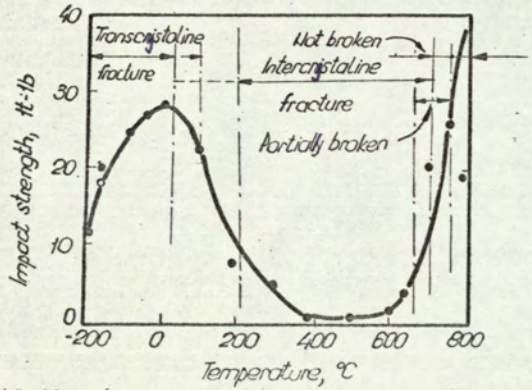

Fig. 240. Variation of impact strength against temperature of high-tensile beta-brass (51).

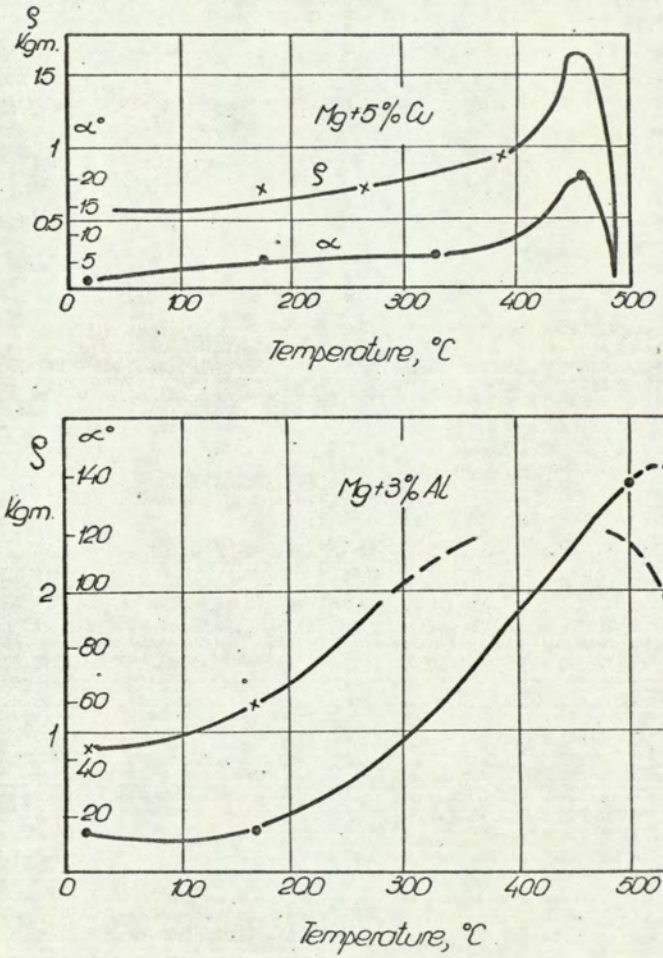

Fig. 239. Variation of energy to facture ϱ and angle of bending α with temperature (10).

with an approximately constant strain rate along the specimen length provided that the temperature is constant. Strain varies across the specimen section, but in a manner that is easily established. Because of this particular feature this method of testing is very suitable for studying the structural changes during deformation.

2) The ductility is affected by strain rate and temperature in different ways for different materials. If the strain rate increases at low temperature the ductility usually increases and the reverse happens at high temperature. At a given temperature ductility is affected by strain rate and for some materials there may be critical points where the ductility changes sharply. Ductility also alters with temperature in a complex manner, hence it is not easy to use for its calculation equations like 2.16 or else such equations will have very limited application .

3) A power law is suitable to relate strain rate and resistance to deformation which gives results comparable with those obtained by other types of testing.

4) An axial force appears during deformation which depends on the material and temperature. Due to this force a complex stress system exists during deformation which differs from metal to metal and from one temperature to another. It is not yet established which factors produce axial force and how it affects the ductility

measurement. It is supposed that axial force may alter the true hot workability measurement which makes comparison of results difficult for various materials and temperatures.

5) Fracture starts in a very complex way. In many cases the cracks appear first inside where the rate of deformation is not maximum. Although there are some explanations for this they cannot yet be regarded as satisfactory because cracks do not always appear within the specimen for all materials even when they have tensile forces of the same order of magnitude. This kind of cracking makes the results obtained by torsion test a little uncertain and show at the same time the necessity for further work to elucidate this aspect.

2.2. 4. Notch-bend impact Test.

This type of testing has been used for studying the brittleness of materials at room temperature for many years. Bunting (56) was one of the earliest who used it for studying the brittle temperature range in brass. He showed that a range of temperature where the brass is brittle exists and it varies with the copper content.

Portevin and Bastien (10) used this test for studying the forgeability of light and ultralight alloys (along with other types of testing). They measured both the energy required for breaking the specimen and the angle of bending and found a connection between them, showing a maximum at the same temperature for alloy Mg-5% Cu, but at

a different temperature for alloy Mg-3% Al (Fig. 2.39).

Bailey, Donald and Samuels (57) used the charpy impact test for studying the impact strength characteristics of high tensile beta-brass in temperature range between -195°C and 800°C and Fig. 2.40 shows the impact strength value against temperature. Making metallographic studies they observed that up to 200°C the fracture was transcrystalline, from 200° to 650°C intercrystalline, and over 650°C elongated grains were seen near the region of the fracture. There appears to be a close connection between impact strength and type of fracture.

Moore, Whishart and Lyon (58) carried out experiments on steels at low temperatures (from -40 to 70°F) using slow bend and impact bend. Some of their results are given in Table 2.VIII from which it can be seen that while for some materials there is no big difference between the energy required to fracture with either the slow or the impact test, for others there is a difference of up to about 50%.

Crussard et al (59) investigated many aspects of this type of testing, but at room temperature only. One of their major aspects was the relationship between the type of fracture, angle of bend and ductility. In most cases, the specimens which broke with low impact strength showed a granular fracture and ductile specimens which required high impact strength showed a fibrous fracture, but it is

TABLE 2 VIII

Material.	Energy for fracture ft-lb							
	Slow bend test				Impact test.			
	70 F	10 F	-20F	-40F	70 F	10 F	-20F	-40F
SAE 3135 heat treated	8.90	7.27	7.27	6.78	11.90	7.80	8.70	8.50
SAE 3135 cold rolled	11.60	6.10	4.72	2.95	9.50	4.00	3.20	3.40
SAE 1020 heat treated	90.50*	97.30*	91.90*	94.20*	108.70*	117.70*	118.70*	119.30*
SAE 1020 cold rolled	10.50	10.21	8.31	6.04	10.00	4.40	4.20	4.20
SAE 1095 heat treated	12.10	10.36	9.74	10.86	17.80	14.30	8.60	13.50
60-40 Brass cold drown	7.71	8.96	8.91	9.50	12.30	14.90	16.20	15.00
Copper cold drawn	51.40*	56.27*	56.70*	57.60*	62.70*	73.40*	78.60*	75.80*
Duraluminium 17-st as received	13.00	13.57	13.37	13.82	18.10	18.90	20.10	19.60

* Specimens did not break in two.

also possible to obtain high impact strength associated with an almost totally granular fracture. It appeared that the poor correlation between ductility and the type of fracture is because the difference between brittle and ductile specimens does not lie in the propogation of cracks but in their initiation. In this way they divided total energy for fracturing into the energy necessary for initiation and the energy for propogation. For brittle specimens there appears to be a straight line relationship between the angle of bend and the impact strength required for fracture, of the form

$$k = 0.9 + 0.38\alpha \qquad 2.20$$

The first term from above equation (0.9) is considered to be not directly connected with the breaking of the specimen, so if it is neglected, it could be argued that brittle fracture requires energy only for initiation of the crack (which corresponds to an angle of bending α) and not for its propogation, while ductile fracture requires energy for both stages of fracture. For ductile fracture however, it is not easy to distinguish the two energy values.

Green and Hundy (60) said that this test is so complex that even a qualitative analysis is difficult because the behaviour of the specimen depends on so many factors, e.g. (i) the shape of the specimen and the system of loading used;

(ii) elastic and plastic properties of the metal and the laws governing its brittle and ductile fracture; and

(iii) speed and temperature at which the tests are carried out.

They showed that the basic general conditions which determine ductile and brittle fracture are still largely unsolved. The various theories proposed conflict with each other and consequently all current ideas are somewhat uncertain. What is clear is that there are two kinds of transitions which can be observed in steels as the temperature of testing is reduced: fracture transition involving a change from fibrous to cleavage type corresponding to a modification of the mode of fracture propogation, and the ductility transition corresponding to a modification in the mode of fracture initiation.

Conclusions

This type of testing is used for hot-workability measurement but it has one great disadvantage; it does not measure directly the capacity of metals to deform, although there seems to be some connection between the angle of bending (which might be a direct measure of ductility) and the energy required for fracture (which is a measure of impact strength). Energy required to fracture depends on both resistance to deformation and ductility for a given temperature.

When in addition the complex mechanism of fracture is considered it is not surprising that it is difficult to relate the energy required to fracture and the ductility.

2.2.5 Other types of test.

For evaluating the ductility Martin and Beiber (61) suggested bending a rectangular bar to an angle of 180°, and the temperature range suitable for forging is denoted by the appearance of cracks in the region of bending. This type of test gives a qualitative information in the sense of 'go' or 'not go' but it is not suitable for evaluating quantitative data.

Josefsson et al (62) used impact bending of unnotched specimens through an angle of about 60°. The degree of brittleness was assessed by the number and intensity of cracks which appeared after bending, for which they used a six point scale. This method has the advantage of simplicity but it may be expected that for some materials no cracks will appear and a quantitative measurement will not be possible.

Chizikov (63) proposed a method of testing by rolling a wedge bar. The section of the specimen varies proportionally and the point of critical reduction (where first crack appears) is used as a criterion of hot workability.

Henning and Boulger (64) proposed a test technique consisting of forging a wedge specimen. The final forged specimen contains zones with various degree of

deformation from zero to a maximum value. This specimen provides quantitative data for hot-workability measurement and may also be used for studying the influence of deformation and temperature on structure.

2.3 Summary of hot-workability tests.

From the above review of literature a few main conclusions can be drawn:

1) The deformation process is a very complex phenomenon and materials have critical points for various factors which may or may not have some connection with each other. Thus, for example;

a) The energy required for producing a certain amount of deformation by tensile test is about constant on increasing strain rate up to a particular value, then it decreases quite sharply without any marked alteration in ductility. This critical value of strain rate is different for different materials as well as different conditions of the same material (Fig. 2.5 and 2.6).

b) Yield stress, maximum stress; elongation, reduction in area and the energy required for fracture by tensile stress are affected by strain rate in different ways for various materials. Even for the same material in the same state, the ratio of dynamic average to static average is different for various characteristics (Table 2.1).

c) The ratio of energy required for fracture by impact bending to that of slow bend varies in a complex way for

for various materials at a given temperature. For some materials this ratio is bigger than 1, for others smaller (Table 2.VIII). Furthermore the variation of impact strength with the temperature is different than the angle of bending. There is a range of temperature where the angle of bending increases and the impact strength decreases (Fig. 2.39).

d) The ductility is affected by strain rate in a different way, depending on temperature and strain rate value, in some ranges of strain rate a small temperature change producing a great change in ductility (Fig. 2.10), and similarly a slight change in strain rate may have the same effect (Fig. 2.30).

Thus it appears that materials behave differently in different types of testing as well as in various conditions of testing. Two main conclusions may be drawn from this:

First, it is not possible to compare quantitatively results obtained by using a certain type of testing with those obtained by using another test; and second, that data obtained in some conditions of testing may differ more or less from those obtained in industrial practice if the conditions of testing differ from those used in practice.

2) Each type of test has some specific character created by the deformation process which then affects the behaviour under subsequent deformation. Thus for example

due to necking in the tensile test a change in the stress system occurs and hence also in real value of strain rate; due to barrelling in the compression test a change in the uniformity of deformation and stress system again occurs. The barrel-shape depends largely of friction which in turn depends on other factors such as strain rate, temperature, lubrication, surface quality etc. Furthermore, by increasing the ratio $\frac{d}{h}$ during deformation the real stress necessary to deform the specimen increases too. Thus, in this test both stress system and their values change very much during deformation, which cannot be easily controlled and which will certainly affect the ductility. Due to axial force which appears during twisting in the torsion test (compression or tension) a complex stress system is present too, which is also likely to influence the ductility measurement.

All the above factors affect the ductility in different ways. Increasing the ratio $\frac{a}{r}$ in the tensile test, and increasing tensile force in the torsion test will decrease the ductility; increasing the stress value inthe compression test and applying compressive force in the torsion test will increase the ductility. Hence the conditions of testing may become better or worse if the degree of deformation increases.

On increasing the temperature the ratio $\frac{a}{r}$ in the tensile test seems to decrease, hence, from this point of view, the conditions of testing are better

at high temperatures. On the contrary, tensile force developed in the torsion test increases if the temperature rises, hence, the conditions of testing become worse if the temperature increases. Thus, it can be seen that the deforming conditions change in different ways in different types of test upon increasing the temperature. From these aspects it seems also that the results obtained with various types of test cannot be usefully compared.

3) The specimens break in different manner in each type of test. This appears more pronounced with materials having a well developed fibre structure. In the compression test the cracks appear at the specimen edge orientated usually in the direction of pressing. Thus, if the specimen is deformed in the direction of the fibre structure, then the cracks appear along it too. In the torsion test the fibre structure changes its direction in respect to the acting shear stress so that in specimens cut along the fibre structure, by its reorientation the cracks appear along it. Hence the anisotropy of material plays a more complex role at this test.

From the above considerations it can be seen that the anisotropy of materials manifests itself differently in respect to fracture for each type of testing.

In the light of the preceding discussion it would appear that the coefficients C_1, C_2, C_3, and C_4 from the equation 2.1 change their values in various conditions of deforming in a manner difficult to predict.

However, it may be supposed that the coefficients for tensile test and torsion test change least. It seems likely that the least change in coefficient would occur with the torison test if the axial force were zero or very small, but because this may show considerable variation from metal to metal and from temperature to temperature the tensile test is least affected.

From the above it is clear not only that a true comparison between the results, for hot-workability, obtained by various types of testing is not possible, but also that it is difficult to make a comparison between results obtained using a given test for various materials and even for the same material at various temperatures. For example, with a given material a peak for ductility at one temperature may be given by one test and at a different temperature using another. Lyons (65) showed such differences in results obtained by torsion and tension (Fig. 2.41), (although his results might be affected by other factors connected with the material history prior to testing), and the results obtained by Guenssier and Castro (66) and by Martin (9) show that differences in ductility due to this effect may exist. However, it may be concluded that the characteristics of the test largely determine where the peak of ductility occurs.

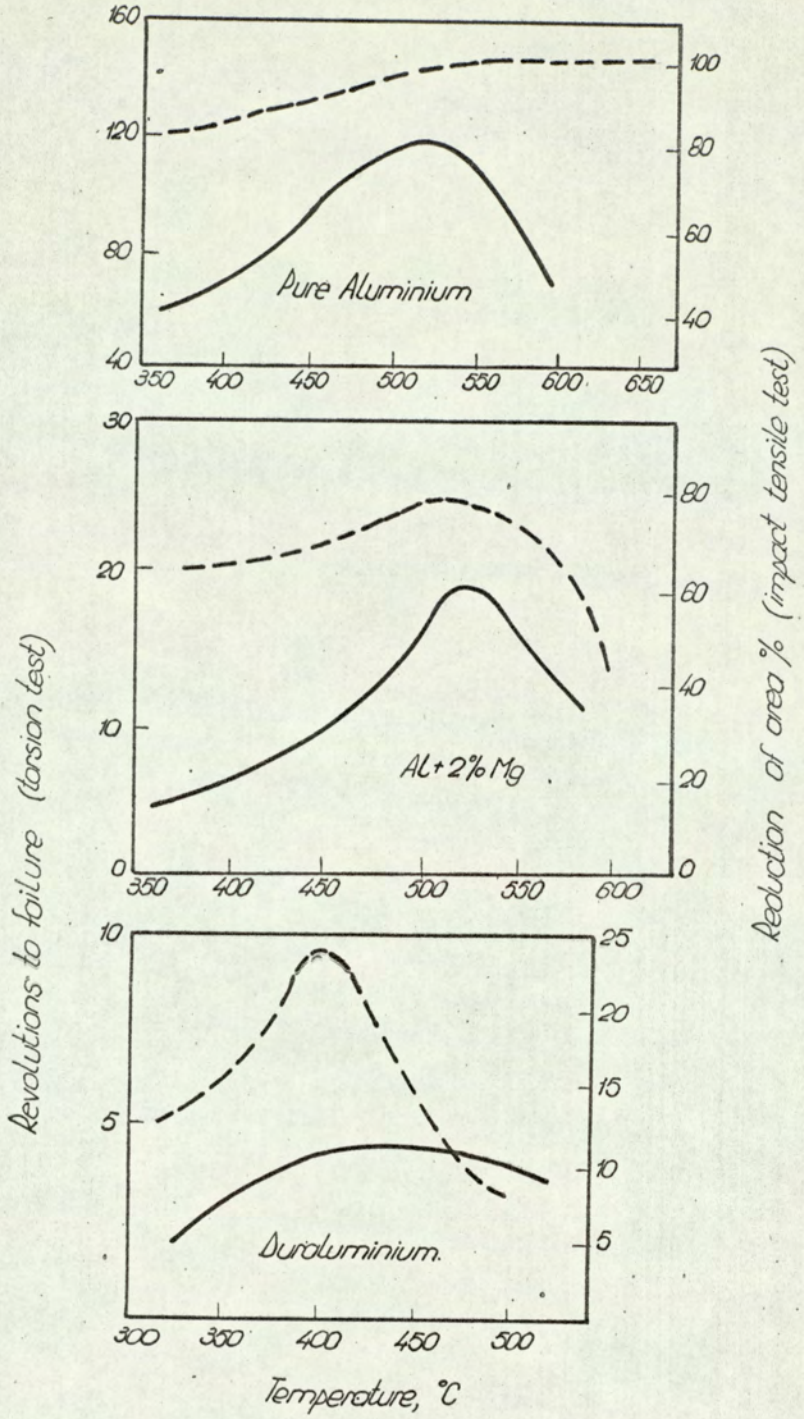

Fig. 2.41. Variation of ductility with temperature for various materials (65).
--- impact tensile test; —— torsion test.

It has been shown that it is not possible to keep constant conditions during deforming or if one parameter is changed whilst others remain constant. Therefore, in order to find a true peak of ductility by varying one factor it is necessary to take account of other factors which also change. In this way, instead of using the ductility value which is actually measured it is necessary to establish a relative value which takes account of the factors which change during testing. Such ductility might be calculated with an equation of the form:

$$P = Po + Cx \, f(x), \qquad (2.21)$$

where P is a relative ductility;

Po - measured ductility;

C_x - a proportionality coefficient;

$f(x)$ - a function composed from the factors which change their values during testing (ex: $\frac{a}{r}$ for tensile test, $\frac{d}{h}$ and $\frac{Dmax}{Dmin}$ for compression test, $\frac{Paxial}{Torque}$ for torsion test etc.).

Such equations like 2.21 cannot take account of all the factors which affect ductility, but if the deformation is at a given strain rate and temperature the main factors which change, which are characteristic for each type of testing, are taken into account. Only in this way is it possible to represent more or less correctly the variation of ductility with temperature and to compare the ductility of metals with each other.

Because each type of test has some characteristic, each has advantages and disadvantages with regard to hot

workability measurement. Tensile tests can show differences in behaviours between specimens cut along and across the fibre structure much better than torsion or compression. Compression tests can show superficial defects, being able to use specimens with the same diameter as rolled bar, aspects which cannot be investigated with tensile or torsion tests. The torsion test allows greater strains and more uniform deformation along the specimen length than tensile or compression tests and also provides an easy quantitative appreciation of the ductility. Impact bending detects the brittle range in materials much better than other tests. Thus, before choosing a method of testing it is necessary to bear in mind the main purpose. The best method of testing will certainly be that which approaches the practical operations. However, taking account of its advantages torsion testing may be regarded as a suitable method of testing for defining the temperature range with highest ductility, especially if some means of correction for axial loads could be established.

CHAPTER 3.

Some problems connected with torsion testing.

For a better understanding of this type of testing and for a better appreciation of the hot-workability measurement there is a need to clarify the following aspects:

1). The conditions giving rise to axial force and its effect on hot-workability measurement.

2). Why the fracture takes place in such a complex manner.

3). Why specimen size affects the ductility measurement.

The experiments described in the following pages were carried out in an attempt to solve the above problems.

2.1. Testing equipment, specimens and material used.

In order to be able to investigate the above aspects a special hot torsion testing device was necessary. This device had to have the following two main features:

a). to measure the torque and axial force which are present during deformation; and

b). to permit application of an external axial force in the conditions of combined deformation (torsion and axial force).

A machine was designed and built, as shown in Fig. 3.1. The solid shaft (1) fixed in the hollow shaft (4) by means of the axial bearing (3) and the nuts (2) may rotate with no axial movement with respect to the hollow shaft (4). The hollow shaft (4) may slide axially in the supports (5) on the bearings (6). On the solid shaft (1)

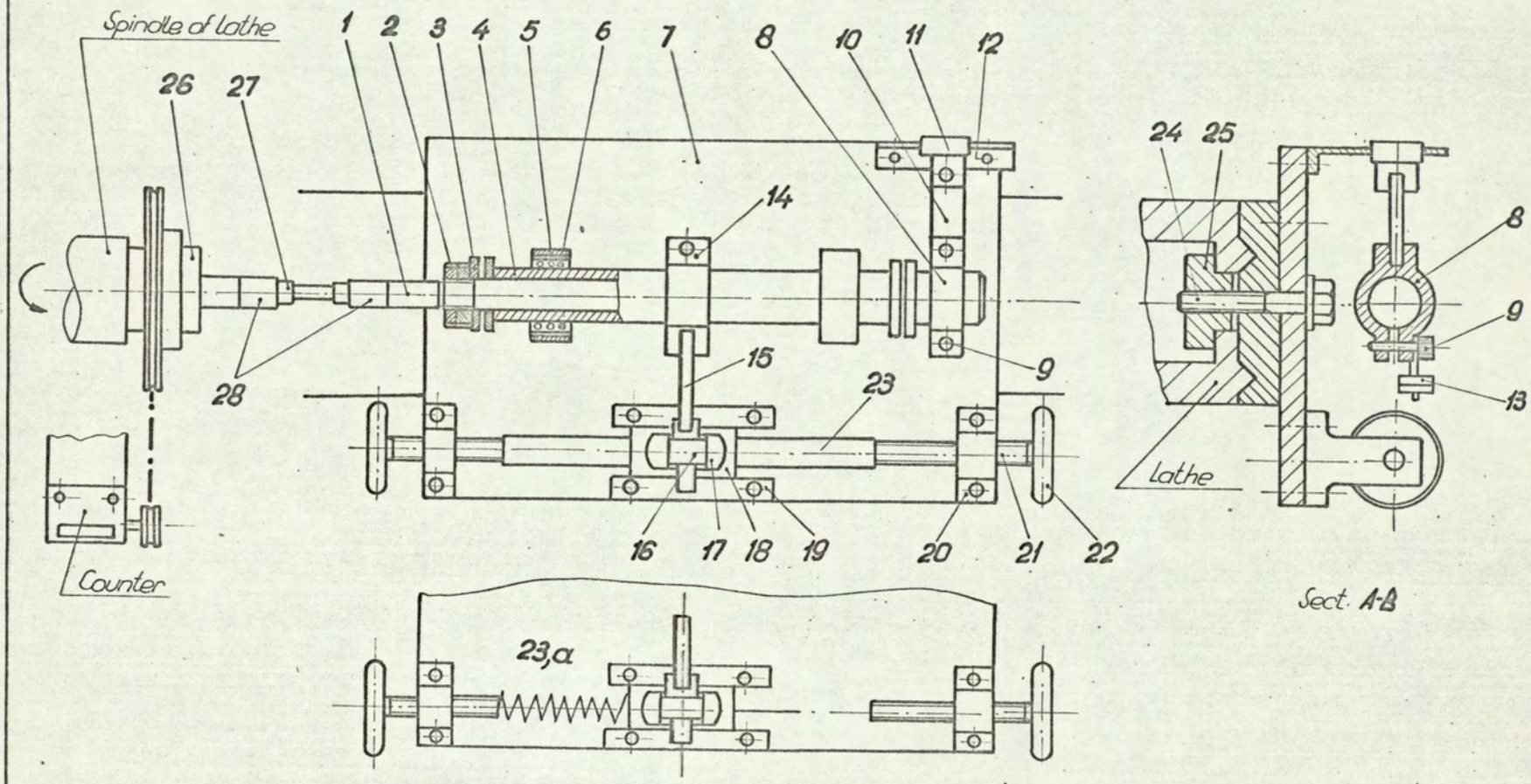

Fig. 3.1. Function sheme of the torsion device.

a circular clamp (8) is fixed, with the bolt (9) which holds the beam (10). At the other end of the beam (10) there is a ball race(11) which may easily slide along the support (12). For balancing two rings (13) are used, fixed at the opposite side of the clamp (8). Strain gauges are attached to the beam (10) so that by its deflection the torque may be measured.

To measure axial force a second beam (15) is clamped on the hollow shaft (4) at the end of which is a bearing fitting into a housing (17) free to rotate in the support (18). This support is able to slide parallel with the spindle (L) between two guides (19) fixed onto the base plate (7). Two supports (20) are mounted at the ends of the base plate (7) aligned with the bearing support (18) through which pass screwed rods (21) operated by handwheels (22). By adjusting these screw attachments (21) the support (18) may be fixed in a desired position by using tubes of fixed length(23) or forced in one direction (or the opposite) by using a compression spring (23, a) in place of one of the tubes (2.3). In Fig. 3.1 the detail showing (23a) is the arrangement used to apply tensile forces to the specimen; to apply compression the spring would be transferred to the right hand side.

The device was designed for a torque of 400 kg cm. max and an axial force of up to 300 kg. and was mounted on a lathe in place of its sledge so that it could be fixed in

a desired position along the lathe bed with the bolts (24) and the pieces (25).

The specimen (27) is mounted for testing in the spindle of the device and the lathe shaft (26) by using two threaded grips (28) made from austenitic steel.

This apparatus has the following advantages:

1) It is simple in operation.
2) The specimen may be easily changed.
3) The accuracy of measurements is affected only by the forces which appear in the bearings.
4) Because the support (18) may be moved by using the bolts (21), its position can be regulated for eliminating axial force which appears into specimen during heating, so that the test can be started with no axial force.
5) By using a spring for creating an axial force it is a simple matter to obtain various values without other equipment. Furthermore, during deformation if the specimen lengthens axial force exerted decreases.

From the equation

$$V = So\ lo = (So + \Delta S)(lo + \Delta l) \qquad 3.1$$

where So and lo are the initial dimensions of the specimen gauge;

ΔS and Δl - the variation of area and length during deformation,

ΔS as a function of Δl (considering an uniform elongation along the specimen gauge) is given by the equation:

$$S = - \frac{So.\Delta l}{lo + \Delta l} \qquad 3.2$$

For small value of Δl - comparing with lo - a linear variation of ΔS with Δl may be considered. The variation of the axial force ΔP given by spring when its length varies is linear too, given by the equation:

$$\Delta P = k.\Delta l \qquad 3.3$$

where k is the spring constant.

In these conditions, for small values of Δl, an approximately constant stress may be maintained during deformation. However, because for big elongation ΔS does not vary linearly and the elongation is not uniform along the specimen gauge, axial stress cannot be kept constant. Thus for instance for a specimen $\frac{3}{8}$ in dia and $1\frac{1}{2}$ in length deformed under an initial axial force of 200 kg (corresponding to an axial stress of 300kg/cm^2), after a deformation with Δl = 9mm a reduction in area of 30% was obtained and the real stress was 260kg/cm^2. This was the largest value for Δl and stress which were used. But because shear stress τ decreases during deforming (over some temperature range) the real value of σ/τ does not alter appreciably and this value has much greater significance. This advantage of uniformity only applies of course for tensile stresses that are externally applied.

One disadvantage is that using a unilateral beam for axial force measurement, creates an axial force of friction in the bearing (6) such as shown schematically in the Fig. 3.2. The value of frictional force is given by the equation:

$$P_f = 2\mu P_2 = 2\mu \frac{P_1 l_2}{l_1} = C.P_1 \qquad 2.4$$

where P_f is frictional force;

P_1 = axial applied force;

P_2 = normal force which acts in bearings;

l_1 = the spindle length (between bearings);

l_2 = the beam length;

μ = frictional coefficient;

c = constant.

Because $l_2/l_1 \approx 2.2$ and for such bearings $\mu \approx 0.015$ -0.02 it means that $C \approx 0.01$ -0.015. Hence this secondary frictional force does not alter the measured axial force more than 1.5%. Of course, this force could be eliminated by using two beams, but this would have considerably complicated the device and the slight gain in accuracy did not appear to be justified.

Torque and axial force are recorded by an ultraviolet recorder type SE 200 5 with a very rapid response. For low voltage supply necessary for the strain gauges, a stabilised power supply was used giving constant 0 to 1 amp and 0 to 15 volts.

For heating radio frequency current was used from a valve generator using a suitable coil

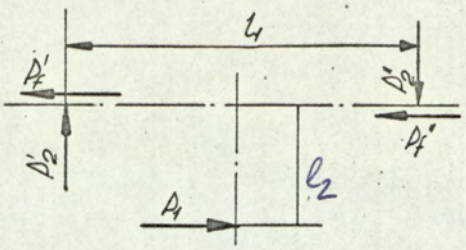

Fig. 3.2. The forces which act in device due to axial applied force.

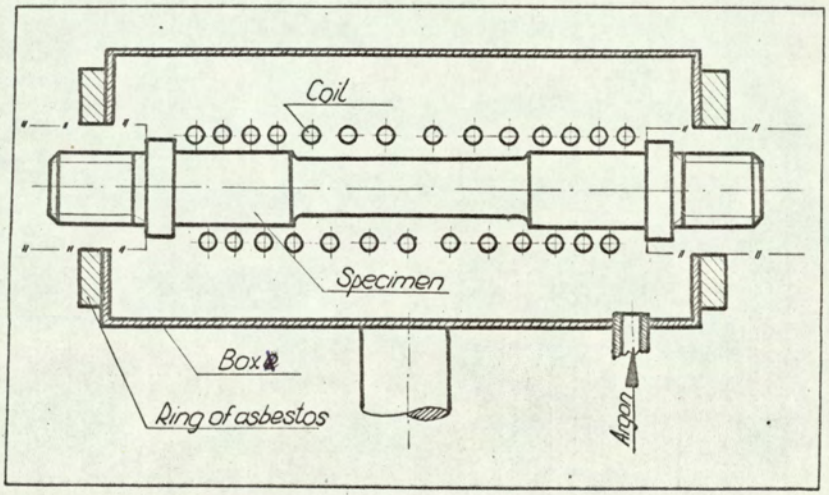

Fig. 3.3. Diagram of heating with high frequency current.

design for the specimen, and for some experiments a resistance furnace fitting onto the lathe bed.

The H.F. heater had an output power of 2.8 KVA and a frequency of 5000 c/sec. It was set near the lathe in order to have a minimum loss in current. The coil, made from flattened copper tube $\frac{1}{8}$ in dia, was $\frac{5}{4}$ in internal diameter, $2\frac{1}{2}$ in length and 16 turns. The distance between neighbouring turns is varied, being less at the specimen shoulder and greater at the centre of specimen gauge (Fig. 3.3). In this way it was possible to get a variation in temperature along the specimen gauge of less than 5°C. For regulating the temperature a variac controlling the valve anode current was used. The time for heating a specimen $\frac{3}{8}$ in dia and $1\frac{1}{2}$ in length was 40-50 sec. for 900°C, $1\frac{1}{2}$-2 minutes for 1100°C and $2\frac{1}{3}$ - 3 minutes for 1200°C (some specimens could be heated up to 1300°C in 3 - 4 minutes, but not for each type of steel). In order to reduce oxidation the coil was enclosed in a box through which argon was passed during heating and deforming (Fig. 3.3). This method of heating was very suitable up to temperatures of 1200°C, and especially for structural studies, because the specimens could be quenched immediately, at any period of deformation.

The resistance furnace provided temperatures up to 1400°C. In order to be able to obtain a constant temperature along the specimen gauge the furnace length was divided in three zones, each having a length of 2 in.

A variable resistance was connected to the mid-sector (Fig. 3.4). In this way the temperature along the furnace could be regulated (by cooling the mid-sector) with no more than 3°C variation along the specimen length (measured on the hollow specimen). The time for heating a specimen $\frac{3}{8}$" in dia and $1\frac{1}{2}$" in length was about 15 minutes for 900°C, 30 minutes for 1100°C and 60 minutes for 1300°C. For reduction of oxidation rate two rings of asbestos were put at the ends of furnace and argon was introduced as in the previous method (Fig. 3.4). For regulating the temperature a variac was again used.

Before starting the deformation the specimens were soaked at temperature for 2 minutes for high frequency heating and about 5 minutes for heating in furnace. No sensible difference in ductility was observed using the two treatments when duplicate tests were made under similar conditions.

For temperature measurement platinum / platinum 13% rhodium thermocouples were used. One thermocouple was connected to a galvanometer in the ultra violet recorder so that the temperature could be recorded during deformation. The temperature was measured at the fixed end of specimen, inside, near the shoulder (Fig. 3.5), the top of the hole being in the same plane as the edge of shoulder. Such specimens could be used only at lower temperatures. Over 1150°C if the hole was made near the specimen gauge, a greater deformation occured due to axial force, and the

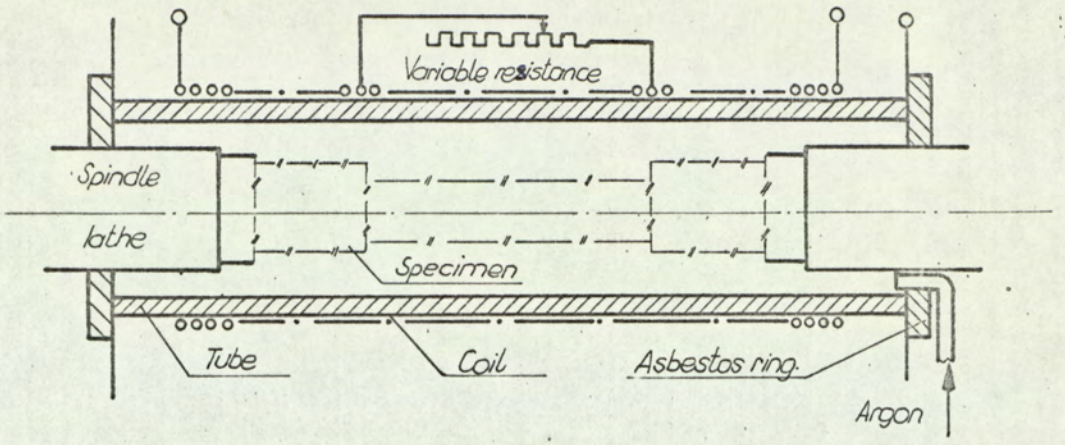

Fig. 3.4. Diagram showing furnace heating assembly.

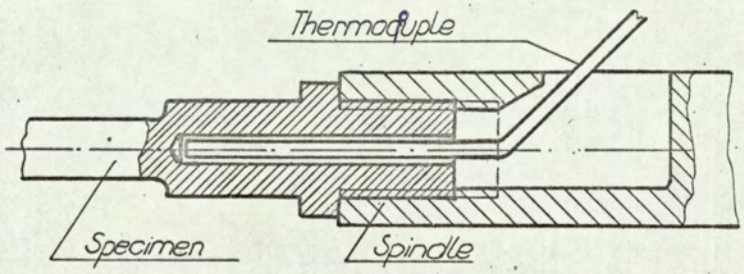

Fig. 3.5. Location of thermocouple within specimen.

specimen usually broke in this place. However, even this close to the gauge length the temperature seems to be lower than the temperature which exists along the specimen gauge during deformation.

For the number of revolutions measurement a counter was connected to the spindle of the lathe. For one revolution of the spindle five revolutions were recorded by counter. In this way the number of revolutions could be known with an accuracy of 0.2 turns. Using timing marks printed on the torque curves by the recorder the number of revolutions to failure were also recorded, and this was the most reliable guide to number of turns to failure as the lathe continued to rotate after the specimen had broken or rewelded, whereas the point of fracture was always revealed by a discontinuity in the torque curve. In Fig. 3.6 is shown a general view of the testing installation using high frequency current for heating. In Fig. 3.7 is shown the device for measuring the torque and axial force which appears in the specimen during twisting, and in Fig. 3.8, the coil used for heating in its box (in the open position). Fig. 3.9 is a general view in the conditions of using the resistance furnace for heating. The stress measuring device in this picture has a spring (23, 6) instead of tubes (23,a) in the position for applying an external axial force.

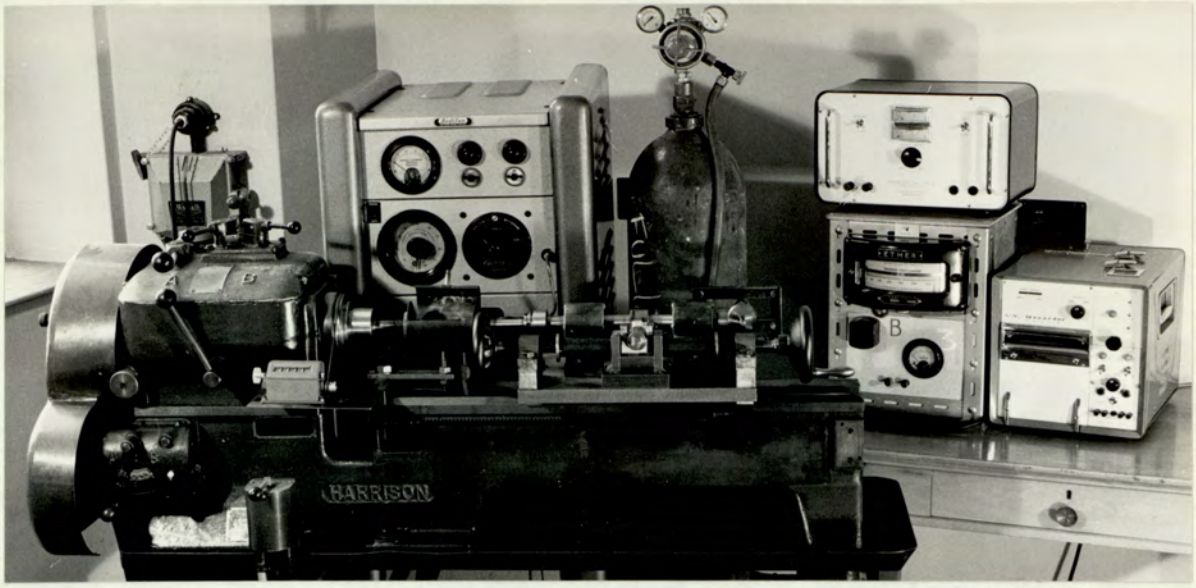

Fig. 3.6. General view of testing installation using high frequency current for specimen heating

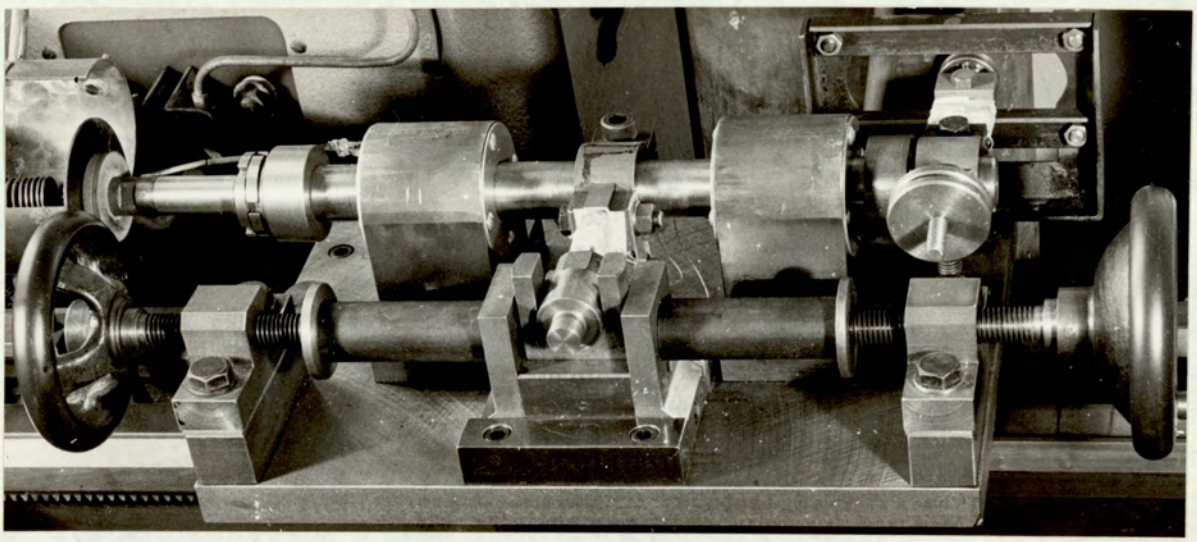

Fig. 3.7. Stress measuring assembly

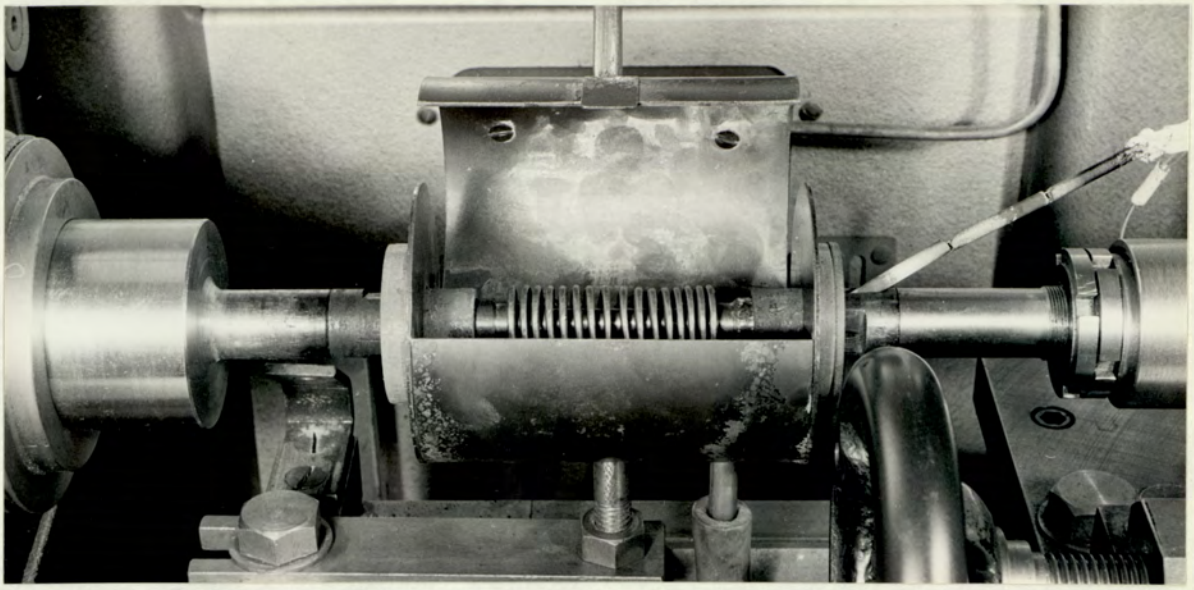

Fig. 3.8. High frequency coil in its box in open position

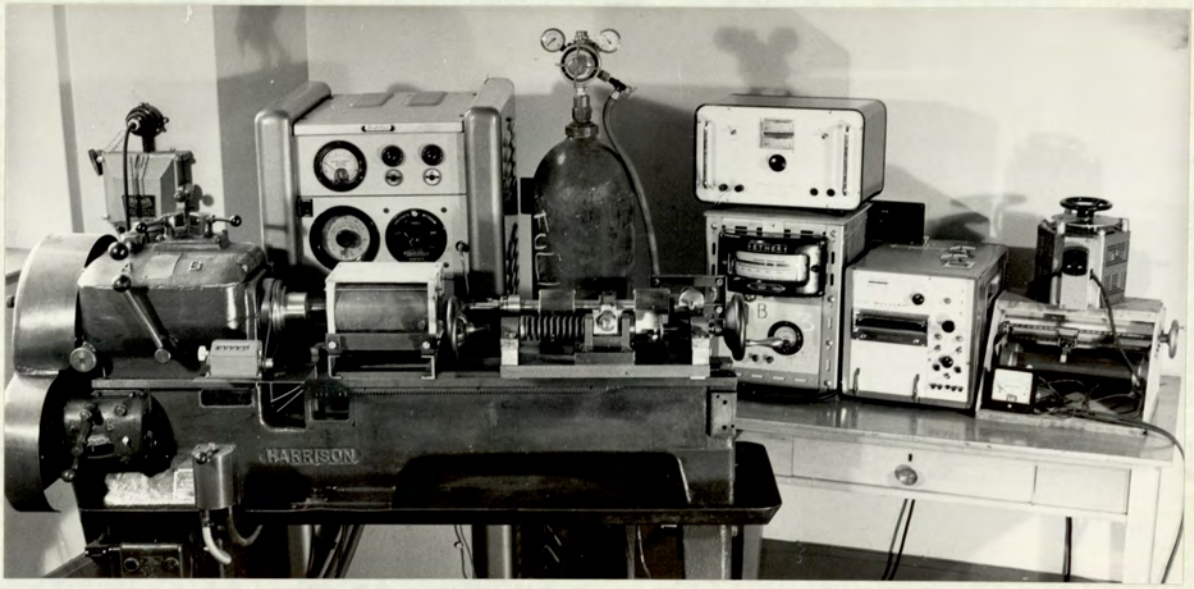

Fig. 3.9. General view of testing installation using furnace for heating

The calibration of torque, axial force and temperature measurement.

By using a free contact between beams and their supports no distortion arose during their deflection, and a linear relationship was obtained between the current variation due to deflection of the torque and axial force beams.

Using flat type strain gauges 1" long having a resistance of 70Ω, galvanometers type C300 with a sensitivity of 0.5 mv/cm and 0.13 MA/cm, and a current of 0.07A, at 3.4 volts, 1mm on the paper corresponded to 3 kgcm for torque and 2.2 kg for axial force.

For temperature recording a type C40 galvanometer was used with a sensitivity of 0.0016 MA/cm and 0.072 MV/cm. 1000°C was taken as a datum and by insertion of a resistance into the circuit 10°C was set to 1 mm on the chart between 700°C and 1300°C.

The accuracy measurements was about ± 1 kgcm for torque, 2% for axial force and ± 3° C for temperature.

In Fig. 3.10 is shown a diagram illustrating the variation of torque, axial force and temperature against time recorded by ultraviolet recorder for a specimen made from mild steel deformed at 950°C.

Specimens

Two types of specimens were used: solid and hollow (Fig. 3.11). Both types had various dimensions

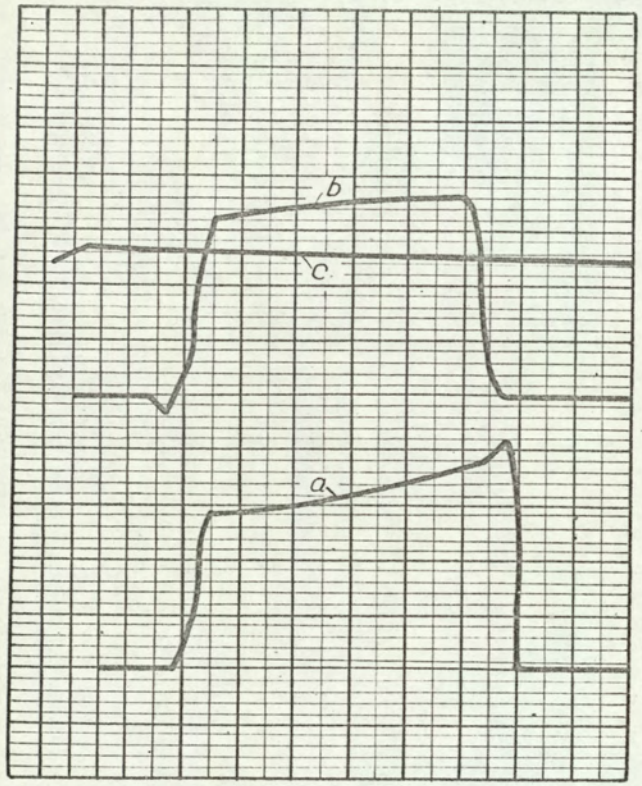

Fig. 3.10. Diagram recorded by ultraviolet recorder for a specimen made from mild steel deformed at 950°C with 75 rev/min. a - torque; b - axial force; c - temperature.

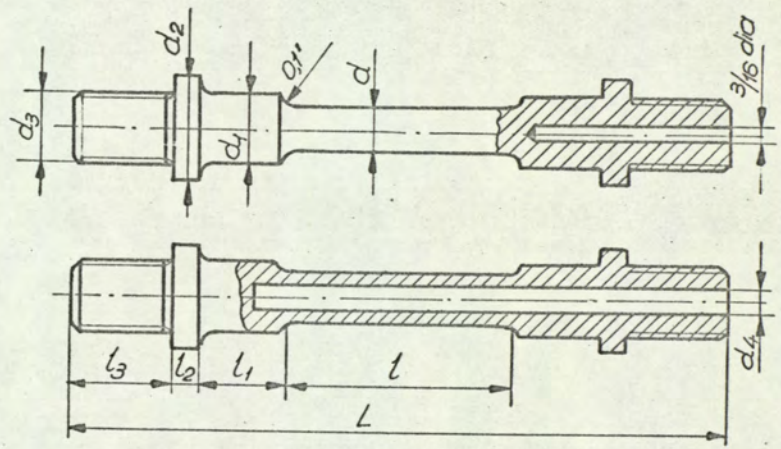

Fig. 3.11. Specimens used for torsion test.

according to the experiment. Their dimensions are given in table 3.1.

Table 3.1. The dimensions of the specimens showed in Fig. 3.11.

Nr.	d in	d_{in^1}	d_{in^2}	d_{in^3}	d_{in^4}	l in	l_{in^1}	l_{in^2}	l_{in^3}
1	1/4	7/16	5/8	1/2		1	7/8	1/4	5/8
2	1/4	7/16	5/8	1/2		1 1/2	5/8	1/4	5/8
3	3/8	1/2	5/8	1/2		1 1/2	5/8	1/4	5/8
4	3/8	1/2	5/8	1/2	3/16	1 1/2	5/8	1/4	5/8
5	3/8	1/2	5/8	1/2	1/4	1 1/2	5/8	1/4	5/8
6	3/8	1/2	5/8	1/2		1	7/8	1/4	5/8
7	3/8	1/2	5/8	1/2		1.6	5/8	1/4	5/8
8	3/8	1/2	5/8	1/2		2.5	5/8	1/4	5/8
9	7/16	1/2	5/8	1/2		1 1/2	5/8	1/4	5/8
10	5/16	7/16	5/8	1/2		1 1/4	5/8	1/4	5/8
11	.582	1	-	3/4	.437	2 1/2	5/8	-	3/4

Materials.

In order to be able to make comparisons several materials were used. Because differences were observed from bar to bar of nominallythe same material, for each experiment specimens used were made from the same length of the bar.

Mild steel and medium carbon steel were used in the form of 5/8 in dia. hot rolled bar. Another mild steel was obtained as ingot slice and was forged 30% and

75% reduction of area. For one experiment aluminium alloy 1 in dia rolled bar was also used. Some experiments were made using the material as received, for other the material was heat treated. Material compositions and their heat treatment before testing are given in Table 3.2.

Table 3.2 The content of the main materials used and their heat treatment before testing.

Material	Content %					Heat Treatment
	C	Mn	Si	S	P	
Steel 1	0.13	0.47	trace	0.047	0.068	Heated at 930°C, for 30 minutes, furnace cooled.
Steel 2	0.57	0.61	0.22	0.016	0.021	Hot rolled bar.
Steel 3	0.18	0.42	0.085	0.032	0.016	Ascast. After forging annealed as Steel 1.
Steel 4	0.20	0.46	0.026	0.036	0.062	Hot rolled bar
Aluminium	Commercially pure.					Extruded bar.

Microstructural studies.

For microstructural work, specimens were heated by using high frequency current. After deformation to a desired degree they were quenched with water immediately. The time between the moment of stopping the lathe and quenching was less than 0.5 sec. It required another 2.3 sec. according to the temperature recorded at the axis until the specimens were cooled below 700°C (depending on temperature).

The structure was studied by cutting the specimens longitudinally and transversely. After polishing they were

etched with a solution of 2% nital.

3.2 Some aspects relating to axial force

Swift (67) and L'Hermite (68) appear to be the first to report that during torsion a permanent change in specimen length occurs at room temperature. This has since been confirmed many times by Hughes (45), Guenssier and Castro (47), Hardwick and Tegart (51, 53). Data at high temperatures have established that an axial force, sometimes compression but more commonly of tension, appears during deformation by torsion if the specimens are fixed in grips, or a change in length occurs when they are free. However, some features have not been resolved, viz:

(a) What factors cause axial force to arise,

(b) How axial force is distributed across the specimen cross section, and

(c) To what extent the ductility measured by revolutions to failure is affected by axial force.

The experiments described below were designed to study these aspects.

3.2. 1. Factors producing axial force

Herson (69), considering unrestrained specimens that become shorter during twisting said that this phenomenon is quite normal, quoting as an example that if a towel is twisted

it becomes shorter. In this way he considered that axial force appears due to fibre structure which tends to wrap helically and shorten the specimen length. Swift (67), who observed that the specimen at first becomes longer if it is twisted at room temperature, supposed that there is a tendancy for slip in the crystalline aggregate to occur so that it contributes more to an axial elongation than to the normal strain in other directions. He also related this phenomenon to crystal structure, pointing out that a fibrous structure in rolled metals cannot be responsible for the lengthening effect. Nadai (70) considered several factors which can explain the longitudinal extension of plastically twisted bar: i.e.

(1) The finite rotation of the principal direction of strain under a large simple shear may cause a simultaneous rotation of the principal direction of stress, because it is found that less mechanical work is required to plastically deform an element of a round bar if in addition to the system of shearing stress a normal stress in the direction of the axis of the bar is also present, through which the shearing stress at the plastic limit remains unchanged.

(2) It is known that the density of several cold worked metals decreases slightly by an order of magnitude comparable with the elastic dilatation in volume produced when a mean stress acts.

If a round bar after considerable torsional strain should carry a system of certain tensile and compression stresses in an axial direction, varying with the radial distance from the axis but representing an equilibrium system of stresses whose resultant would still vanish, this stress will produce in the radial and tangential directions elastic strain of a magnitude varying with radius and giving rise to a secondary system of radial and tangential stress. The small permanent increase of the volume in the outer portion nearest to the surface of the barwhich was worked the most, together with the variable elastic parts of the strain, must contribute to the increase in length of a severely twisted bar.

(3) Under the increasing permanent strain the metal ceases to deform in the simple manner postulated in all theories of isotropic flow. The permanent increase in length of twisted bar is also due to the anisotropic way polycrystalline metals distort after the strain increases to finite magnitude.

Rossard and Blain (54) said that increase in length is connected with work-hardening and decrease with non work hardening. Hardwick and Tegart (51) investigating this problem in detail came to the conclusion that change in length during twisting is not of geometrical nature, but depends on the

material and temperature. They said that if the extension may be explained by increasing the specimen volume due to increase in the number of dislocations during deforming, decrease in length is still obscure, and further investigations are necessary to explain it,

From the above it can be seen that axial force during twisting may appear due to several reasons but none has yet been proved to be directly responsible for it. The difficulty of establishing the main factors which produce axial force is that it is not easy to make determinations directly, and it is necessary to make deductions based on interpretations of other phenomena.

It is true that axial force of compression (or increase in specimen length) may be due to increase in specimen volume during deformation, but axial force of tension certainly cannot be attributed to this phenomenon. If axial tensile force is due to nonhomogenity of materials why does it appear in pure metals and, especially, why has it various values for various materials? If its variation is due to the form of crystal structure why is there great difference in its magnitude for materials which have the same type of structure? If it is attributed to some change in principal direction of strain and stress why does this change occur differently in various materials and at various temperatures? Furthermore, why does axial force return from compression to zero and then change to tension when a specimen is deformed at a given

temperature? These characteristics imply that the main factor which produces tensile force during twisting may be different from those so far considered.

Being in agreement with Hardwick and Togart that this phenomenon is dependent on the material and temperature the problem was studied as detailed below.

EXPERIMENTS AND RESULTS

(1) The Influence of Fibre Structure

For this experiment solid specimens $\frac{3}{8}$" in dia, and $1\frac{1}{2}$" gauge length made from steels 1, 2, and 3 (Table 3.2) were used. Steel 1 had a low content in carbon, (0.13) high content in sulphur (0.047) and phosphorus (0.068) and a pronounced fibre structure. Steel 2 contained 0.5% carbon, lower content in sulphur (0.016) and phosphorus (0.021) and a less pronounced fibre structure. Steel 3 was used in the as-cast state (0.18C, 0.036S, 0.068P) and forged with 30% and 75% reduction in area respectively. From forged material specimens were cut longitudinally and transversely with respect to the forging direction.

Torsion tests were carried out in the temperature range from 600 to 1300°C using a strain rate of about 60% s^{-1} corresponding to 75 rev/min.

The variation of torque and axial force against number of revolutions at various temperatures for steels 1 and 2 are shown in Fig. 3.12. The curves for steel 3

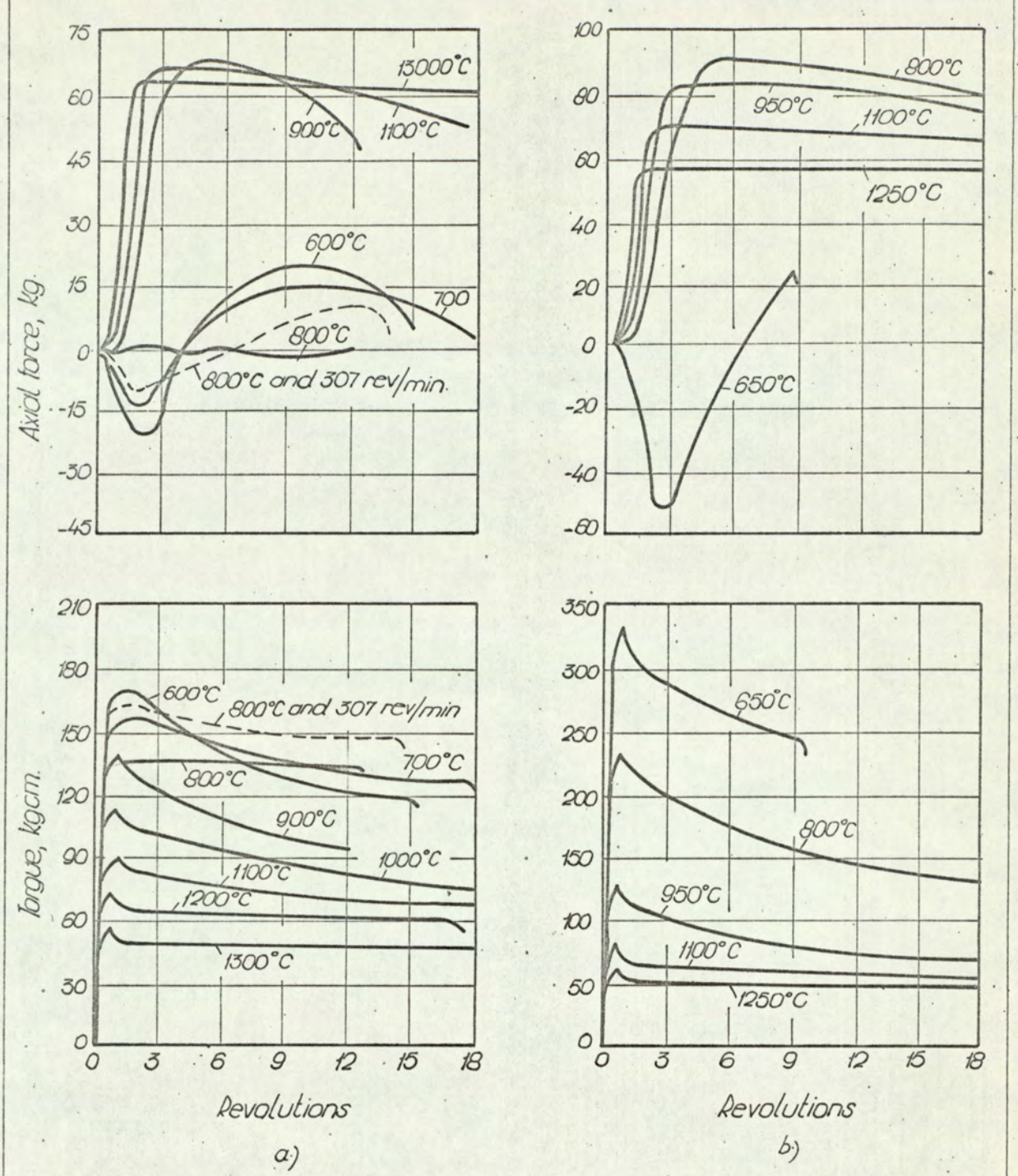

Fig.3.12. Variation of torque and axial force against number of revolutions to failure for two steels deformed at various temperatures with 75 rev/min.

had about the same shape as for steels 1 and 2. The variation of maximum axial tensile force with temperature is shown in Fig. 3.13 for steels 1 and 2 and in Fig. 3.14 for steel 3. Because the three steels have different compositions and therefore different strength and melting point, for a better comparison in Fig. 3.15 is shown the variation of the ratio σ/τ with the ratio $\frac{T}{Tm}$ (σ being maximum tensile stress, τ - shear stress corresponding to maximum tensile stress, T - testing temperature and Tm - melting temperature).

(2) The Effect of Strain Rate

For this test specimens of steels 1 and 2 were used. The tests were carried out in the temperature range from 700 to 1300°C using speeds of 30 and 307 rev/min. In Fig. 3.16 is shown the variation of the ratio σ/τ with temperature (σ and τ have the same meaning as before).

(3) Variation of Axial Force With Temperature Using Hollow Specimens

Because solid specimens deform nonuniformly on their cross section it was considered useful to deform hollow specimens which exhibit a much more uniform deformation. For this test hollow specimens with $\frac{3}{8}$" external diameter, $\frac{1}{4}$" internal diameter and $1\frac{1}{2}$" length, made from steel 1 were used. The deformation was carried out with 75 rev/min.

Because the hollow specimens changed their form very quickly before axial force attained its maximum value, a core was inserted as shown in Fig. 3.17. This core extended the life

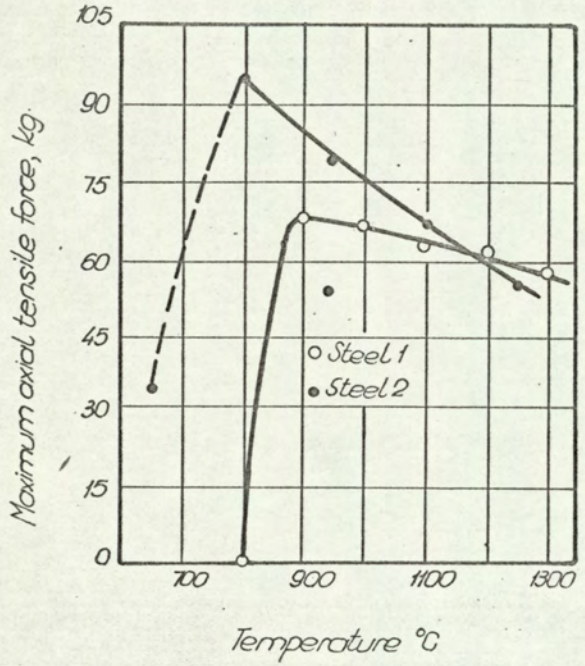

Fig. 3.13. Variation of maximum tensile force against temperature for steel 1 and 2 deformed with 75 rev/min.

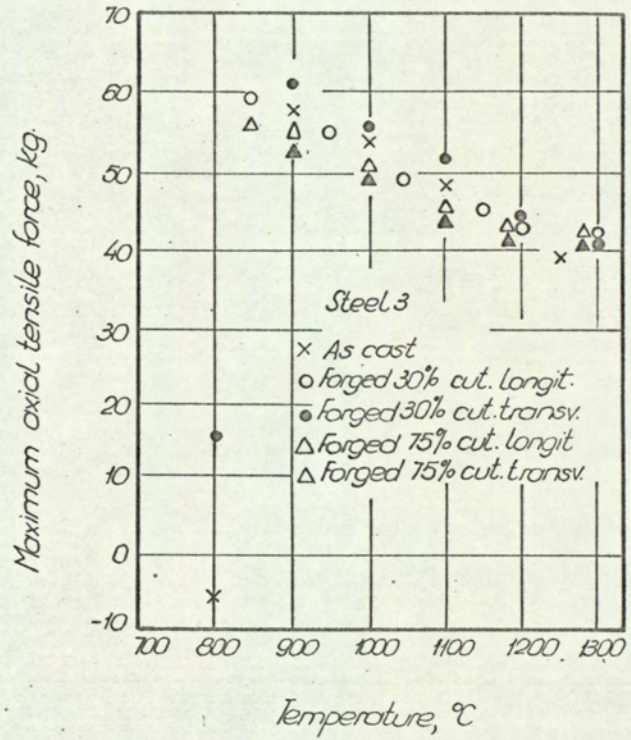

Fig. 3.14. Variation of maximum tensile force against temperature for steel 3 deformed with 75 rev/min.

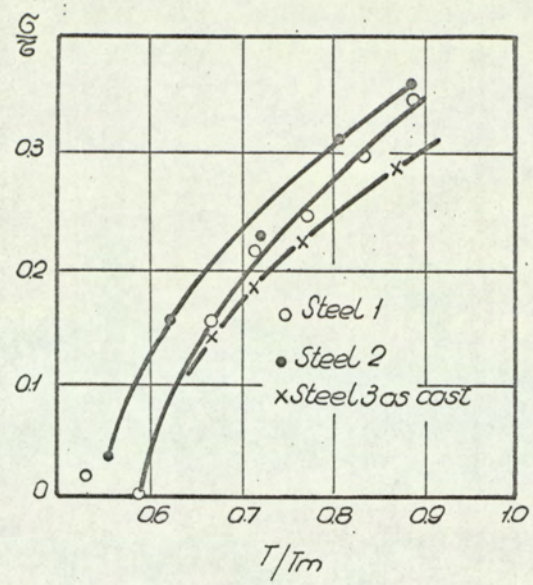

Fig. 3.15. Variation of ratio σ/σ against ratio T/T_m for the three steels.

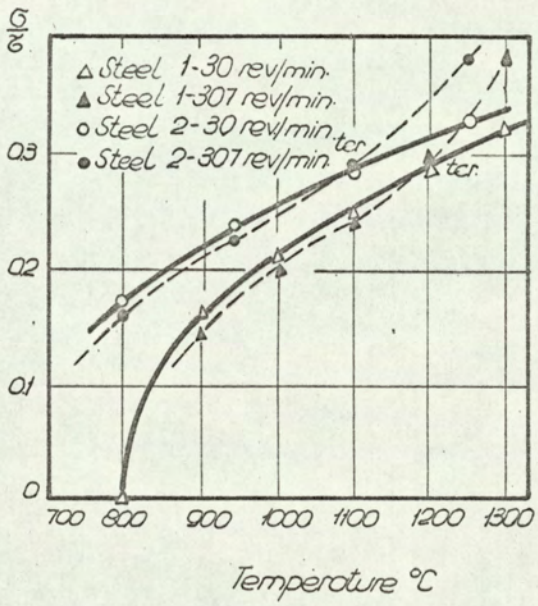

Fig. 3.16. Variation of ratio σ/σ against temperature for steel 1 and 2 deformed at 30 and 307 rev/min.

of the specimen so that with these conditions it was possible to obtain a stabilized value for axial force and torque before its form altered but only at temperatures above 900°C. Although the core slightly influenced the values of torque and axial force the change in their value can be neglected because the specimen length was kept constant, and the torque necessary to deform the core was much less than that necessary to deform the specimen. The core could also produce a nonuniformity in deformation along the specimen gauge, but because the value of torque and axial force were taken at the stage when they first reached steady values, it may be considered that the nonuniformity effect was also insignificant. On the basis of comparison between the dimensions of specimen and of core, the measured results were estimated to be in error by no more than 10%.

The variation of maximum axial force and of the ratio $\frac{S}{G}$ against temperature are shown in Fig. 3.18. For comparison and results for solid specimens made from the same material ~~and~~ deformed in the same conditions are also shown.

(4) The Effect of Temperature

The aim of this test was to see how axial force which appears during twisting is eliminated with time after stopping deformation in comparison with a force of the same magnitude applied from outside to an nondeformed specimen at the same temperature. For this test solid

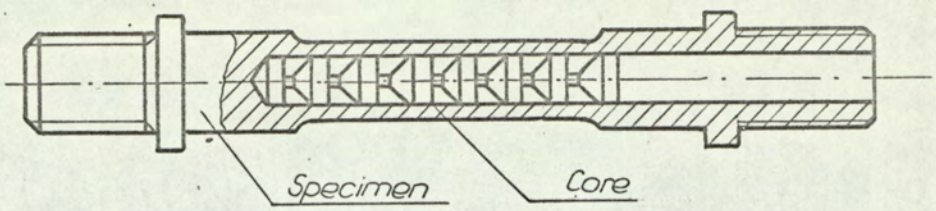

Fig 3.17. Hollow specimen with a core inside.

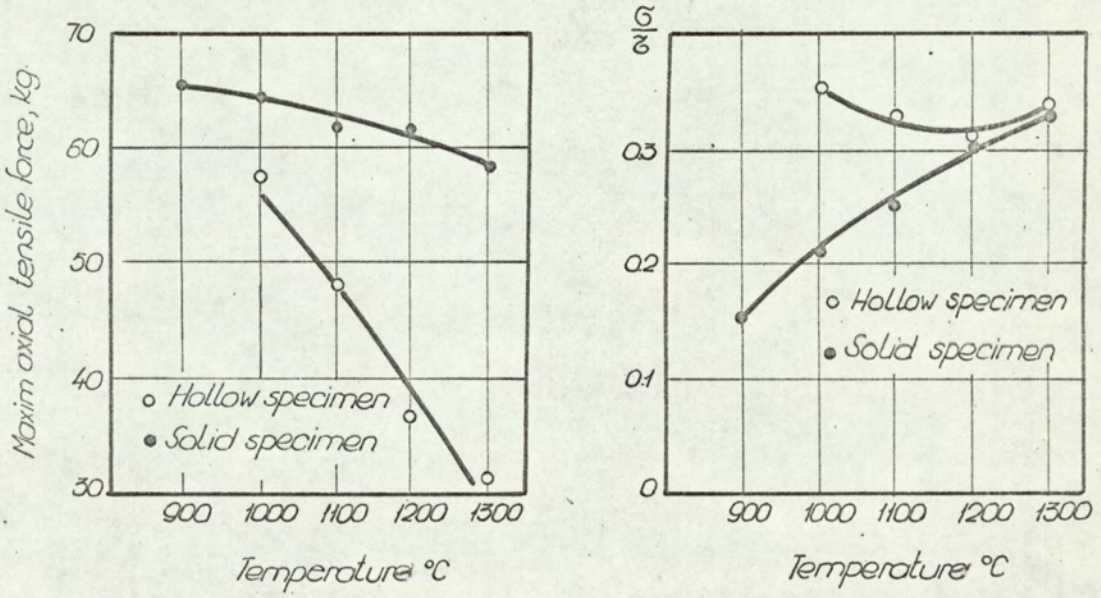

Fig. 3.18. Effect of temperature on the axial force and σ/σ for hollow and solid specimens made from mild steel and deformed at 75 rev/min.

specimens $^{7}/_{16}$" dia. and $1\frac{1}{2}$" length were used. A bigger diameter was chosen in order to work with higher values of axial force for more accuracy in measurement. For deformation a speed of 75 rev/min was used. Three temperatures were chosen for testing 700, 800 and 950 °C (800°C for undeformed specimens only). For 700 and 950°C specimens made from steel 2 (0.5 % C) were used which exhibited a high compression force at 700°C and a high tensile force at 950°C. For 800°C specimens made from steel 1 were used in the undeformed state, because the axial force which appeared during deformation in specimens made from this material at 800°C is almost zero. (Fig. 3.12). The tests were made in the following manner:

At 700°C. The specimen was heated at 700°C (by high frequency), held 2 minutes, deformed 3 turns and then the deformation stopped. An axial force of compression of 93 kg. had by then appeared. Its decay was recorded for a 15 minute period, keeping the temperature constant. Another specimen was heated at 700°C, held 2 minutes, a compression force of 93 kg was applied and its decay recorded over 15 minutes. The decrease of axial force against time for the two tests are shown in Fig. 3.19, a.

At 950°C. The same technique as at 700°C was used but the deformation was stopped after two stages: after 5 turns when an axial tensile force of 105 kg has appeared, and after 26 turns when the axial force has a value of 89 kg.

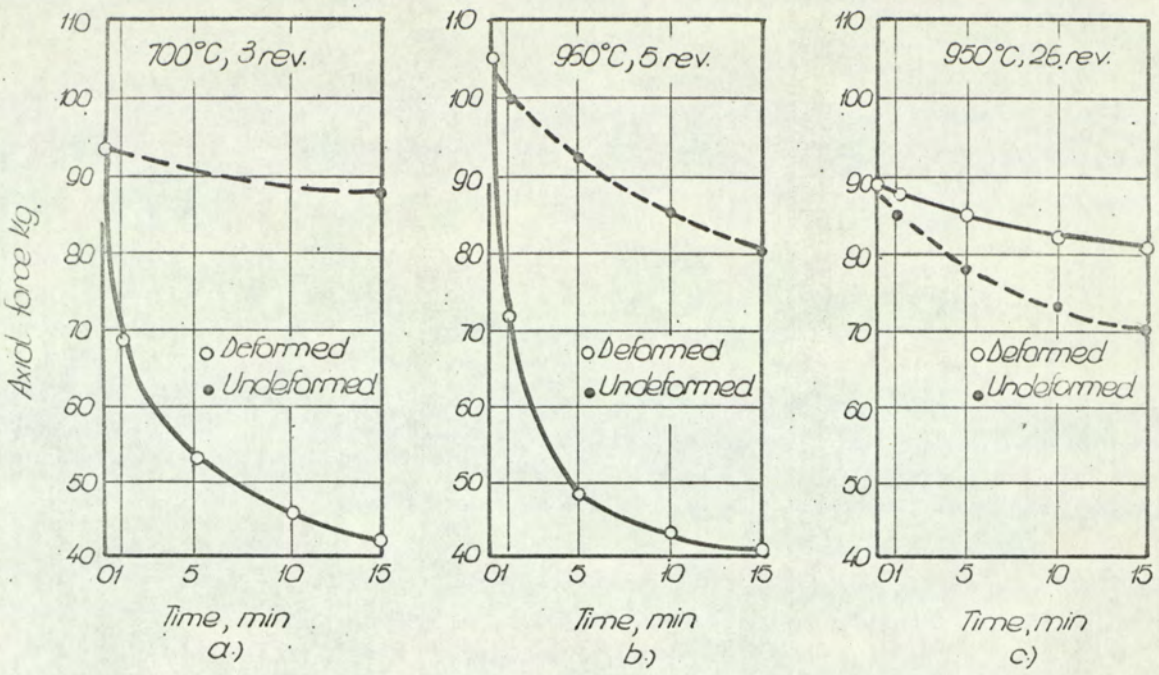

Fig.3.19. Decay of axial force with time for deformed and undeformed specimens.
a- 700°C; b- 950°C after 5 rev.; c- 950°C after 26 rev.

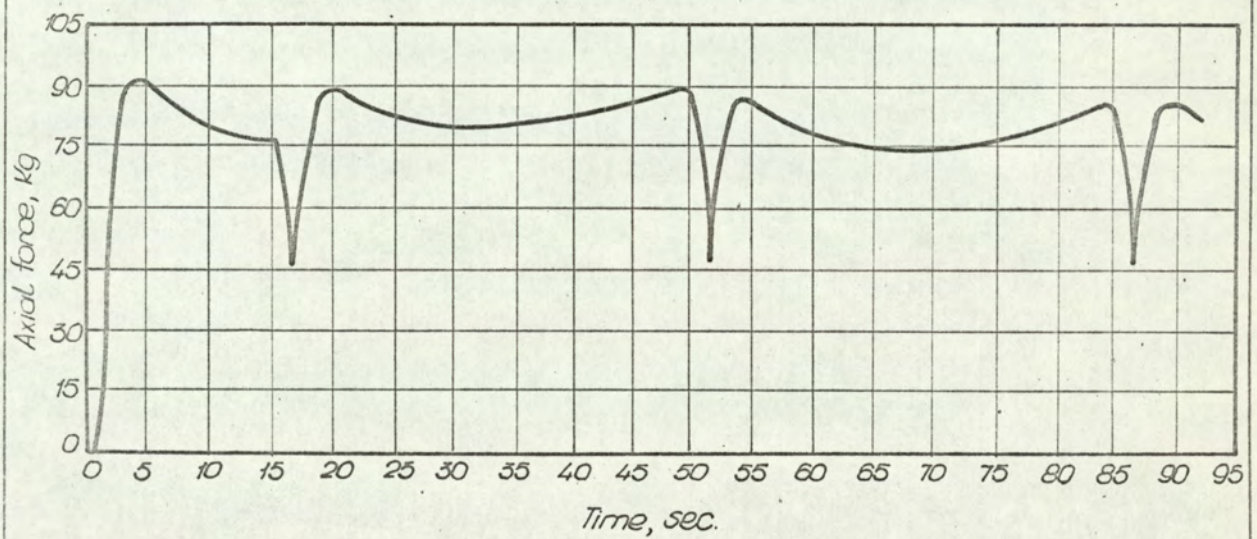

Fig.3.20. Changes in axial force in time for interrupted deformation at 950°C.

Axial tensile forces of the same magnitude, 105 and 89 kg. respectively were applied to undeformed specimens, and the decay curves are shown in Fig. 3.19, b (for 5 turns) and 3.19, c (for 26 turns).

Another specimen was deformed at 950°C with interruptions. The variations of axial tensile force against time are shown in Fig. 3.20 which also shows the testing sequence. Twisting was recommenced when the axial force had decayed to 45 kg after each interruption.

During deformation the temperature rises and after stopping deformation it falls to its initial value. The change in temperature affects axial force by specimen expansion or contraction. In order to lessen the change in temperature the anode current was slightly decreased at the beginning of deformation and after deformation it was increased again to the value corresponding to working temperatures. The change in temperature of the specimen was recorded and did not vary by more than 20°C. However, a curve of variation of axial force against temperature was determined using an undeformed specimen (Fig. 3.21, a). Because a decrease in temperature of 50°C occurred in less than 7 sec. the effect of temperature in the decay experiments lasting over 15 min. periods, such as shown in Fig. 3.19, may be considered negligible. In fact the curves in Fig. 3.19 have been corrected for the slight initial variation in temperature using the correction diagram of Fig. 3.21, b.

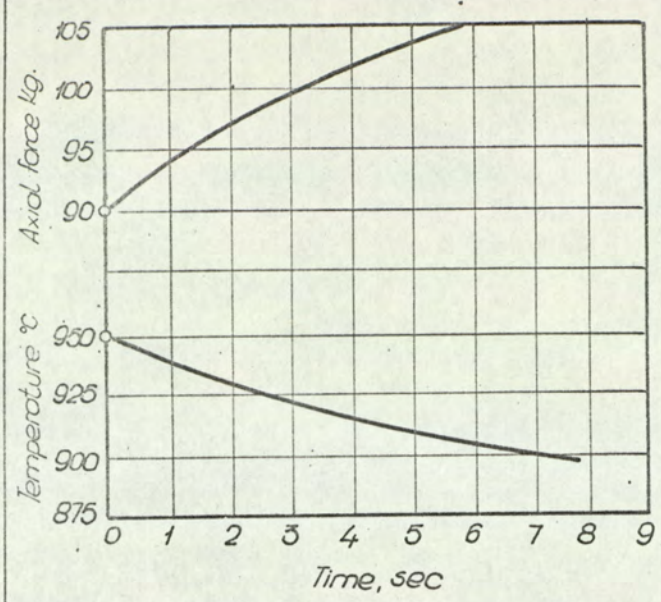

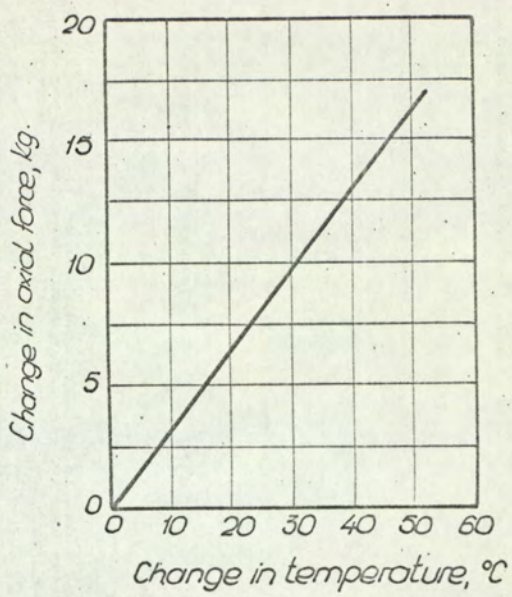

Fig. 3.21. Effect of time on the axial force and temperature (a) and effect of temperature on the axial force (b) after stopping the heating current.

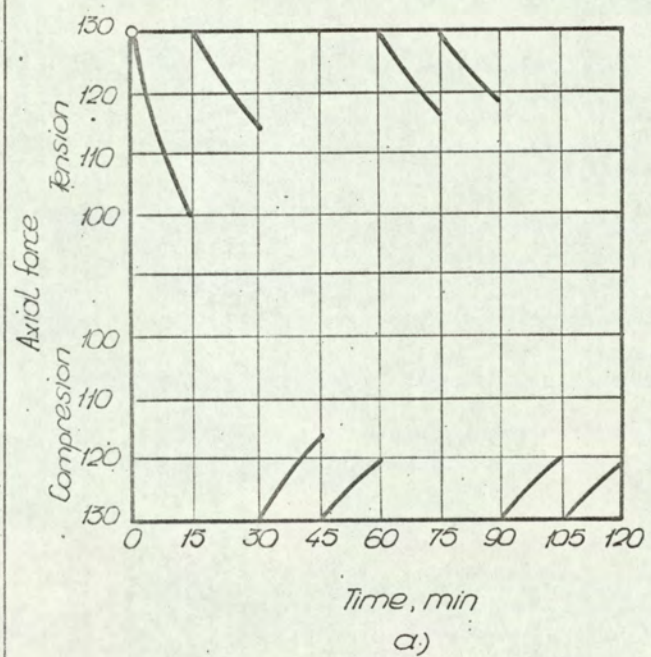

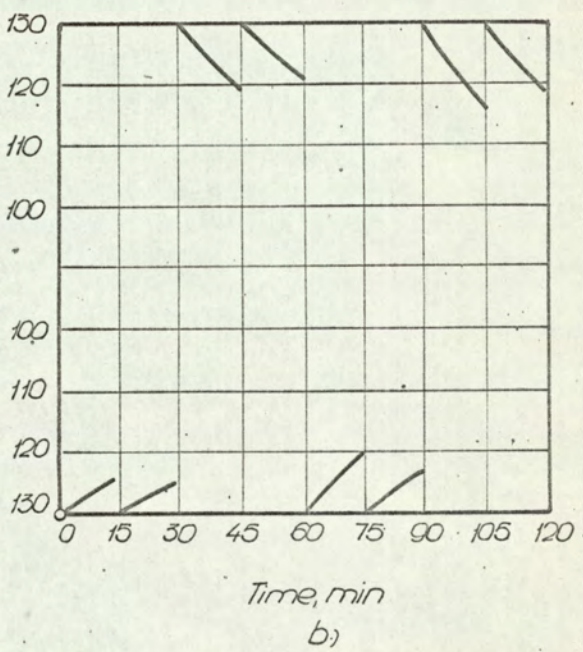

Fig. 3.22. Effect of time on the axial force variation in undeformed specimen heated at 800°C
a-: axial force applied after 1 min; b-axial force applied after 30 min.

At 800°C. The aim of this test was to discover whether the ferrite/austenite transformation has any particular effect on axial force, and whether for a given temperature axial force of compression is eliminated at a similar rate to the axial force of tension when they both have the same order of magnitude. Thus a specimen was heated at 800°C held for 1 minute and an axial force of tension applied having a value of 130 kg. Its decay was recorded over 15 min. after which the axial force was raised again to its initial value, and the decay again recorded. After this an axial force of compression of 130 kg. was applied and then a similar procedure followed. Another specimen was heated to 800°C, held for a longer period than before of 30 minutes equivalent to two 15 minute decay periods and then an axial force of compression was applied of 130 kg. The test was then continue as that described before. The variation of axial force for the two tests are shown in Fig. 3.22.

DISCUSSION OF RESULTS

The specimens made from steel 1 and deformed at 750°C developed helical surface markings whereas specimens made from steel 2 showed no trace of such form at any temperature. Fig. 3.23 shows two specimens made from steel 1 and 2 deformed at 750°C. The microstructure of the specimens made from steel 1 and deformed at 750°C was found to be non-uniform along the specimen gauge length. The grains were smaller in the portion with smaller diameter as illustrate in Fig. 3.24,a. In Fig. 3.24,b is shown this nonuniformity in grain structure which shows very distinctly in a macro section. Similar

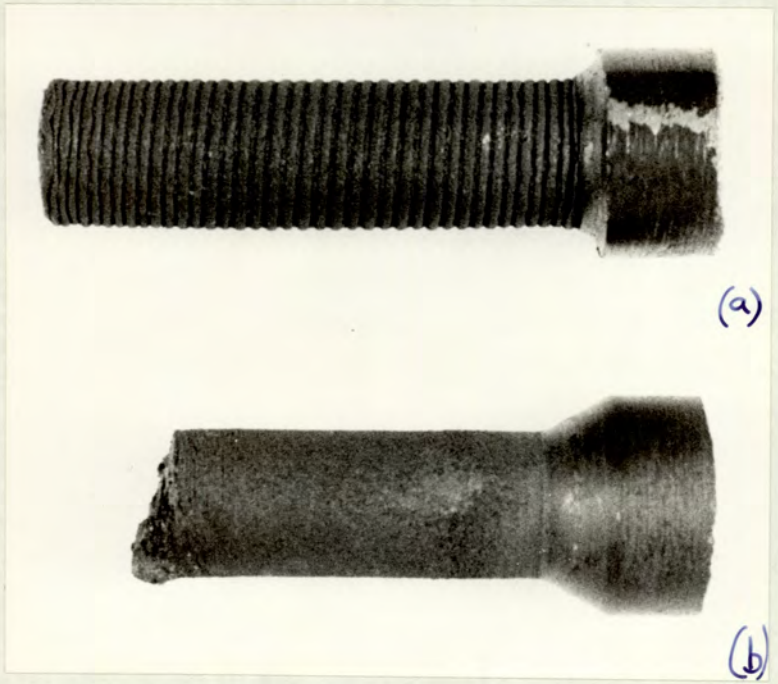

Fig. 3.23. Specimens deformed at 750°C(x2)
a - steel 1 ; b - steel 2.

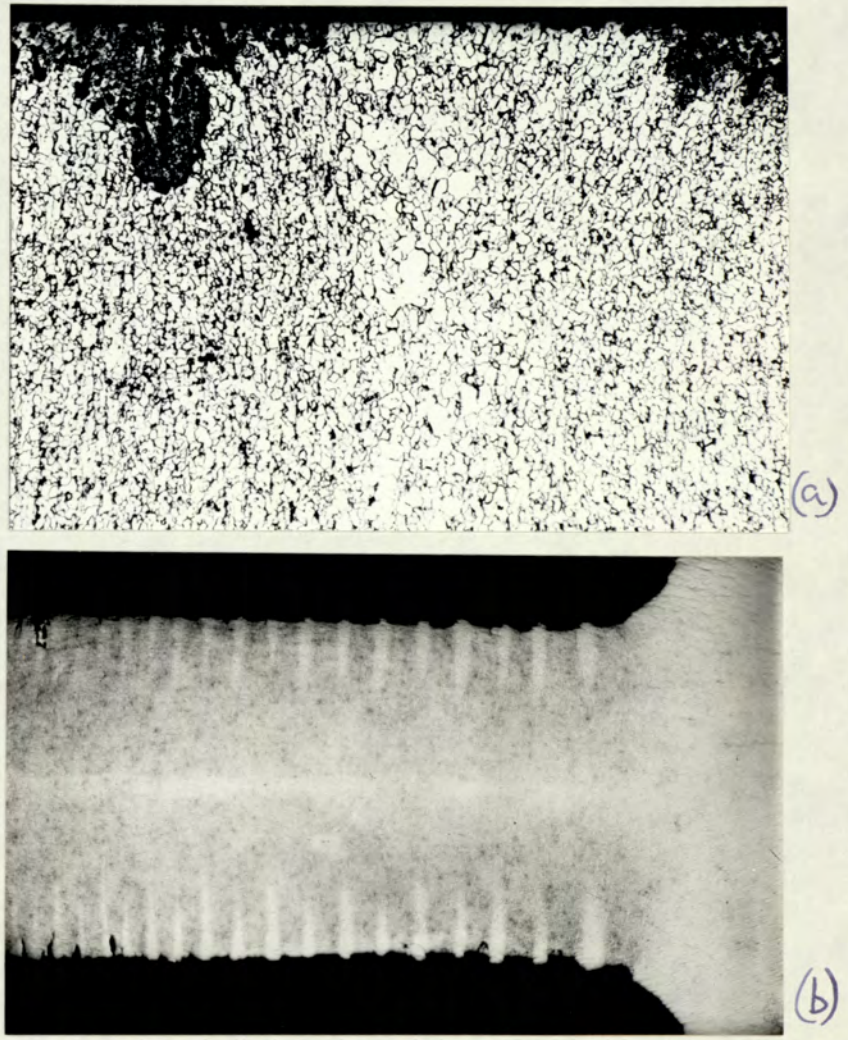

Fig. 3.2.4. Longitudinal section of a specimen made from steel 1 and deformed at 750°C with 75 rev/min. a - x100; b - x4

nonuniformity was not observed in specimens made from steel 2. This aspect shows that steel 1 compared with steel 2 is quite different from the point of view of isotropy. However, although the specimens made from steel 1 and deformed at 800°C gave an axial force almost zero (Fig. 3.12), at other temperatures axial force curves had about the same shape for both steels and the same order of magnitude for the ratio σ_z/σ_φ.

No large difference was observed in variation of axial force with the temperature for steel 3 (as-cast and forged state) or between specimens cut longitudinally or transversely with the forging direction (Fig. 3.14) , Taking account of small differences in composition, strength, number of revolutions to failure, errors of measuring etc. some spread in results may be expected. However, the shape and magnitude of axial forces ($\frac{\sigma}{\sigma}$) show that fibre structure, impurity variation, and even carbon content, have very little influence on axial force appearance; hence the main factor (or factors) which gives rise to this force must be other than those so far considered

Looking at the Fig. 3.13 and 3.14 it can be seen that an axial tensile force, having a sensible value, appears at the temperature range just over 0.5 Tm which corresponds with the equicohesive point for steels reported by Crussard and Tamhankar (71). At this order of temperature a sensible grain boundary sliding starts to occur (72). This coincidence suggests that there may be some Connection between axial tensile force and grain boundary sliding.

Comparing the variation of axial force with temperature for hollow and solid specimens from Fig. 3.18,a it can be seen

that the values of axial force alter. as the temperature is raised, i.e. the force falls steeply for hollow specimens in which the deformation takes place more uniformly over the cross section than in solid specimens. Furthermore, between their ratio $\frac{P}{\sigma}$ from Fig.3.18,b there is a big difference at lower temperatures which is reduced by increasing the temperature.

Two conclusions may be drawn from this aspect:

1) Two factors (or two groups of factors) produce axial force: one compression and the other tension. They are present together all the time, at any temperatures, but their intensity is different at various temperatures and stages of deformation. Those which produce compression have greater intensity at lower temperature and at the beginning of deformation, and those which produce tension have greater intensity at higher temperature and towards the end of deformation.

2) The factors which give rise to tensile force appear to have a limited effect when the temperature is increased in that only up to a certain temperature does the tensile force continue to rise, thereafter it begins to fall.

From Fig. 3.19,a it can be seen that compression force which appears in specimens spontaneously during deformation is much more quickly eliminated by temperature than a similar compression force applied to an undeformed specimen. This suggests that axial force of compression is connected with defects which appear in structure due to deformation (dislocations and vacancies) which are cured in time at high temperature if the deformation is stopped. This conclusio

is in good agreement with Swift's conclusion (discussed previously) with regard to lengthening of the specimen during twisting at room temperature.

From Fig. 3.19,c an opposite effect can be seen which occurs with tensile force. Tensile force which appears during deformation decayed more slowly than the same force applied (force) to an undeformed specimen. On the other hand from Fig. 3.20. it is apparent that at every commencement of deformation tensile force decreased by about the same amount and then increased again to a fairly constant value everytime the twisting was restarted. From these results it may be implied that during deformation a dynamic equilibrium of dislocations and vacancies (corresponding to given conditions of deforming) are present which contribute to making the specimen longer than in the undeformed state. Hence, this may be the reason why in Fig. 3.19,c the tensile force which appeared due to deformation disappeared more slowly than force applied to the undeformed specimen (i.e. the dislocations and vacancies associated with twisting decrease with time after stopping the deformation and contribu to shorten the specimen length thus helping to maintain axial tensile force). But this also shows that there are two factors (or two groups of factors) which produce axial force, both being present together all the time during deformation. Furthermore, it can be argued that while the factor which produces compression is connected with the crystal defects [illegible] (which appear during deformation and are curing or redistributing when the deformation ceases), the factor(s) which produces tensile force is not.

From Fig. 3.19,b we see that tensile force which appears due to deformation, after 5 turns, is eliminated by temperature faster than applied tensile force to underformed specimens, which is at first sight in contradiction with the effect after 26 turns in Fig. 3.19,c. Before further discussions on this figure it is necessary to analyse the results in Fig. 3.22. From this figure it can be seen that axial force decreased faster when it was applied after 1 minute, and more slowly when it was applied after 30 minutes. Also while the rate of axial force decrease became smaller with time in Fig.2.22, it increased with time in Fig. 2.22,b. But rate of axial force decay after 120 minutes is about the same in both cases. The bigger difference in the rates of axial forces decrease at the beginning may be attributed to the $\alpha \rightarrow \gamma$ phase transformation. In the first case (Fig. 2.22,a) at the moment of applying the axial force transformat $\alpha \rightarrow \gamma$ had not reached equilibrium whilst in the second case (Fig.2.22,b after 30 minutes an equilibrium $\alpha + \gamma$ had been established, correspondi to the temperature of 800°C. This would suggest that axial force is much faster eliminated by temperature when a phase transformation occurs. In the light of this conclusion one may examine Fig. 3.12 for steel 1, where, deformed at at 800°C, with 75 rev/min, the axial force was almost zero, while it was greater at both 700° and 900°C. Deforming with 307 rev/min at 800°C axial force has about the same shape as at 700°C. although it has a smaller value, due to the shorter time taken to complete a given number of revolutions.

It would be expected that any rearrangements of atoms would contribute to faster elimination of axial force. Applying this

conclusion to the results from Fig. 3.19,b we have to accept that the rate of recrystallisation is greater at the beginning of deformation, and due to this process the axial force, either compression or tension, is eliminated faster at this stage. It appears that there is a close connection between the rate of axial force elimination and the speed of atomic rearrangement, and that the factor which produces axial force of tension is closely connected with some intrinsic property of the material rather than with impurities and minor structural changes.

From the aspects connected with temperature effect on axial force elimination it is suggested that compression force arises from grain deformation (by slip lines or subgrains formation) and tensile force from relative grain boundary sliding.

A general feature evident in Fig. 3.12, 3.13 and 3.14 is a steeply increasing axial force on passing from 800 to 900°C, i.e. from α range to γ one. This shows more clearly on comparing the results of steel 1 with those of steel 2. For steel 2, which is richer in carbon (0.57) axial tensile force increased more rapidly at lower temperature than for steel 1 (0.13) and for steel 2 the transformation finished at a lower temperature. However, on passing from α to γ range two phenomena are known that occur:

1) The resistance to deformation of γ grains is greater than of α ones (50).

2) Due to the transformation finer grains are present just above the transformation temperature than just below.

From the first phenomenon a question arises: does the

resistance of the grain boundary to deformation increase in the same ratio as the grain on passing from α to γ range? Because at grain boundary the atoms do not lie in a well determined structure, the transformation from α to γ may give a smaller increase in its resistance compared with the increase in resistance of grains; this change may cause a marked increase in the difference between the resistance of grains and grain boundaries, hence a sudden increase in grain boundary sliding might occur. On the other hand it is known that with decreasing grain sizes grain boundary sliding occurs more readily, up to a particular grain size (72), hence a marked increase in grain boundary sliding at this particular temperature may also occur. The range of temperature where the transformation $\alpha \rightarrow \gamma$ takes place is critical from ductility point of view, too. From the results of Reynolds and Tegart (50) shown in Fig. 2.31 it appears that there is a close connection between increase in resistance to deformation and ductility in the lowest γ range. It could be that such decrease in ductility is due only to decrease in ductility of γ grains with respect with α grains. But it is well known that F.C.C. structures are favourable for deformation in most metals and even for steels at other temperatures and it is difficult to understand why the ductility of pure irons should be so low at this temperature. However, the pronounced fall in ductility at this temperature may well be due to a sharp rise in the difference between the resistance of grains and grain boundaries, which favours grain boundary sliding and facilitates fracture. Results like those of Reynolds and Tegart were obtained by Randall too (73) using creep tests. Carrying out tests on low carbon

steel in the range of temperature 1200° to 1800°F he found that the time to fracture has a maximum and the ductility a minimum just above Ar_3 (Fig. 3.25). It may be supposed that the maximum in time to fracture against temperature is due to increase in the resistance to deformation of grains and minimum in the curve of ductility against temperature due to increase in intensity of grain boundary sliding.

From the above aspects, accepting that at the transformation temperature a marked rise in grain boundary sliding occurs, it again appears that there is a close connection between tensile force and grain boundary sliding.

It is to be noted that for a given material, specimen size, strain rate and temperature, the ration $\frac{\sigma}{\sigma}$ is a well defined value. Deforming specimens with an applied initial tensile force greater than that corresponding to given conditions resulted in the specimen lengthening up to the value of $\frac{\sigma}{\sigma}$ which appeared if the specimen had been fixed. From creep tests it was reported by more investigators (7,72) that the ratio $\frac{\epsilon_{gb}}{\epsilon_t}$ (ϵ_{gb} being the ratio of grain boundary sliding and ϵ_t the ratio of total deformation) has also a well determined value for a given material, temperature, strain rate and grain size. This ratio seems to increase with temperature and decreasing strain rate.

Now if it is assumed that axial compression force is given by grain deformation and tensile force by grain boundary sliding, and for given conditions of torsion testing both $\frac{\sigma}{\sigma}$ and $\frac{\epsilon_{gb}}{\epsilon_t}$ have well definable values, then some relationship should exist between these two terms. The ratio $\frac{\sigma}{\sigma}$ increases with temperature from 900°C

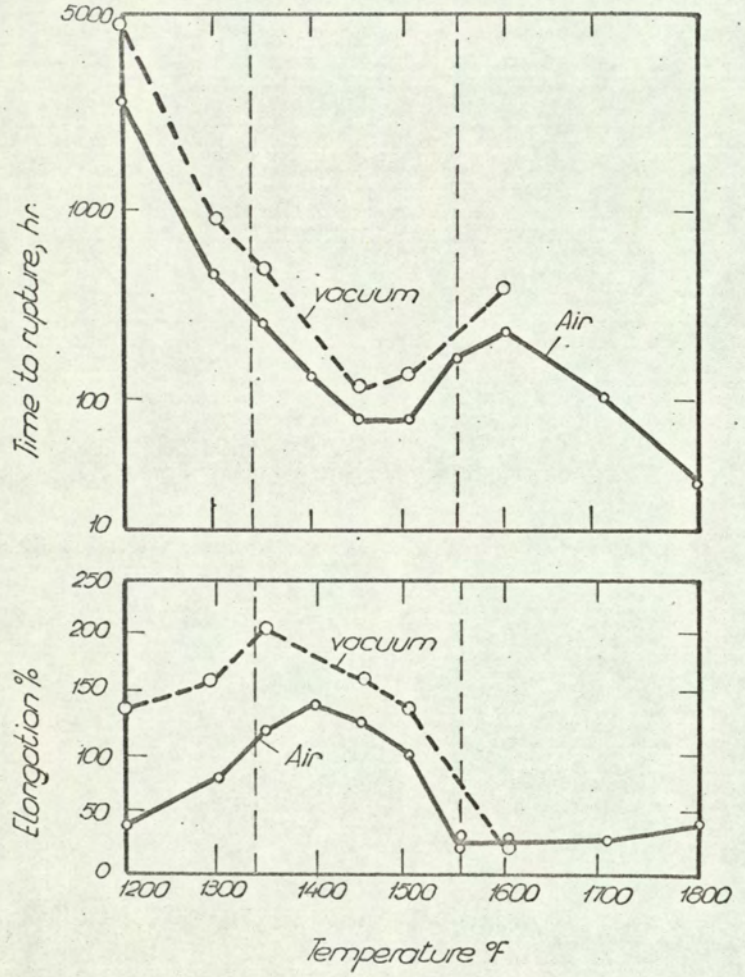

Fig. 3.25. Effect of temperature on the time to fracture and elongation for a carbon steel [13].

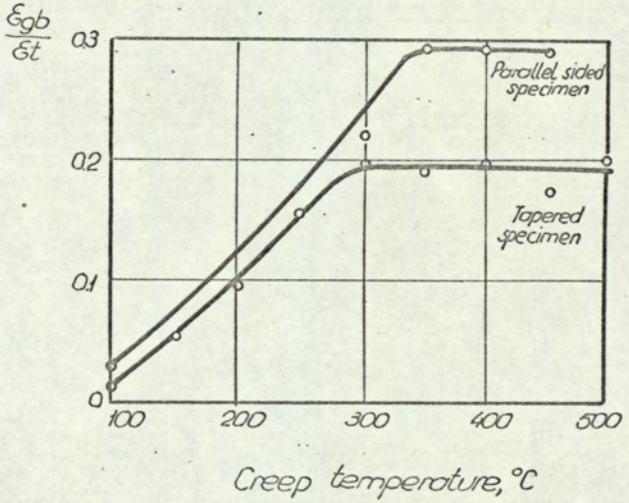

Fig. 3.26. Effect of temperature on the Egb/Et for aluminium [16].

to 1300°C for solid specimens but it varies hardly at all for hollow specimens (Fig. 3.18,b). Thus it appears that the ratio $\frac{\sigma}{\epsilon}$ is in agreement with $\frac{\epsilon_{gb}}{\epsilon_t}$ only for solid specimens, but it was shown before that a hollow specimen has more uniform deformation on its cross section. However, grain boundary sliding is a complex process, especially during deformation at high temperature and at high strain rates. By increasing the temperature, the ratio $\frac{\epsilon_{gb}}{\epsilon_g}$ would tend to increase for a given grain size, but by increasing the deformation temperature the grains grow and, as a consequence, the ratio $\frac{\epsilon_{gb}}{\epsilon_g}$ would tend to decrease. Hence, the value of $\frac{\epsilon_{gb}}{\epsilon_g}$ may not change appreciably by increasing the deformation temperature, above a certain value, and there may exist a connection between $\frac{\sigma}{\epsilon}$ and $\frac{\epsilon_{gb}}{\epsilon_t}$ even for hollow specimens above 900°C. That the ratio ϵ_{gb}/ϵ_t does not always change its value on altering the temperature was reported by several investigators:- Martin et al (74), making experiments by creep on β brass, showed that the ratio $\frac{\epsilon_{gb}}{\epsilon_t}$ was independent of temperature for a given stress. Similar results were also reported by Fazan et al (75). Mclean and Farmer (76) found by creep test on aluminium that ϵ_{gb}/ϵ_t increased up to 300 - 350°C and above this temperature remained almost constant (Fig. 3.26). If we compare the variation of ϵ_{gb}/ϵ_t with temperature from Fig. 3.26 with the variation of σ/ϵ with temperature for hollow specimens from Fig. 3.18,b they would be in quite good agreement if it is assumed that the results for the hollow specimen are on the plateau, and σ/ϵ would decrease below 900°C.

From Fig. 3.16 it can be seen that the ratio σ/ϵ

decreases slightly if the strain rate is raised up to a certain temperature (different for the two steels) above which a much greater change occurred. From this point of view it seems that there is an agreement up to a particular temperature only. Above this temperature strain rate has an opposite effect with respect to $\frac{\epsilon_{gb}}{\epsilon_t}$. This aspect seems to be more complex and it is necessary to be further analysed. It is well known that the grains behave as plastic material and grain boundary as viscous material (6,72) At high temperature, considering the deformation process as a competition between strain hardening (due to deformation) and restoration (due to recovery and recrystallization), the amount of work hardening corresponding to some value of strain in an equilibrium state of deformation depends on strain rate; hence the real deformation strain present in specimen is a function of strain rate. Thus both the resistance to deformation of grains and of grain boundaries depend upon strain rate and temperature, expressed in the form:-

$$\tau_{gb} = f(t, \dot{\varepsilon}_{gb}); \qquad 3.5,a$$
$$\tau_{g} = f(t, \dot{\varepsilon}_{g}),$$

where τ_{gb} is shear stress for grain boundary;

τ_g - shear stress for grains;

t - testing temperature;

$\dot{\varepsilon}_{gb}$ - strain rate for grain boundary sliding;

$\dot{\varepsilon}_g$ - strain rate for grains deformation

Considering the increment of shear stress with strain rate for grains and grain boundaries separately, and comparing them with the variation of the ratio $\frac{\epsilon_{gb}}{\epsilon_t}$ against temperature from Fig. 3.16

for the two values of strain rates, it seems that

$$\frac{d\sigma_{gb}}{d\dot{\varepsilon}} > \frac{d\sigma_g}{d\dot{\varepsilon}} \quad \text{up to Tcr} \qquad 3.6,a$$

$$\frac{d\sigma_{gb}}{d\dot{\varepsilon}} < \frac{d\sigma_g}{d\dot{\varepsilon}} \quad \text{above to Tcr} \qquad 3.6,a$$

where $\bar{\dot{\varepsilon}}$ represents a medium strain rate which includes both grain deformation and grain boundary sliding. Hence, up to Tcr, by increasing strain rate the resistance to sliding of grains will increase more than the resistance of their deformation and the ratio $\frac{\varepsilon_{gb}}{\varepsilon_t}$ will decrease. Above Tcr. by increasing strain rate the resistance to sliding of grains will increase less than the resistance to their deformation and the ratio $\frac{\varepsilon_{gb}}{\varepsilon_t}$ will increase.

Now if this criterion is accepted, during deformation σ_{gb} ought to have the same value as σ_g and instead of an equicohesive point (which may be valid in static state or at slow strain rates) there should be an equicohesive line. However, the condition $\sigma_{gb}=\sigma_g$ may be valid only if two conditions are satisfied:-

- first, if at lower temperature (below Tcr) a strain rate with a certain value acts, capable of increasing σ_{gb} at the same value of σ_g , and

- second, if grain boundary sliding may occur with any value at temperatures above Tcr.

If the first condition may be realised without difficulty by increasing strain rate the second cannot. Grain boundary sliding is dependent on grain deformation and it cannot increase independently above a particular value corresponding to given conditions of deformation. The values of $\frac{\varepsilon_{gb}}{\varepsilon_t}$ from Fig. 3.26 and of $\frac{\sigma}{\bar{\sigma}}$ from

Fig. 3.18,b show that such a limit exists. In this way σ_{gb} will have the same value as σ_g as long as ϵ_{gb} real (for a given value of strain rate) is smaller or at most equal to the maximum ϵ_{gb} possible for these conditions of deformation. If ϵ_{gb} ' necessary to keep the condition $\sigma_{gb} = \sigma_g$ needs to be greater than ϵ_{gb} possible, this condition cannot be realised and consequently $\sigma_{gb} < \sigma_g$. Fig. 3.27,b shows schematically the effect of taking account of the equations 3.6, in representing the deformation state in relation to that considered in static state, Fig. 3.27,a. Point t_1 will be determined by temperature and may correspond to the equicohesive point for the static state (or very low strain rate), the second point, t_2, will be determined by temperature and strain rate. In this way it seems that at high temperatures there is the possibility of a difference between the strength of grains and grain boundary during deformation even if in static state such a difference will not exist, and for this difference to increase if the strain rate is raised. Furthermore, there may exist a certain range of temperature over which a particular value of strain rate will keep the condition $\sigma_{gb} = \sigma_g$. Smaller and greater than this will give $\sigma_{gb} < \sigma_g$. In this way t_2 may be at the highest temperature for a medium value of strain rate rather than the highest value.

It was shown above that ϵ_{gb}/ϵ_t may have a limiting value above a certain temperature which is attained at about 300 - 350°C for aluminium and about 900°C for steel. However, from Fig. 3.16, upon increasing strain rate ϵ_t increases steeply above Tcr, against the existence of a limit for ϵ_{gb}/ϵ_t.

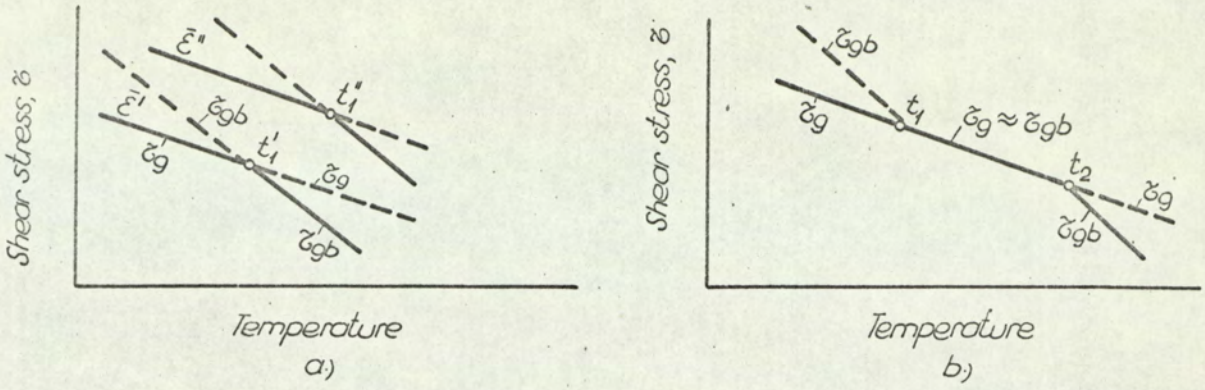

Fig. 3.27. Variation of τ_{gb} and τ_g with temperature (schematic).
a - conditions of equicohesive point; b - conditions of equicohesive line.

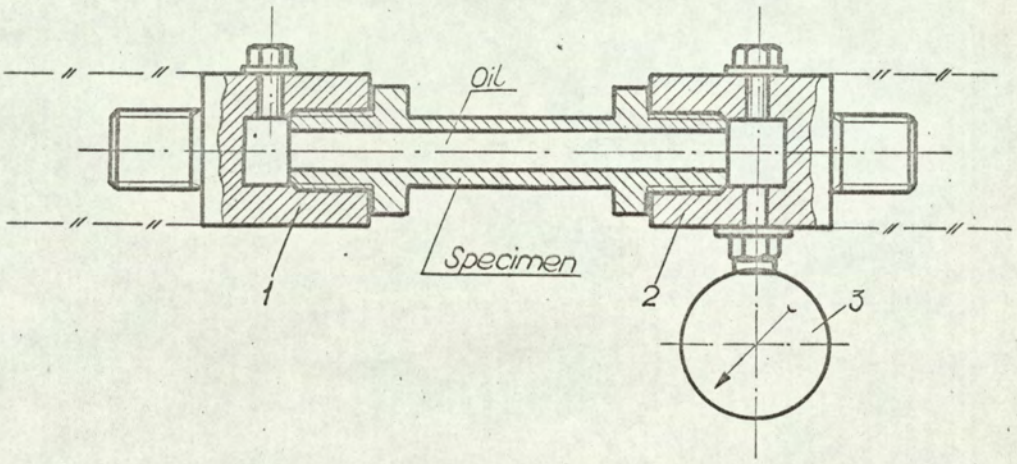

Fig. 3.28. Diagram showing deformation of hollow specimen using internal pressure.

Three explanations amy be put forward for this phenonenon:-

(1) A greater local deformation of grains near grain boundaries may occur upon increasing the strain rate. A greater deformation of grains near grain boundary was observed by Fazan et al (75)

(2) Grain size decreases on increasing strain rate. Decrease of grain size by increasing strain rate, for a given temperature, was observed by Rossard and Blain (54).

(3) The width of grain boundaries may increase by increasing the strain rate.

An investigation of grain boundary thickness variation during deformation has not yet been made. It is supposed that the width of a grain boundary is of the order of 2 - 3 atoms (7), but because a greater deformation of grains near grain boundaries is possible, an increase in grain boundary thickness during deformation at very high temperature may also be possible. However, even if ϵ_{gb}/ϵ_t increases by increasing strain rate it does not follow that ϵ_{gb} actual has the same value as ϵ_{gb} necessary to keep condition $\sigma_{gb} = \sigma_g$, and at high temperatures (above Ter) by increasing strain rate above a particular value, σ_{gb} will be smaller than σ_g, and a decrease in ductility may occur.

If we compare the results of Martin and Parker (77) with those of Manjoine and Nadai (19) it will be seen that deforming copper at high temperature Martin and Parker obtained an intergranular fracture using low strain rate. Nadai and Mangoine

also deforming copper, found a ductile fracture with high values of strain rate and a brittle fracture (with very small reduction in area) occurred using a very high strain rate. Nordheim et al (17) deforming steel with low content in carbon at 1800°F found that a strain rate of 0.001% sec^{-1} produced an intergranular fracture with about 75% reduction in area, a strain rate of 0.1% sec^{-1} produced a transgranular fracture with about 93% reduction in area, and a strain rate of 50% sec^{-1} although giving a fracture which looked to be transcrystalline, intergranular cracks were seen near fracture and the reduction in area was smaller than with 0.1% sec^{-1}.

Because results obtained by creep tests show that at a given temperature the higher the value of grain boundary sliding the lower is the ductility, the decrease in ductility by increasing strain rate (above a certain temperature) may be partially due to raising the ratio $\varepsilon_{gb}/\varepsilon_t$, such as the ratio $\varepsilon_g/\varepsilon$ shows in the present work. The results of Castro and Poussardin (18) on mild steel show a decrease in ductility by increasing strain rate from 5 sec^{-1} to 400 sec^{-1} over 1200°C (Fig. 2.10) From Fig. 3.16 Tcr for mild steel is also at about 1200°C. Hence there is agreement between the temperature at which harmful effect of increasing strain rate on ductility was observed and the temperature at which an increase in the ratio $\varepsilon_g/\varepsilon$ was recorded by increasing strain rate. From this statement, two inferences may be drawn:-

1) Above a certain temperature, a decrease in ductility, on increasing the strain rate, may be due to increase in the ratio $\frac{\varepsilon_{gb}}{\varepsilon_t}$

in comparison with lower strain rates (Several other factors may of course, contribute to this phenomenon).

2) There may be some connection between ϵ_{gb}/ϵ_t and $\frac{\sigma}{E}$ even over Ter.

Considering now that between $\frac{\epsilon_{gb}}{\epsilon_t}$ and $\frac{\sigma}{E}$ there is an established connection, it may with some approximation be expressed in the form: $\frac{\epsilon_{gb}}{\epsilon_t} = a + b\frac{\sigma}{E}$ (3.7) where a and b are two constants which could be determined by making parallel tests in torsion and creep for measuring $\frac{\epsilon_{gb}}{\epsilon_t}$ and $\frac{\sigma}{E}$ in conditions as near identical as possible.

The equation 3.7 has this form because when $\sigma = 0$ it does not follow that the factor which gives rise to tensile force is not present; on the contrary, it would merely have an intensity of the same order of magnitude as the factor which produces compression.

CONCLUSIONS

1) Although it is not possible to establish directly which factors produce axial force during deformation by twisting, two main factors can be put forward to explain this phenomenon:

(a) axial force of compression appears due to grains deformation by build up of dislocations and vacancies;

(b) axial force of tension appears due to grain boundary sliding.

Both factors are present together during deformation at any temperatures but their magnitude is different. Grains deform more

under steady conditions of deformation, and grain boundary sliding is less at lower temperatures and at the beginning of deformation, whereas grains deform less and grain boundary sliding occurs more at higher temperatures and towards the end of deformation. However, at high temperatures, after a few revolutions in the torsion test a steady state is reached and the intensity of both factors seems to remain almost constant throughout the remainder of the deformation.

Fibre structure seems to have no or very little effect on axial force. Alloy elements and impurities seem to affect axial force appearance only from the point of view of their influence on grain boundary sliding and phases transformation.

2) For the materials tested the ratio $\frac{\sigma'}{\tau'}$ decreases slightly up to a particular temperature (about 1200°C for mild steel) on increasing strain rate and thereafter rises steeply. According to the equation 3.7 the ratio $\frac{\varepsilon_{ab}}{\varepsilon_t}$ would vary in the same manner. In this way may be explained why the ductility of some materials decreases at high temperature when strain rate increases, as well as why the ductility of pure irons decreases steeply just above 900°C, (a decrease which may not be entirely due to a decrease in ductility of grains but also to a bigger difference between the strength of grains and of grain boundary which may appear at this particular temperature compared with just above or just below.)

3) Axial force which originates in specimens due to deformation by twisting or which is applied from exterior to an undeformed specimen may be used for studying the following phenomena:-

(a) The rate of grain boundary sliding $\frac{\varepsilon_{gb}}{\varepsilon t}$ by measuring the ratio $\frac{\sigma}{\tau}$ and using an equation similar to equation 3.7. Even if the coefficients a and b are not known, from the point of view of grain boundary sliding it is possible to use such as a basis for comparison with other materials.

(b) Rate of recrystallization or transformation in various stages of deformation may be assessed by measuring the decrease in axial force against time.

Together with metallographic observations axial force in the torsion test may be of assistance in studies of a range of metallurgical phenomena.

3.2.2. Distribution of Axial Force Within the Specimen

From the results of Nadai (46), Rossard and Blain (53), Ornerod and Tegart (55), discussed previously shear stress distribution on the specimen cross section seems to be quite clear, having a maximum value outside and zero at the specimen axis. Axial stress distribution over the specimen cross section, when both axial force and torque act (neglecting radial and circumferential stresses) can be calculated from the plasticity law of the form.

$$\sigma^2 + 3\tau^2 = 3k^2 \qquad 3.9$$

where σ is axial stress;

τ - shear stress;

k - maximum shear stress

and outside where $\tau = k, \sigma = 0$. Inside, at the specimen axis

where $\bar{\sigma} = 0$, $\bar{\sigma} = \sqrt{3}k$ which is its maximum value. In this way axial stress distribution was given by Nadai (46) and its variation is shown in Fig. 2.29 alongside shear stress. Because this problem seems to be very clear no other studies were made from other positions.

In the same work Nadai made a connection between stress and strain in the presence of both axial and shear stresses. Starting from the equations:

$$x = \phi[\varepsilon_x - \tfrac{1}{2}(\sigma_y + \sigma_z)]; \quad \gamma_{xy} = 3\phi\tau_{xy} \qquad 3.10$$

$$y = \phi[\varepsilon_y - \tfrac{1}{2}(\sigma_x + \sigma_z)]; \quad \gamma_{yz} = 3\phi\tau_{yz} \qquad 3.11$$

$$z = \phi[\varepsilon_z - \tfrac{1}{2}(\sigma_x + \sigma_y)]; \quad \gamma_{zx} = 3\phi\tau_{zx} \qquad 3.12$$

Neglecting the elastic portion; assuming Poisson's coefficent $v = \frac{1}{2}$, and $-\epsilon_y = \varepsilon$; $\epsilon_x = \epsilon_z = -\frac{\varepsilon}{2}$; $\gamma_{yx} = \gamma$; $\gamma_{zy} = \gamma_{zx} = 0$, he obtained

$$= \phi\bar{\sigma} \qquad 3.13$$

$$\gamma = 3\phi\tau \qquad 3.14$$

Dividing 3.14,a into 3.13, he obtained the equation

$$\frac{\gamma}{\epsilon} = \frac{3\tau}{\bar{\sigma}} \qquad 3.15$$

Hill (78) studying the problem of conbined torsion and tension of a thin-walled tube, ignored the component of elastic strain in the conditions of strain hardening, and derived the equations:

$$d\epsilon_z = \frac{dl}{l} = \frac{\sigma d\bar{\varepsilon}}{H'\bar{\sigma}}; \quad d\epsilon_r = \frac{dt}{t} = -\frac{\sigma d\bar{\varepsilon}}{2H'\bar{\sigma}}$$

$$d\epsilon_\theta = \frac{dr}{r} = -\frac{\sigma d\bar{\varepsilon}}{2H'\bar{\sigma}}; \quad d\gamma_{\theta z} = \frac{r d\theta}{2l} = \frac{3\tau_z d\bar{\varepsilon}}{2H'\bar{\sigma}} \qquad 3.16$$

Combining the expressions of dE_z and $d\gamma_{\theta z}$ he obtained:

$$r\frac{d\theta}{dl} = \frac{3\tau_z}{\sigma} \qquad 3.17$$

where r is the specimen radius;

θ - angle of twisting;

ℓ - specimen length;

τ - shear stress;

σ - axial stress,

which is similar to that derived by Nadai.

Considering a cylindrical bar composed from many tubes Hill claimed that this theory will also be valid for solid bar.

However, it may be questioned whether the above relations hold when axial and shear stress are present together : In order to consider this question, it is necessary to examine the equations 3.15 or 3.17 and to apply them to this particular case.

During twisting when the specimen is kept fixed, $dl = 0$ but an axial force is present, hence $\sigma \neq 0$. When the specimen is let free $\sigma = 0$ but $dl \neq 0$. The equation 3.17 shows that when $\sigma = 0$, $dl = 0$. Hence, in this particular case the equations 3.15 respective to 3.17 cannot be used; they are valid for ideal material only which produces no axial force during twisting. Furthermore, axial force in torsion arises from the deformation process, - it is not applied from outside - and it is necessary to distinguish between the two kinds of forces; axial stress which appears in specimen due to deformation is present in those places where the deformation occurs.

Let us suppose that at the specimen axis no deformation takes place; this part may be considered as an ideal material and using the equation 3.17 it results that as $dl = 0$, $\sigma = 0$, too. Outside where deformation occurs and the material cannot be

considered as ideal, due to the presence of an axial force it appears that although dl = 0, $\delta \neq 0$. From this simple analysis it is clear that during twisting, when the specimen is kept fixed and an axial force appears, for axial stress distribution the equations of plasticity cannot be applied in a simple way. Furthermore, it seems that in this particular case axial stress is bigger outside and smaller at the specimen axis which is in contradiction to what would be expected from the equation 3.12.

In the above equations radial and circumferential stresses were neglected. But from Dewis' results (79) it can be seen that radial and circumferential stresses have defenite values when an axial force is present along with torque. Using tubular specimens with thin wall ($1\frac{1}{8}$" external diameter, and 1" interval diameter) made from steel, Dewis applied forces in conbinations of torsion, tension nd internal pressure. He varied axial stress and internal pressure in such a way that the medium diameter of the specimen remained constant. The true normal and shear stresses and also principal normal stresses are given in Table 3.3 for various values of axial stress. Although the values of radial and circumferential stresses may have little effect on the equations 3.12, 3.15 and 3.17, for ideal materials, in this particular case they may certainly affect axial stress distribution on the specimen cross section.

Useful results on this problem have also been obtained by Crossland and Hill (80). They studied plastic behaviour of thick tube under combined torsion and internal pressure, using for

3.III

Tab. ~~33~~ 33 Values of true normal and shear stresses for combined torsion, tension and internal pressure [79]

Tab. 33.

Stresses	Their values, p.s.i.			
Axial stress, σ_x	100.500	89.500	74.500	59.500
Circomferent stress, σ_ϕ	50.640	46.900	37.300	29.000
Radial stress, $\sigma_r = -\frac{p}{2}$	-2.700	-2.520	-2.050	-1.670
Shear stress, τ	0	21.000	34.000	41.000
Principal stress, σ_1	100.500	98.750	94.700	87.800
σ_2	50.640	38.250	17.100	600
σ_3	-2.700	-2.520	-2.050	-1.670

plastic state the equations:

$$po = 2k \log \frac{b}{a} \quad ; \qquad 3.18$$

$$to = \frac{2\pi}{3} k (b^3 - a^3) \qquad 3.19$$

where po is internal pressure able to produce plastic deformation of tube without the presence of torque; to - torque able to produce plastic deformation of tube without the presence of internal pressure; a - internal and b - external radius of tube;
k - maximum shear stress,
Noting with p a certain internal pressure and with t a torque which has a value corresponding to p in such a way that together they can produce plastic deformation of tube, they found the equation:-

$$\left(\frac{p}{po}\right)^2 + \left(\frac{t}{to}\right)^2 = 1, \qquad 3.20$$

This expression gave satisfactory results with a limit of error of only 2% approximately.

From the above results it may be deduced that the internal pressure affects the behaviour during deformation by torsion.

Rossard and Blain (53) measuring the torque using various values for strain rate found that at 1200°C (for steel) by varying the number of revolutions per minute from 0.24 to 697, an increase in torque was noticed of about 5 times. This experiment implies that because there is a big difference in strain rate between specimen axis and its surface a big difference in resistance to deformation also exists.

Considering the results of Dewis, Crossard and Hill and Rossard and Blain it may be supposed that during deformation. in

the presence of an axial force alongside of torque an internal pressure may be created at the specimen axis which will affect axial stress distribution on the specimen cross section.

In the light of the above the following experiments were carried out to study axial stress distribution during the torsion test.

EXPERIMENTS AND RESULTS

Several types of experiments were used, as detailed below:-

1. Study of Internal Pressure that Appears in Specimen During Twisting with the Presence of An Axial Force.

For this experiment hollow specimens with 0.588" external diameter, 0.437" internal diameter and 2" gauge length were used, made from aluminium. They were held in the testing machine by using two special pieces (1) and (2) from Fig. 3.28) p 96 A pressure gauge (3) was used, attached to piece (2), and the whole assembly filled with oil. The specimens were deformed by twisting until a steady state of internal pressure was obtained. The deformation was carried out in two ways: starting first from an initial pressure of zero and second starting from an initial pressure greater than the steady value reached during the first test. About the same pressure was obtained in both cases at the steady state of deformation. This experiment was repeated on specimens by using various values for axial force, having the order of magnitude corresponding to those which appear in steel at high temperature.

For a better appreciation of this test and in order to

make comparison with the results obtained by Dewis the equation 3.18 was used in the form.

$$p = c2k \log \frac{b}{a} \qquad 3.21$$

where p is internal pressure which appears during deformation;

c - coefficent which takes account of the presence of axial force and torque;

k, b and a have the same significance as in equation 3.18.

The value of c was calculated by using the equation 3.21 re-written in the form:

$$c = \frac{p}{2k \log \frac{b}{a}} \qquad 3.21,a$$

The value of k was determined in the conditions of internal pressure p = o and axial force a = o.

In Fig. 3.29 the variation of the coefficent c with the ratio $\frac{\sigma}{\tau}$ is shown (σ being true axial stress and τ true shear stress).

From Dewis results, taking $p = 2\sigma_f$ (he considered a medium value for $\sigma_f, \sigma_f = -\frac{p}{2}$) and calculating the value of k from principal normal stresses (given in Table 3.3) using the equation

$$(\sigma_1 - \sigma_2)^2 + (\sigma_2 - \sigma_3)^2 + (\sigma_3 - \sigma_1)^2 = 6k^2 \qquad 3.22$$

the value of c against the ratio $\frac{\sigma}{\tau}$ is shown in Fig. 3.29, too.

From Fig. 3.29 it appears that the two curves fit together quite well, and that the value of c is independent of material and specimen size; therefore this experiment was not continued by using specimens with other dimensions.

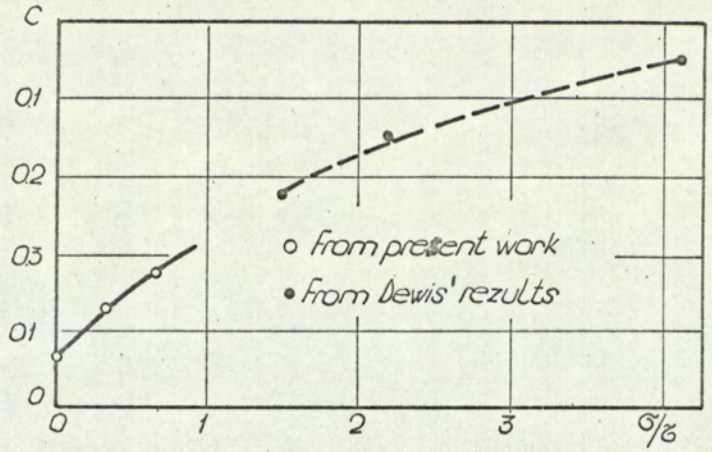

Fig. 3.29. Variation of c with $\frac{\sigma}{c}$.

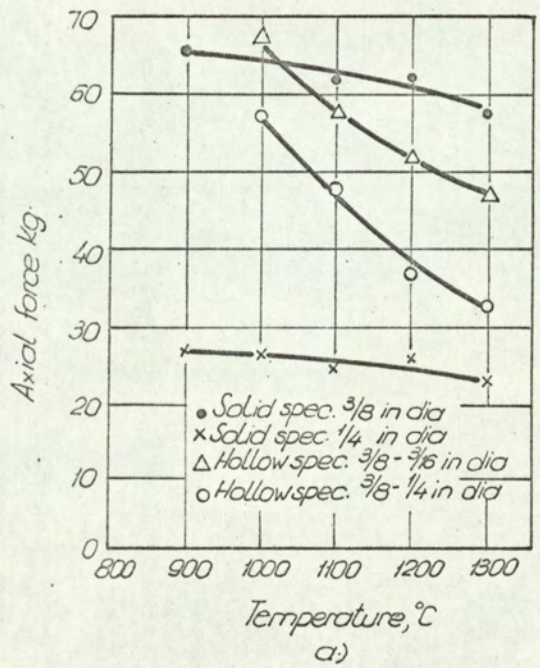

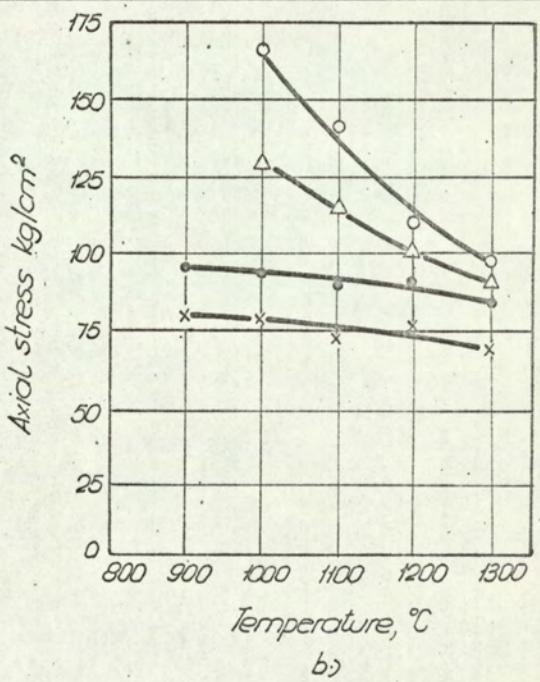

Fig. 3.30. Effect of temperature on the axial force (a) and axial stress (b) for various types and sizes of specimens.

2. Measurement of Tensile Stress

For these tests solid specimens with $1\frac{1}{2}$" length, $\frac{1}{4}$ and $\frac{3}{8}$" dia. were used together with hollow specimens of $1\frac{1}{2}$" length, $\frac{3}{8}$" external diameter and $\frac{3}{16}$" and $\frac{1}{4}$" internal diameters. These dimensions were selected to make comparisons between axial stress present in various places along the specimen radius. All specimens were machined from mild steel (steel 1). The experiments were carried out at 75 rev/min in the temperature range from 800 to 1300°C (except hollow specimens which were only tested above 900°C). For comparison the value of maximum axial forde which appeared was chosen together with the corresponding torque at that point along the number of revolutions axis. Variation of maximum axial force and of maximum axial stress with temperature are shown in Fig. 3.30.

Considering a medium circle on the cross section such that the area inside is equal to that outside, the variation of axial stress on this circle with specimen radius, for various temperatures, is shown in Fig. 3.31. The specimen length and the number of revolutions per minute are the same for all specimens but their diameters differ and this produced different true strain rates. In Fig. 3.32 and 3.33 are plotted the variation of $\frac{\varepsilon}{\bar{\sigma}}$ against temperature and against specimen radius respectively for various temperatures.

3. Metallographic Study on the Specimen Cross Section in Various Stages of Deformation

For this test specimens of $\frac{3}{8}$" dia. and $1\frac{1}{2}$" length made

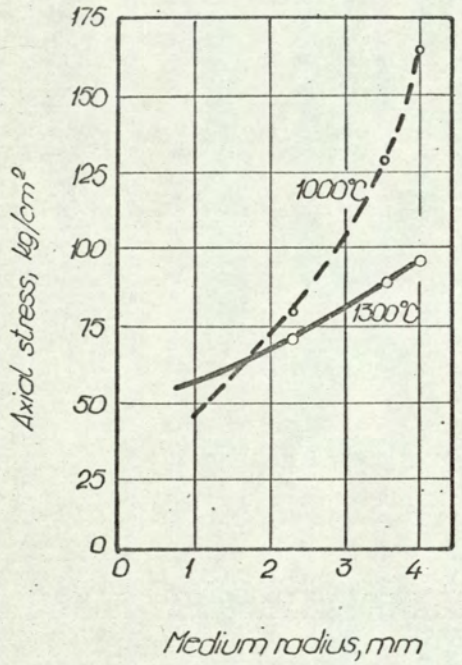

Fig. 3.31. Variation of medium σ along the specimen radius for 1000 and 1300°C.

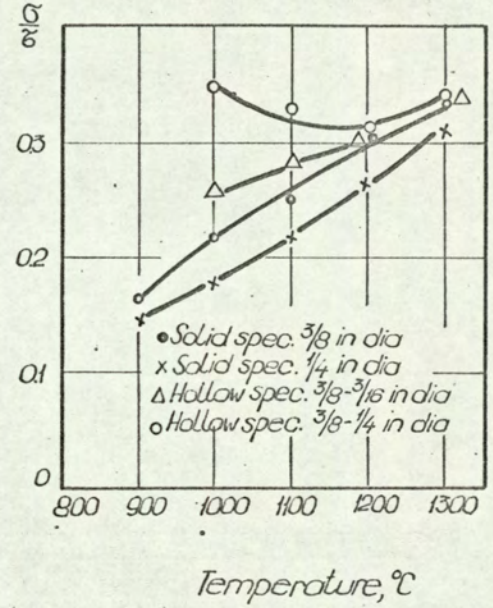

Fig. 3.32. Variation of $\frac{\sigma}{\sigma}$ with temperature for various types and sizes of specimens.

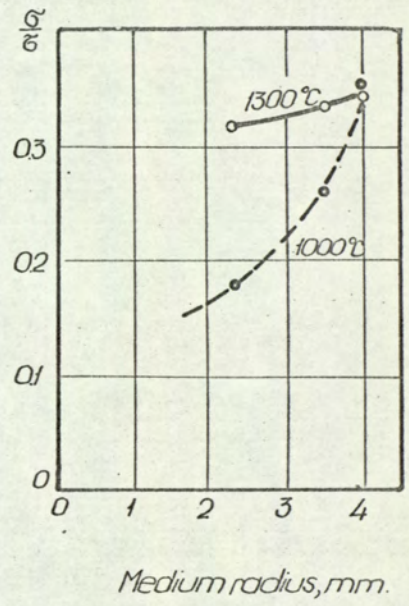

Fig. 3.33. Variation of $\frac{\sigma}{\sigma}$ along the specimen radius for 1000 and 1300°C.

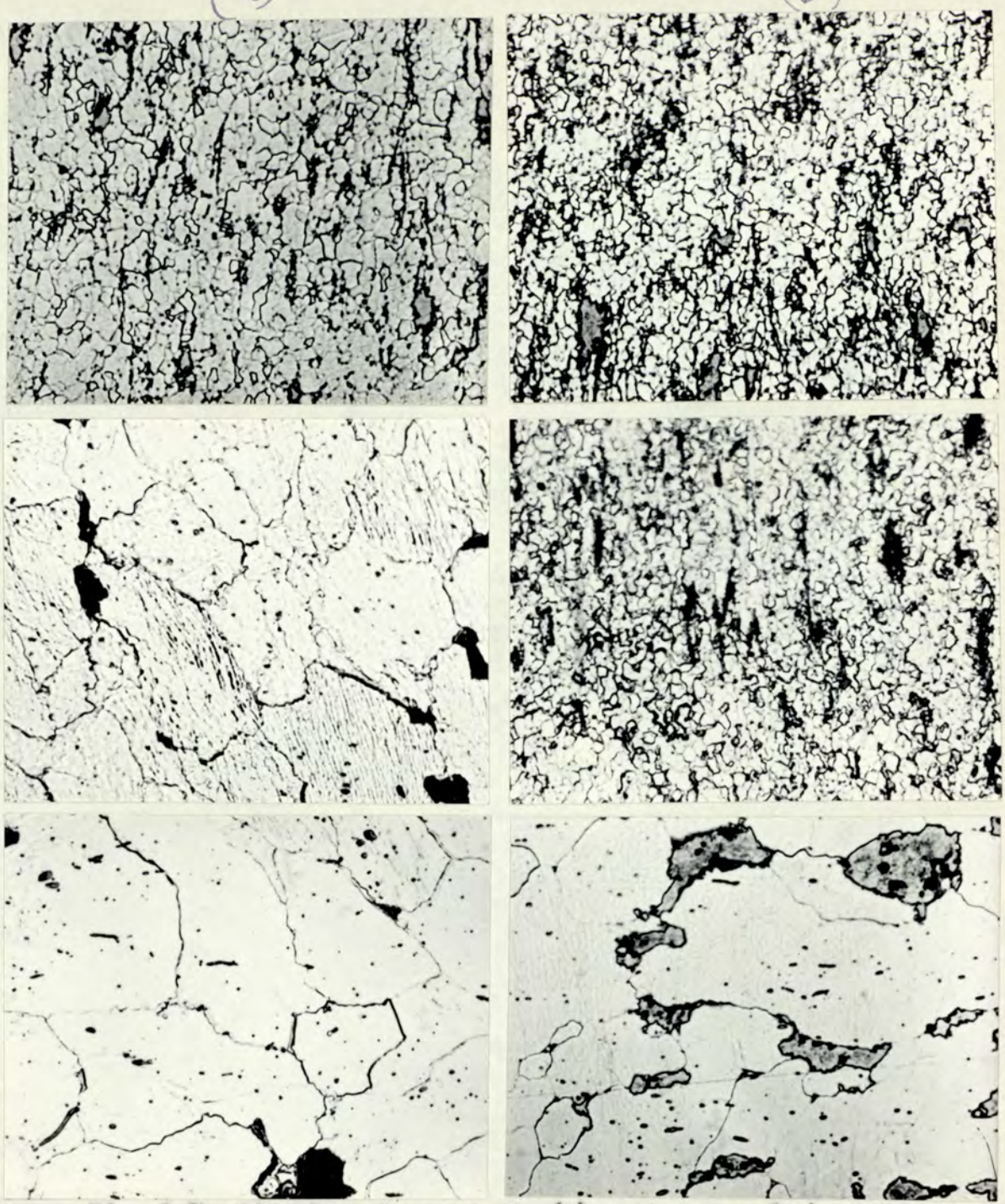

Fig. 3.34. Structures from outside (I), mid-radius (II) and axis (III) of specimens made from steel 1 and deformed at 600°C with 75 rev/min x 300.
a - after 4 rev.; b- after 13 rev.

from steel 1 were used. The deformation was effected at 75 rev/min. The specimens were quenched at a desired stage, immediately stopping the deformation. The structure from outside, mid-radius and specimen axis after deformation for 4 turns and 13 turns respectively for the specimens tested at 600°C are shown in Fig. 3.34. This temperature was chosen because both types of force appear; compression at the beginning and tension towards the end of deformation. The variation of torque and axial force against the number of revolutions at the above temperature is shown in Fig. 3.35 and of the ratio $\frac{\sigma}{\tau}$ in Fig. 3.36.

DISCUSSION OF RESULTS

From Fig. 3.34 it appears that at the specimen axis almost no deformation occurred even after 13 turns. Comparing the change in structure with the change in axial force from 4 turns to 13 turns it appears clear that compression force is associated with substructure formation. No appreciable difference can be seen in the structure near the outside surface after 4 turns and 13 turns. Thus the degree of grain deformation decreases with time, and an increase in grain boundary sliding (subgrain boundaries probably behaving as grain boundaries) gives axial tensile force. Neglecting any deformation at the specimen axis the variation of axial stress across the specimen section would be expected to have the form shown schematically in Fig. 3.37. Hence, during progressive stages of deformation the factor which produces tensile force has a bigger and bigger effect outside whilst that which produces compression acts only inside the specimen up to a stage when

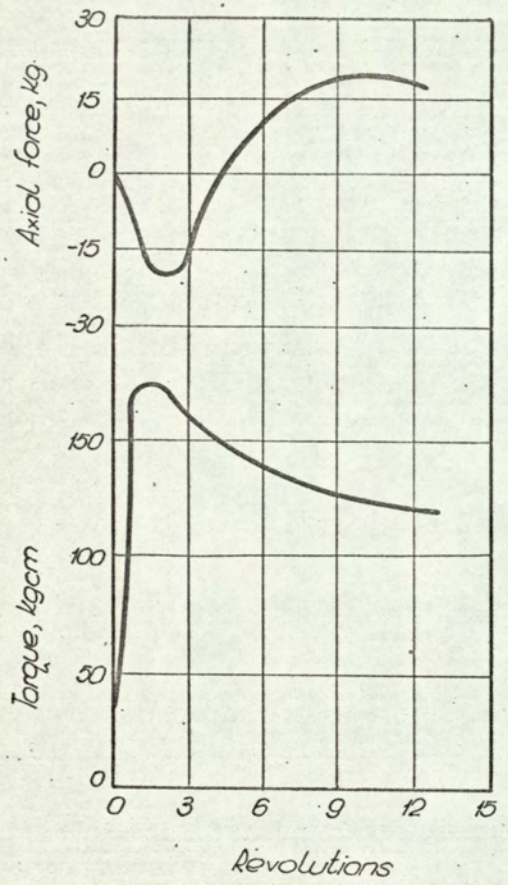

Fig. 3.35. Variation of torque and axial force with number of revolutions for a specimen deformed at 600°C with 75 rev/min.

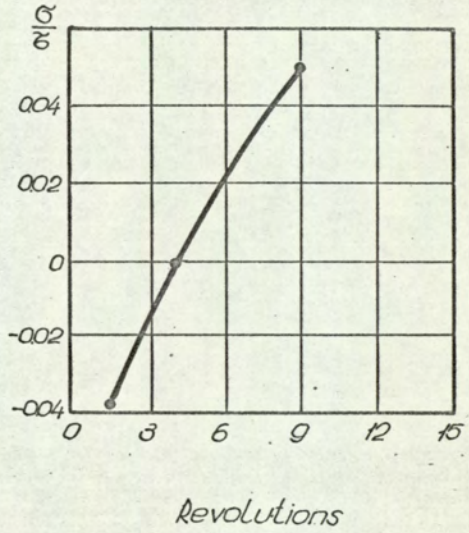

Fig. 3.36. Variation of σ/σ with number of revolutions for a specimen deformed at 600°C.

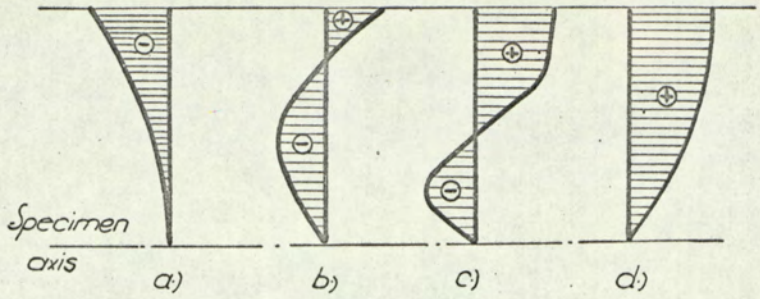

Fig.3.37. Scheme of axial stress variation along the specimen radius in various stages of deformation.

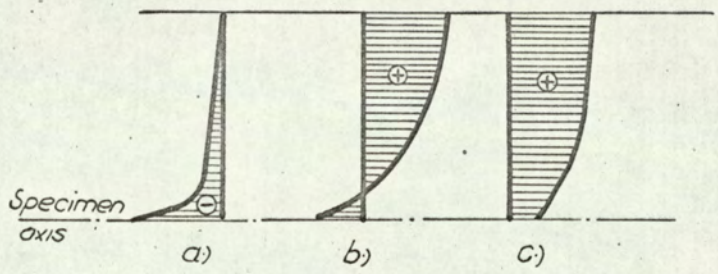

Fig.3.38. Scheme of radial and axial stress variation along the specimen radius in various conditions of testing.

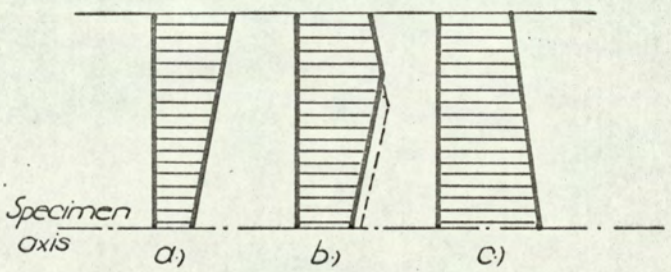

Fig.3.39. Scheme of temperature distribution along the specimen radius in various stages of deformation.

it begins to decrease.

Using the coefficent c from Fig. 3.29 and the equation 3.21 it appears that a compressive stress is present at the specimen axis due to radial stress too, regarding $\sigma_3 = p$. But because the value of c is quite small, the radial stress has a sensible value only at the specimen axis, its variation along the specimen radius being schematically such as in Fig. 3.38,a. Combining the pattern shown in Fig. 3.37,d with the variation of radial stress from Fig. 3.38,a it appear that at the specimen axis it is possible to have a compression stress even while at the outside a tensile stress is present. In these conditic the axial stress distribution on specimen cross section, when a tensile force is measured during twisting and the specimen length remains constant could be such as in Fig. 3.38,b.

The presence of a compressive stress at the specimen axis and tensile stress outside can also be deduced from Fig. 3.30,a. In this figure the axial tensile force for hollow specimens (with 3/16" internal diameter) deformed at 1000°C is bigger than for a solid specimen of the same external diameter deformed at the same temperature (the area of the solid specimen being greater than that of the hollow specimen). The differences in stresses, between the ratio σ/σ from outside and inside for solid and hollow specimens respectively, decrease when the temperature rises. Furthermore, between 1200 - 1300°C the ratio for hollow specimens is about the same as for solid specimens with the same external diameter. This shows that by increasing the temperature the deformation takes place at the specimen axis too, but of a nature that produces tensile stress. Under the conditions of

deformation at temperatures above 1100 - 1150°C after a relatively large number of revolutions, axial stress distribution may be such as in Fig. 3.38,c, showing the existence of a tensile stress even at the specimen axis, although of course this would have a much smaller value than at the outside.

Comparing the variation of axial force with temperature for solid and hollow specimens from Fig. 3.30, the variation of the ratio σ_z/σ with the number of turns from Fig. 3.36 and the structural changes from Fig. 3.34, it appears that the breakdown of the grain structure occurs in mild steel with less and less intensity up to a temperature of about 1150°C. Above 1150°C this phenomenon becomes less important in creating compressive force. Hence, above 1150°C a tensile force appears almost from the beginning of deformation in nearly the whole cross section of the specimen and exists at about the same value of σ_z/σ throughout the deformation.

The axial stress distribution discussed above and shown schematically in Fig. 3.38 may be accepted as one of the conditions of the test, and regarded in the same way as constitution, content in impurities and strain rate over the whole cross section. However, these conditions of stress distribution probably do not remain constant. During deformation, due to the energy required for deformation, the temperature of the specimen increases. Because the development of heat in the specimen is proportional to the energy required for deformation, it follows that near the outside the temperature rises faster than inside, and after a few turns it

will be distributed on the specimen cross section such as shown in Fig. 3.39,a. But because the temperature will be greater outside heat will be conducted to the inside and also lost from the outer surface by radiation. After a certain number of turns an equilibrium may be reached at a particular position between the loss in heat and its generation. At this stage of deformation the temperature distribution across the specimen section will be such as in Fig. 3.39,b. The maximum temperature across the section will then tend to move further inside the section. Going on in this way, after a large number of turns it may be considered that the highest temperature will be near specimen axis, such as in Fig. 3.39,c. Because the energy required for deformation decreases and the coefficent of heat transmission by radiation increases with increasing the temperature, the first distribution (a) will be present at relatively low temperatures and small number of revolutions, the second at higher temperatures and larger numbers of revolutions, and the third at very high temperatures and very large number of revolutions. Of course, distribution of temperature in the way shown above is purely relative, and would also be markedly influenced by strain rate. Although the strain rate may change the values of axial stress it would not alter the shape of the curves shown in Fig. 3.38.

Due to variation in temperature and possibly composition across the specimen section, a variation in phases present at a particular temperature may also be possible. It was shown before that on passing from α to γ range a steep change in axial

force occurs. Hence, a variation in temperature and phase content may alter the form of stress distribution across the specimen section. Of course, this effect would only be pronounced in the vicinity of the transformation range.

Another factor which may also affect stress distribution across the specimen section is the nonuniformity of temperature along the specimen gauge. Even if nonuniformity is not present at the beginning of deformation it may appear during deformation. It has already been shown that due to deformation the specimen temperature rises and becomes higher than its surroundings and, in particular higher than the shoulders of the specimen. A greater loss in heat occurs near specimen shoulder and the temperature will thus be lower than at the mid-gauge, as shown schematically in Fig. 3.40,a. The difference in temperature will result in inhomogeneous deformation along the specimen gauge. The torque T has the same value in sections I and II, so from the equation

$$T = \frac{2\pi}{3} r_I^3 \tau_I = \frac{2\pi}{3} r_{II}^3 \tau_{II} \qquad 3.23$$

where r_I and r_{II} are the specimen radius in the sections I and II;

τ_I and τ_{II} - shear stresses in the sections I and II,

it is clear that because $r_I = r_{II}$ (at the beginning of deformation) τ_I must have the same value as τ_{II}. But

$$\tau_I = f(\theta_I / t_I) \qquad 3.24,a$$

$$\tau_{II} = f(\theta_{II} / t_{II}) \qquad 3.24,b$$

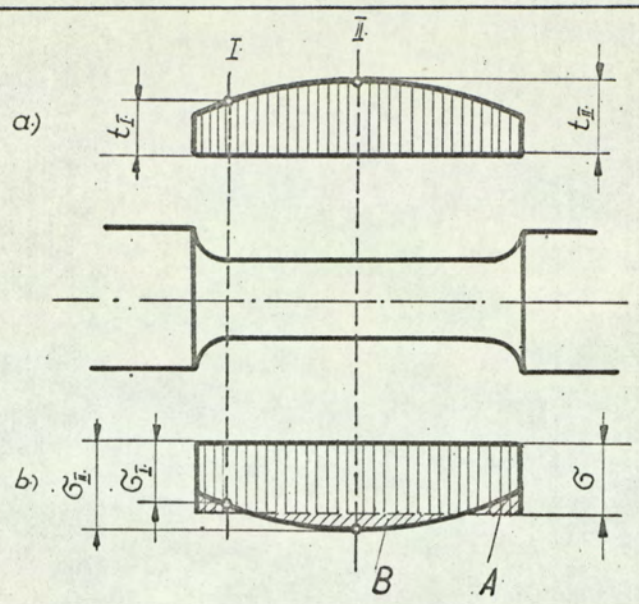

Fig. 3.40. Scheme of temperature variation (a) and σ variation (b) along the specimen gauge during deformation.

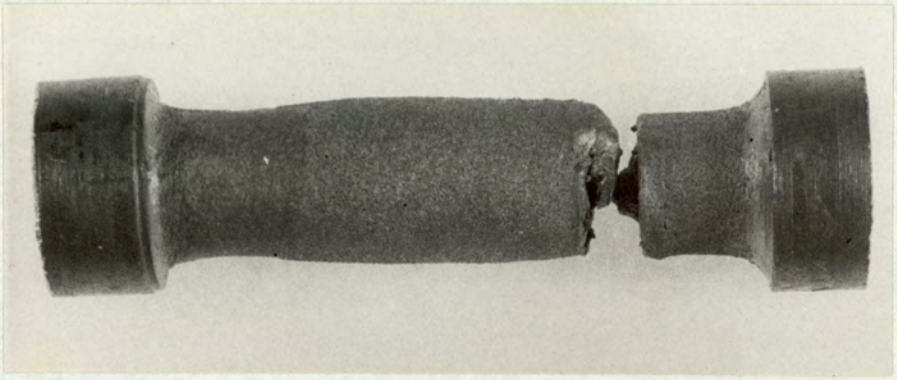

Fig. 3.41. Specimen deformed at 1200°C in special conditions.

where t_I and t_{II} are temperatures in the section I and II.

$\bar{\theta}_I$ and $\bar{\theta}_{II}$ - strain rates in the section I and II.

and because $t_I < t_{II}$, θ_{II} will be greater the θ_I.

Because the ratio $\frac{\sigma}{\bar{\sigma}}$ increases with temperature (for solid specimens) and at high temperature also with strain rate it is to be expected that σ_I (corresponding to the conditions in sectionI) would be smaller than σ_{II} (corresponding to the conditions in section II). However, during deformation the axial force must be the same along the whole specimen gauge, so that true axial stress σ will be bigger than σ_I in the section I and smaller than σ_{II} in the section II, varying along the specimen gauge as illustrated in Fig. 3.40,b.

The difference between the real axial stress σ and that corresponding to the true conditions of testing will produce elongation in the portion A (where $\sigma > \sigma_I$) and compression in the portion B (where $\sigma < \sigma_{II}$). This implies that during deformation in the presence of an axial force, due to the difference in temperature between the section I and II, γ_I tends to decrease and γ_{II} to increase. In Fig. 3.41 is shown such a specimen, deformed at 1200°C with 480 rev/min. In this instance, in order to create a bigger difference in temperature between the sections I and II, the current for high frequency heating was stopped when the deformation began. Alterations in diameters of specimens can often be seen especially in the temperature range of 1100 - 1200°C after a fairly large number of revolutions. This

phenomenon appears usually in this temperature range because a difference in temperature along the specimen gauge is possible (the energy required for deformation being high) and a high ratio $\frac{\sigma}{\tau}$ exists. In this special case axial stress distribution on the specimen cross section would be such as is schematically shown in Fig. 3.42.

CONCLUSIONS

1) The equations for axial stress distribution given in the theory of the plasticity, valied for ideal materials, cannot be applied in a simple way to hot torsion testing.

2) Axial stress on the specimen cross section starts from outside and develops towards inside. The value of tensile stress at specimen axis is smaller than at the surface and, at lower temperatures and small numbers of turns, it may even be of opposite sign i.e. in compression.

3) Axial stress distribution may be altered by the differences in temperature across the specimen section and along its length, which may be created during deformation. It may also be influenced by differences in phases content, composition and strain rate, but in general to a much smaller degree.

4) The difference in stress magnitude and distribution, created by the difference in temperature along the specimen gauge, may result in nonuniformity of deformation and consequently a change in specimen geometry.

3.2.3 Axial Force Influence on the Hot-Workability Measurement

It is well known that any metal will sustain a higher

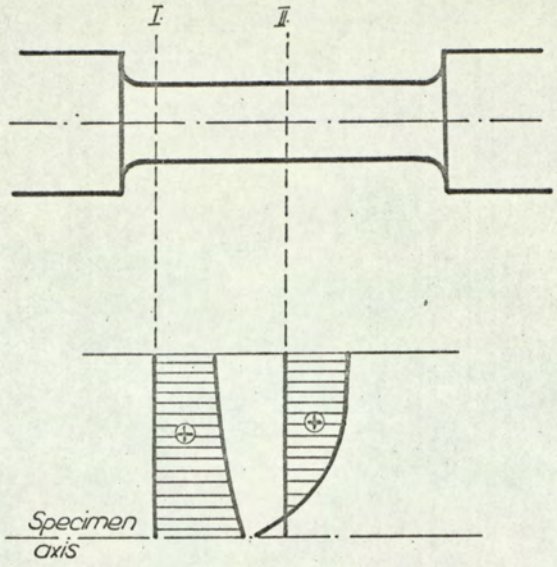

Fig. 3.42. Axial stress distribution in the conditions of nonuniform temperature along the specimen gauge.

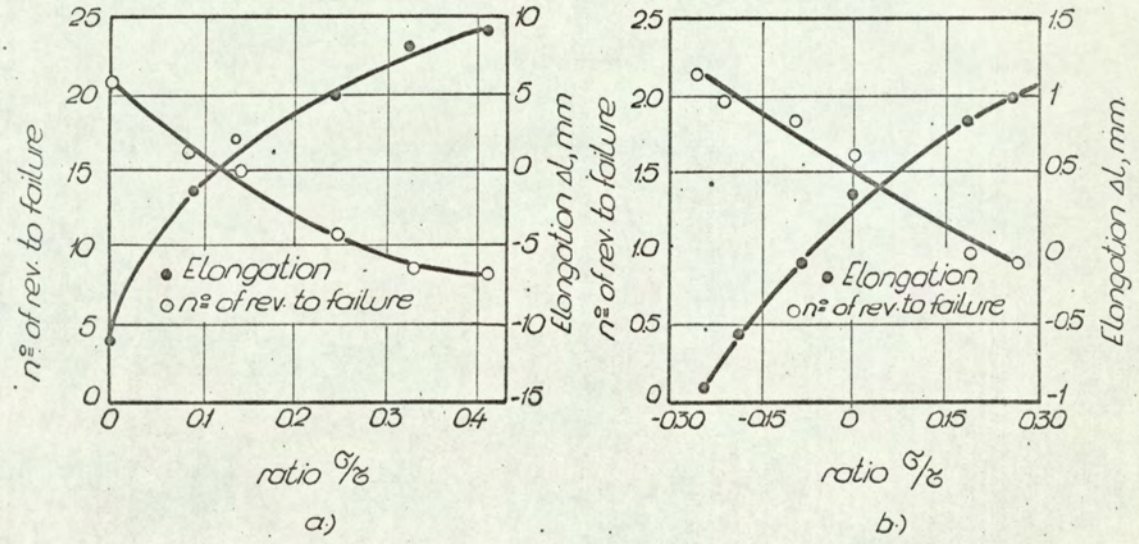

Fig. 3.43. Variation of the number of revolutions to failure and elongation with the ratio σ/σ
a - tested at 900°C; b - test at the room temperature.

rate of deformation if deformed by compression than by tension. Bridgman (20) deforming specimens by tension and compression under high hydrostatic pressure at room temperature observed that the ductility increased almost linearly with increasing hydrostatic pressure. Making tests by torsion combined with compression he also observed an increase in ductility for cast iron. Hughes (45) using torsion test for hot-workability measurement, observing that the ductility of the tested steels fell at temperatures at which in tensile tests it still increased, suggested that, with other factors, the presence of axial force during twisting amy be responsible of this decrease in ductility. Guenssier and Castro (47) stated that the torsion test has many advantages for hot-workability measurement, but because of the presence of axial force, with various value for different materials, the test cannot give true values for ductility.

Although it was agreed that axial force may have some influence on the hot-workability measurement by torsion, no study was made on this aspect.

Two questions arise from this problem, namely:-

1) To what extent does force affect the results of hot ductility measurement, and is its influence samll enough to be neglected?

2) If axial force cannot be neglected how can it be taken into account for a better expression of the hot workability measurement as determined by the hot torsion test?

EXPERIMENTS, RESULTS AND DISCUSSION

To study the first question noted above, specimens of

$\frac{3}{8}$" dia. and $1\frac{1}{2}$" length and $\frac{1}{4}$" dia. and 1" length were used, made from steel 4. A batch from the first size was deformed at 900°C, and the second size deformed at room temperature. The smaller diameter had to be used for room temperature tests due to limitations of stress measurement on the testing machine. Larger sizes at higher temperatures enabled more accurate measurements to be made. A few specimens of the first size were also deformed at 700, 800, 1000 and 1100°C. For deformation at room temperature the torsion was combined with tension and compression. For deformation at high temperatures the torsion was conbined with tension only because when no axial force was present the specimen became shorter; no successful test could be made with applied compression. Axial force both at room temperature and high temperature was chosen such that values for $\frac{\sigma}{\sigma}$ were obtained corresponding to those that appear during deformation at high temperatures (maximum 0.45). The steel used had a characteristic that its ductility was relatively low, the greatest number of revolutions to failure being 21 at 900°C.

From the above experiments the number of revolutions to failure and elongation were plotted as a function of axial force (indicated by $\frac{\sigma}{\sigma}$). These values are given in Fig. 3.43,a. for the test made at 900°C and in Fig. 3.43,b for the test made at room temperature. In Fig. 3.44 is shown the variation of the ratio $\frac{\sigma}{\sigma}$ against the ratio $\frac{\Delta l}{n}$ (Δl being the elongation and n - the number of revolution to failure). The specimens deformed at 900°C with various values of axial force are shown in Fig. 3.45.

From the above results it can be seen that the number of

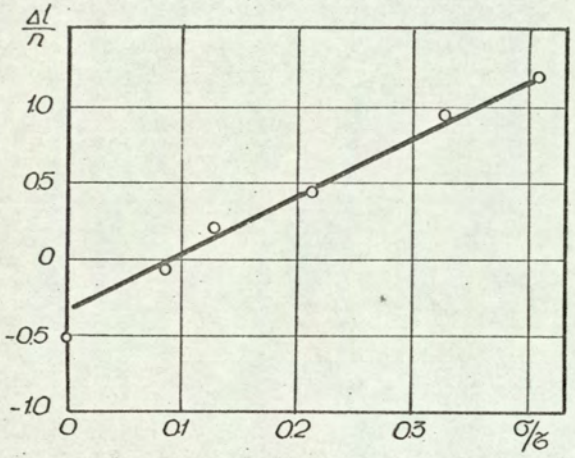

Fig.3.44. Variation of the ratio $\frac{\Delta l}{n}$ with the ratio $\frac{\sigma}{\sigma_c}$ for specimens deformed at 900°C.

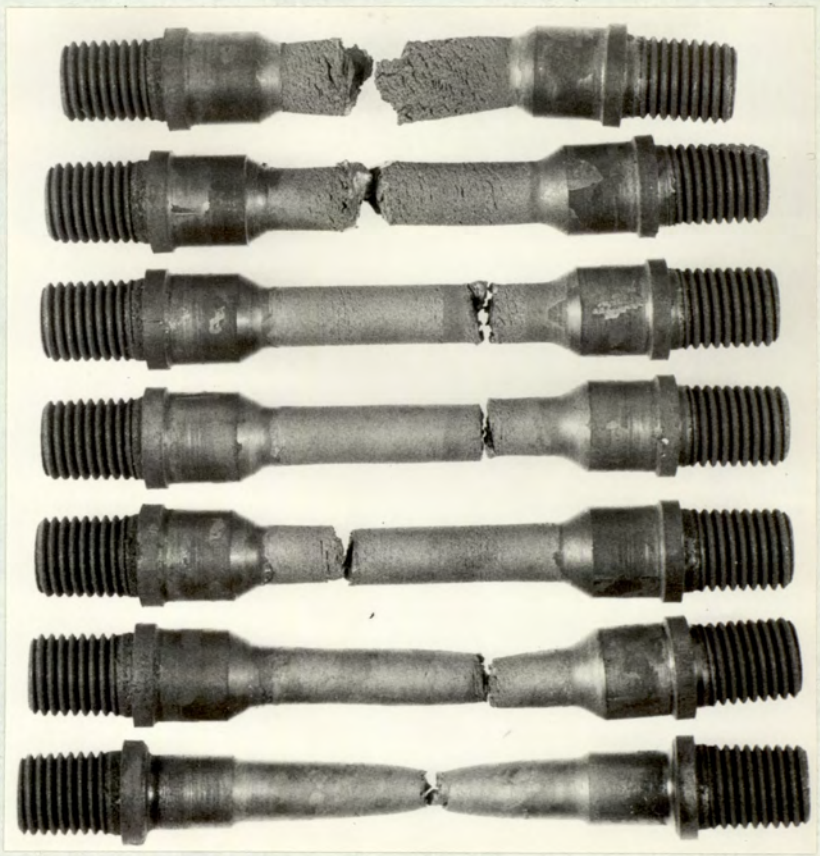

Fig.3.45. Specimens deformed at 900°C with various values of axial force.

revolutions to failure vary appreciably by varying the axial force. Hence, for a more reliable evaluation of hot-workability measurement by torsion test it is clearly necessary to take account of the axial force influence.

With a certain degree of approximation it should be possible to combine the deformation obtained by torsion with elongation, using an equation of the form:

$$\frac{\pi d_o n_o}{l_o} = \frac{\pi d_x n_x}{l_x} + C_1 \frac{\Delta l_x}{l_o} \qquad 3.25$$

where do and lo are initial dimensions of the specimens;

dx and lx - medium dimensions of the elongated specimens;

Δ lx - elongation for given conditions;

no - number of revolutions to failure for Δ lx = 0;

nx - number of revolutions to failure for Δ lx;

C_1 - coefficent.

The coefficent C_1 may be calculated with the equation 3.25 put in the form

$$C_1 = \frac{\pi l_o}{\Delta l_x}\left(\frac{d_o n_o}{l_o} - \frac{d_x n_x}{l_x}\right) \qquad 3.25,a$$

In Fig. 3.46,a is shown the variation of the coefficent C_1 with the ratio $\frac{\sigma}{\tau}$. From this figure it can be seen that C_1 increases when $\frac{\sigma}{\tau}$ increases. Thus on increasing the ratio σ/τ there is an increase the nonuniformity in deformation. In fact, reference to Fig. 3.45 reveals that for high values of $\frac{\sigma}{\tau}$ a neck appeared. Hence it would be better not to use the values of Δ lx measured directly for calculating C_1 but a $\Delta l x^1$ corresponding to reduction in area. For this purpose, considering the specimen volume

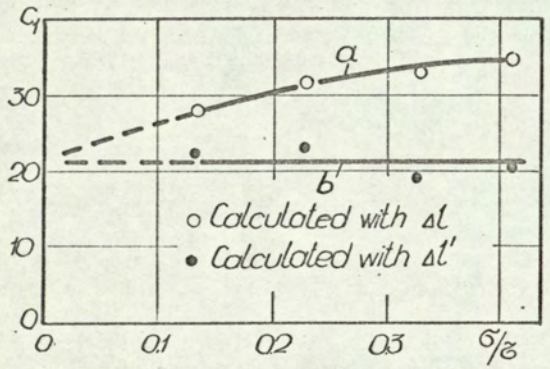

Fig.3.46. Variation of the coefficient c_1 with the ratio δ/ℓ

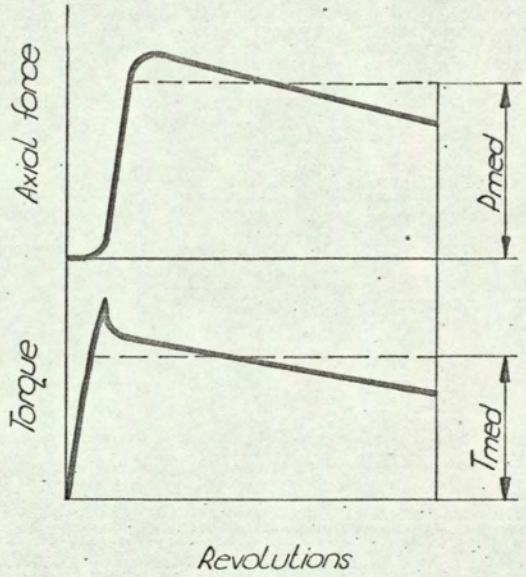

Fig.3.47. Medium values for torque and axial force.

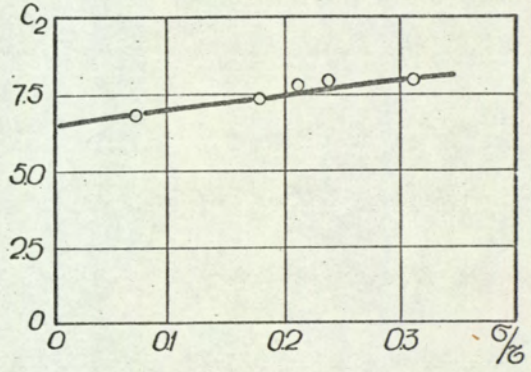

Fig.3.48. Variation of the coefficient c_2 with the ratio δ/ℓ.

constant during deformation, from the relation

$$V = A_o l_o = A_x l_x \qquad 3.26$$

where A_o and l_o are initial area and length;

A_x and l_x - area and length at a given moment, can be obtained a connection between the elongation ratio $\frac{l_x}{l_o}$ and reduction in area ratio $\frac{A_o}{A_x}$ in the following way:-

$$\frac{A_o}{A_x} = \frac{A_o}{A_x + A_o - A_o} = \frac{1}{\frac{A_o}{A_o} - \frac{A_o - A_x}{A_o}} = \frac{1}{1 - \psi}$$

and

$$\frac{l_x}{l_o} = \frac{l_x + l_o - l_o}{l_o} = \frac{l_o}{l_o} + \frac{l_x - l_o}{l_o} = 1 + \epsilon$$

from which

$$\epsilon = \frac{1}{1 - \psi} - 1$$

and hence:-

$$\Delta l_x^1 = \left(\frac{1}{1 - \psi} - 1 \right) l_o \qquad 3.27$$

The variation of C_1^1 (calculated with the equation 3.25,a by using Δl_x^1 instead of Δl) with the ratio ϵ/γ is shown in Fig. 3.46,b. Calculated in above conditions C_1 does not vary much with ϵ/γ and in this way a connection between the number of revolutions to failure and elongation may be possible.

When the specimen is fixed during deformation by torsion no elongation occurs but an axial force appears which can be measured. Suppose that the normal state of the specimen is when axial force is zero, as it is when unrestrained. In this state of

course a change in length occurs, but it is a reasonable assumption that this change in length is proportional to the ratio σ/ε. In this way Δl may be calculated knowing the value of σ/ε using Hill's equation (78) of the form

$$r \frac{d\theta}{dl} = 3 \frac{\varepsilon}{\sigma}, \qquad 3.28$$

where r is the specimen radius;

$d\theta$ - the change in the angle of twist;

dl - the change in the specimen length.

Because Fig. 3.44 shows that the ratio $\Delta\varepsilon/\varepsilon$ varies with the ratio σ/ε almost linearly, it may be approximatly true to express:-

$$\frac{d\theta}{dl} = \frac{\Delta\theta}{\Delta l}$$

It has already been shown that the equation 3.28 was deduced neglecting the radial and circumferential stresses, and in such special conditions does not fit. For instance, from the equation

$$\varepsilon x = \phi \left[\sigma_x - \vartheta(\sigma_s + \sigma_\theta)\right] \qquad 3.29$$

where εx is elongation ratio;

σx, σ_s and σ_θ - axial, radial and circumferential stresses;

ϑ - Poisson's ratio,

in the condition when εx is 0, σx is not zero, hence σ_ρ and σ_θ cannot be zero. Furthermore, because σ_ρ and σ_θ are acting, the real value of Δl, corresponding to a ratio σ/ε is smaller than that given by the equation 3.28 and for calculating Δl; hence instead of the constant 3 a higher value needs to be used.

It is not possible to determine precisely the values of σ_s, σ_θ and γ (or some equivalent ratio holding for plastic deformation rather than elastic), and deduce a precise equation similar to 3.28 with a suitable coefficent for these conditions. However, it is known that $\Delta\theta/\gamma_1$ varies almost linearly (for a given value of r) with σ/τ, so the equation 3.28 may be written in the form:

$$r\frac{\Delta\theta}{\Delta\ell} = C_2\frac{\tau}{\sigma} \qquad 3.30$$

where C_2 is a coefficent which takes account of all factors in these special conditions of deformation.

The value of C_2 was determined in the following way: for a given temperature a specimen kept fixed was deformed and the ratio $\frac{\sigma}{\tau}$ measured (average values for torque and axial force were obtained as shown in Fig. 3.47), and another specimen was deformed free and the ratio $\Delta\ell/\Delta\theta$ measured. The coefficent C_2 was then calculated by using the equation 3.30 in the form:

$$C_2 = r\frac{\Delta\theta}{\Delta\ell}\frac{\sigma}{\tau} \qquad 3.30,a$$

The variation of C_2 with the ratio σ/τ (determined at various temperatures) is shown in Fig. 3.48, p117 which shows that this coefficent varies with the ratio σ/τ almost linearly, rising from just over 6 (at room temperature) to 8 at high temperatures where maximum values of σ/τ are observed. Knowing now the value of C_2 and measuring the ratio $\frac{\sigma}{\tau}$ the value of Δ lx can be determined from the equation 3.30 written in the form:

$$\Delta\,\text{lx} = \frac{\gamma}{C_2}\frac{\Delta\theta}{\tau}\frac{\sigma}{\tau} \qquad 3.30,b$$

If in the equation 3.25 instead of Δl_x we put its value from the equation 3.30,b we have

$$\frac{\pi \, d_o \, n_o}{l_o} = \frac{\pi d_x n_x}{l_x} + \frac{C_1}{C_2} \cdot \frac{\gamma \, \Delta\theta}{l_o} \cdot \frac{\sigma}{\tau} \qquad 3.31$$

When the specimen is fixed and its dimensions are unchanged $d_o = d_x = 2r$ and $l_o = l_x$. Thus writing $\frac{C_1}{C_2} = C$ and $\Delta\theta = 2\pi n_x$ and inserting all the above values, in the equation 3.31.

$$n_o = n_x \left(1 + C \frac{\sigma}{\tau}\right) \qquad 3.32.$$

where n_o is the number of revolutions to failure which takes account of the axial force influence on ductility,

n_x - the number of revolutions to failure measured directly;

C - coefficent which may depend on the material and ductility, and for the mild steel tested its value lies between 2.5 and 3;

σ - average value of axial stress (positive for tensile stress and negative for compression stress);

τ - average value of shear stress.

CONCLUSIONS

1) Axial force significantly affects hot-workability measurement and in conditions of high values of the ratio σ/τ large errors result if it is neglected. The true ductility of the steels used in which an axial force of tension appears during twisting, is greater than that measured directly, the opposite would hold in

those materials in which compression force appears. Hence the true peak of ductility against temperature exists at higher temperatures than normally indicated by the torsion test for those materials at which an axial tensile force is present.

2) An approximate relationship between the number of revolutions to failure and the ratio $\sigma/\bar{\sigma}$ can be established which may be used to correct the results of hot workability measurement by torsion in the presence of an axial force.

3.3 The Mode of Fracture of Specimens in the Torsion Test

INTRODUCTION

The results of Hughes (45), Tegart and Reynolds (50) regarding manner of fracture are very complex. Fracture would normally be expected to start from the surface where the deformation is greatest and it is therefore somewhat surprising when the fracture starts from the interior. The appearance of cracks at the mid radius position might be attributed to axial stress as suggested by Hughes, but from Tegart and Reynolds results it can be seen that they also form within the specimen in the temperature range 800 - 900°C where axial force has only a very small value. However, comparing the ductility variation against temperature with the mode of fracture and taking account of the fact that the temperature

distribution may change over the cross section during deformation, which may produce changes in structure, axial stress night well be associated with appearance of cracks. For example, with iron A (Fig. 2.31) the number of revolutions to failure at 870°C was about ten times greater than at 700°C, and about twenty times that at 920°C. Allowing that the temperature varies on the specimen cross section during deformation, cracks will be expected to appear first in that place where the temperature corresponds to the lowest ductility. Reynolds and Tegart suggested that the cracks appearance inside may be associated with phase transformation, but it is surprising that the cracks appear inside also at temperatures over 1100°C in pure irons, where no phase transformation occurs, and in similar manner as in Hughes' experiments.

The fact that cracks appear in torsion tests in this complex way even though they may be explained for the temperature range 800 - 850°C for pure irons, shows that the reason(s) for their appearance at temperatures over 1100°C in some steels only is still obscure. However, from the above results it may be concluded that three main factors could be responsible for the formation of internal cracks, viz:-

1) Phase transformation.
2) Axial stress distribution.
3) Fibre structure, particularly in relation to impurity content.

The first factor seems to be quite clear and may explain in the above way why the cracks appear inside in the temperature

range where $\alpha \rightarrow \gamma$ transformation takes place. With regard to the second factor it has already been shown that in these conditions of deformation the axial stress is not usually greatest, as supposed by Hughes, at the specimen axis, but at the outside. Although the ductility is affected by axial force differences in the ratio $\frac{\sigma}{\bar{\sigma}}$ across the specimen section (due to minor factors already shown) it cannot be such as to cause the fracture to start from inside, and this cannot be the main reason. It could be that the difference in impurities or inclusions between the inside and outside causes the material to behave differently in the two places. This factor may also be associated with axial force and the change in orientation brought about by the twisting.

EXPERIMENTS AND RESULTS

Specimens with $\frac{3}{8}$" dia. and $1\frac{1}{2}$" length made from steels 1 and 2 were used. In specimens made from steel 1 the cracks appeared first outside up to about 1150°C and around 1200°C they appeared first inside. In Fig. 3.49 ave shown three specimens with their longitudinal sections, which were deformed at 750, 950 and 1220°C respectively at 75 rev/min. In specimens made from steel 2 the cracks started from outside at all testing temperatures, and no interior cracking was detected of the type shown for steel 1.

The cracks which started from outside in Steel 1 were approximately perpendicular to the specimen axis and were not continuous around the specimen but tended to lie on a helix when well developed. Eventually these extend, link together and produce

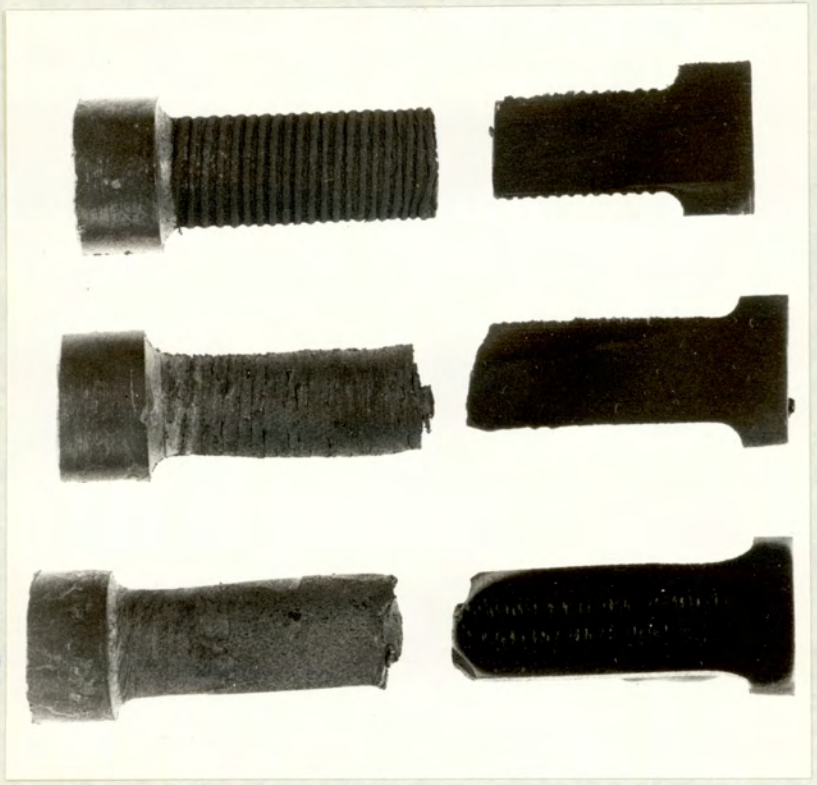

Fig. 3.49 Specimens made from steel 1 and deformed with 75 rev/min. at various temperatures.
a - 750°C, n = 17 rev; b - 950°C, n = 24 rev; c - 1220°C, n = 49 rev.
surface (left); cross section (right)

Fig. 3.50 Crack development on surface of a specimen deformed at 750°C with 75 rev/min, x 6

the fracture. The number of turns of the helix along the gauge length was equal to or multiples of the number of revolutions used for deformation. Cracks developed on a specimen deformed at 750°C can be seen in Fig. 3.50

Electron probe microanalysis of the outer region of the specimen deformed at 750°C showed that the cracks were not associated with segregation of manganese, silicon, sulphur or phosphorus, all of these elements being quite uniformly distributed as shown in Fig. 3.51 for manganese, which is typical of the results also obtained for silicon, sulphur and phosphorus.

To study the cracks which form in the interior the following experiments were made:-

1) A specimen was deformed at 1200°C at 75 rev/min. After cooling a longitudinal section at the specimen axis was taken to observe the cracks formed along the specimen. It was found that individual cracks started and developed from points where impurities were agglomorated. In Fig. 3.52 such a crack is shown which formed by joining two points and another one which is developing in the same manner. Microanalysis showed that these cracks are associated with manganese and silicon rich regions. No increase in sulphur or phosphorus could be seen in the region of cracks such as shown in Fig. 3.53.

2) A specimen was deformed at 1200°C at 75 rev/min and after 32 revolutions (about $\frac{3}{4}$ from the number of revolutions to failure) an external axial force about 4 kg greater than that which appeared during deformation was applied, causing extra elongation to take

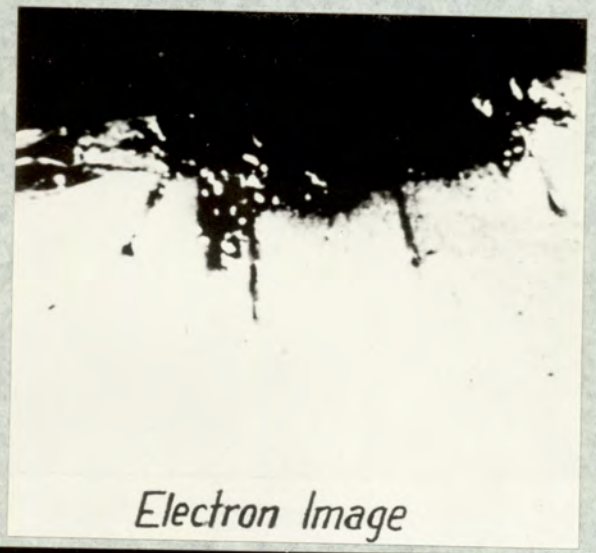

Fig. 3.51. Electron image and manganese distribution in the outer part of the specimen deformed at 750°C (x200)

Fig. 3.52. Crack formation in specimen deformed at 1200°C (x100)

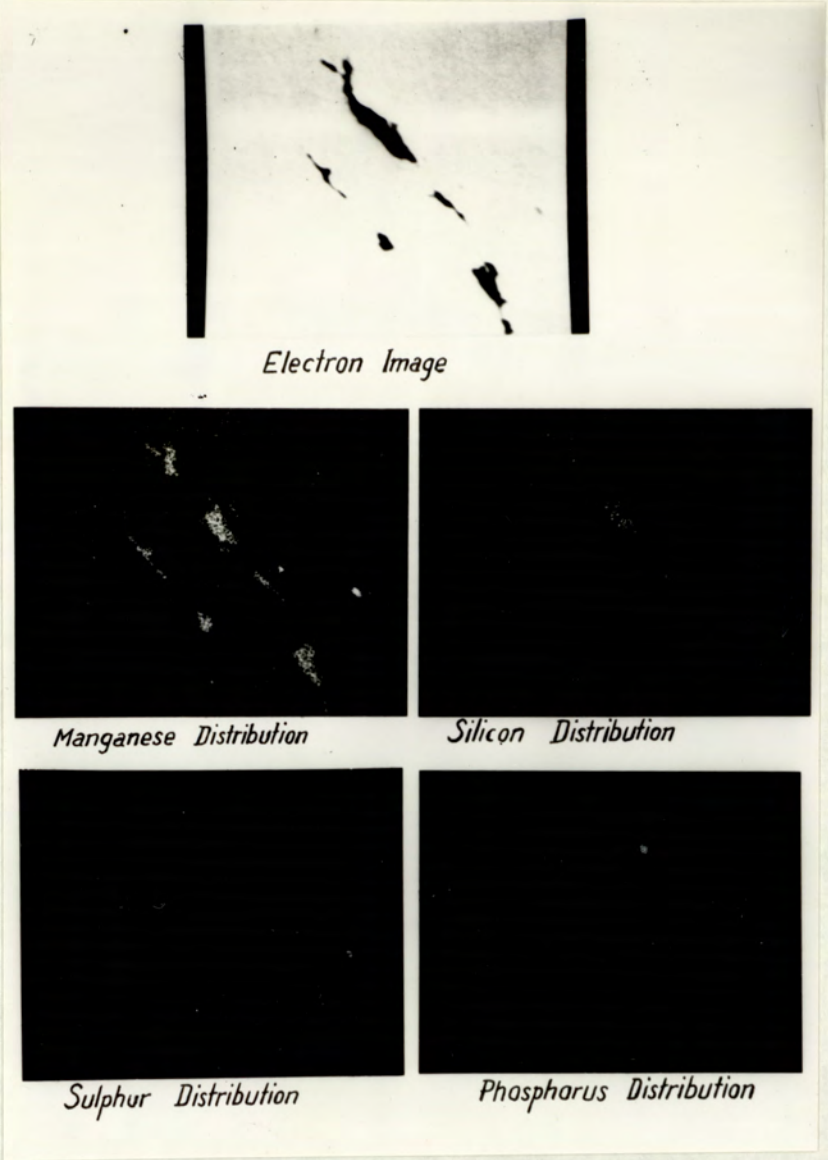

Fig. 3.53. Electron image and manganese, silicon, sulphur and phosphorus distribution in the cracks region of the specimen deformed at 1200°C (x300)

place. This resulted in cracks appearing along the specimen axis as in Fig. 3.54,a. In Fig. 3.54,b the etched macrostructure of a specimen deformed normally at 950°C is also shown, from which it will be observed that the fine grained bands and the fracture itself exhibit an almost identical pattern to the cracking developed when the extra axial force was applied at 1200°C.

3) A specimen was deformed at 1200°C with 196 rev/min. After 30 revolutions the heating current was decreased in order to create a difference in temperature between the regions near shoulder and the mid-gauge after which an axial force of approximately 3 kg more than that which was already present was applied, again causing slight elongation to take place. The distribution of cracks from near shoulder (on the left) towards the middle of gauge (on the right) are shown in Fig. 3.55.

DISCUSSION OF RESULTS

The fact that the cracks from outside are orientated perpendicular on the specimen axis and are not associated with impurities shows that they are produced by shear stress and appear after a certain number of revolutions corresponding to the ductility of the material in this place. However, the fact that they form sometimes on a helix shows that various layers along the specimen length (before twisting) may have different content in certain elements which causes different behaviour on deformation from the remainder. From Fig. 3.49 it may be deduced that the differences in deformation between these banded layers is greater in the temperature range

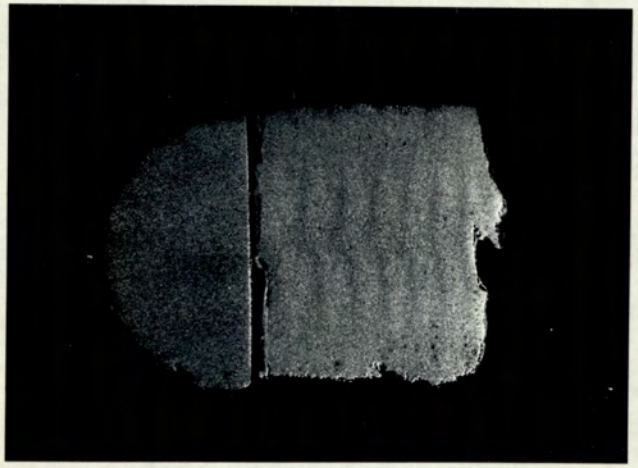

Fig. 3.54. Comparison between cracks which appear at 1200°C (a) and fibre structure reorientated by deforming at 900°C (b)

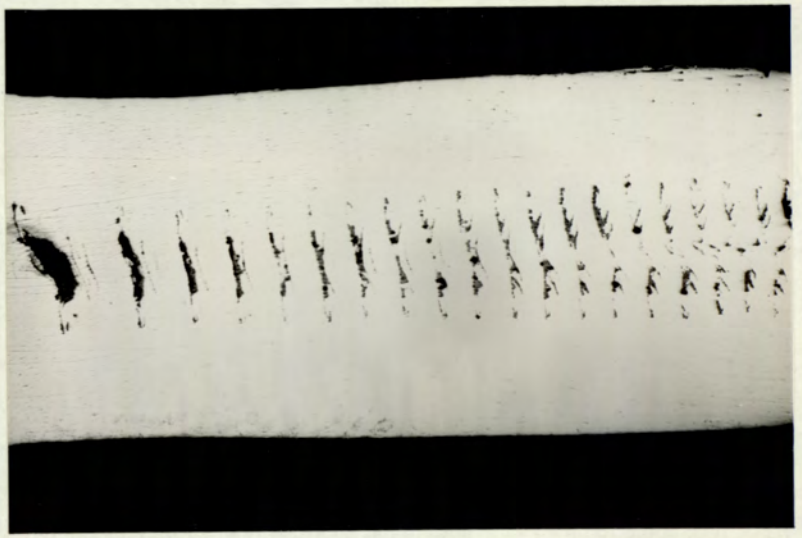

Fig. 3.55 Crack distribution in specimen deformed at 1200°C under special conditions

800 - 1000°C than at the temperatures over 1150°C.

From Fig. 3.54 it can clearly be seen that there is a connection between the cracks which form inside and the reorientated fibre structure. In conjunction with Fig. 3.53 it would also appear that these cracks are associated with manganese and silicon. It is to be expected that more inclusions would be present near the axis of the bar, and the above results confirm that there is more manganese and silicon inside than outside, and this affects the ductility over 1150°C to a marked degree.

Cracks appear at the specimen axis when a higher axial force than usual appears during deformation, which reveals that these cracks are very sensitive to axial force, being fully in agreement with Hughes' suggestions. Furthermore, because these cracks appear at temperatures over about 1150°C it follows that the ductility of these layers in this temperature range become very much reduced compared with the rest of material. Hence, when the uniformity in deformation of the various layers increases near the surface at higher temperatures, it apparently decreases inside. However, this also implies that some elements or inclusions are responsible for lowering ductility in the various layers outside at lower temperatures and others inside at higher temperatures. This conclusion agrees with the pattern of distribution shown in Fig. 3.51 and 3.53.

From Fig. 3.55 it can be seen that cracks from the specimen axis are present near the shoulder (where the tensile

stress is higher at the axis),but spread out towards the mid gauge (where the tensile stress value is lower at the axis corresponding to stress distribution shown in Fig. 3.38 and 3.42). Thus it seems that cracks appear usually on both sides of specimen axis due partly to the fact that at the specimen axis axial stress has a smaller value than at the mid-radius, being in full agreement with stress distribution already discussed in the present work. However, Fig. 3.54 shows that fibre structure reorientated by twisting is not quite transverse to the specimen axis as it is outside, and because of this the axialregion is less sensitive to axial stress than the outside. This explanation is also in agreement with Hughes' suggestion regarding the mode of cracking.

From the above results it is to be pointed out that the cracks which form in the interior are first due to impurities and second due to axial stress. Hence, materials with high contents of manganese and silicon at the specimen axis may crack at the axis after a relatively large number of revolutions and the ductility measured will be largely determined by the type and distribution of impurities.

Fracture in specimens deformed by torsion exhibit characteristics not only across the specimen gauge but also along it. In the experiments made the specimens quite often broke near the shoulder. Two ranges of temperatures were found where this kind of fracture occurred.

1) In and near $\alpha \rightarrow \gamma$ transformation range

2) Between 1100 - 1250°C

One explanation could be found for both ranges of temperature, namely the difference in temperature developed along the specimen gauge during deformation. It was shown before that during deformation the temperature increases more at the mid-gauge and less near shoulder. Hence, near the transformation range where the resistance to deformation increases and ductility decreases steeply with rising temperature, the fracture may readily start from near the shoulder. In the temperature range 1100 - 1250°C due to difference in temperature along the specimen gauge a different axial stress distribution is present near the shoulder and at the mid-gauge (Fig. 3.42). For materials with high ductility the fracture will not start from the mid-gauge where the deformation is greater but from inside near shoulder in a section where a combination of shear and tensile deformation becomes critical. This type of fracture is therefore due largely to tensile stress and shows the marked effect that axial stress has on ductility measured by torsion. But because this fracture depends on axial stress distribution near shoulder and mid-gauge, which in turn depends of the difference in temperature along the specimen gauge, it follows that the bigger this difference in temperature in the presence of high value of axial stress the greater is the possibility of the fracture occurring near the shoulder. Because the temperature gradient will become steeper with increasing strain rate and number of revolutions to failure, it also follows that this type of fracture arises only in these

conditions of testing.

The difference in temperature along the specimen gauge also depends on the ratio $\frac{d_1}{d}$ of the specimen (Fig. 3.11). The bigger this ratio the greater is the temperature gradient along the specimen gauge, (the loss in heat from gauge to shoulder being proportional to this ratio). For this reason the ratio d_1/d should be kept as small as possible, consistent with confining the deformation to the gauge length.

It was shown before that this type of fracture was observed only at temperatures above 1100°C. Three explanations may be put forward to explain its appearance in this range viz:-

1) an increase in temperature during deformation is possible, due to the material still having a relatively high resistance to deformation and requiring appreciable energy which changes into heat;

2) a relatively high axial tensile stress is present;

3) a steep rise in ductility occurs by increasing the temperature, hence, at the mid-gauge the ductility is higher than near shoulder.

Between 900 and 1100°C the deformation is quite uniform along the specimen gauge and the fracture may start from any place.

In Fig. 3.56 three specimens are shown which exibit the three types of fracture discussed above. The upper specimen (Fig. 3.56,a) was deformed at 800°C and the fracture started from both sides near shoulder. The middle specimen (Fig. 3.56,b) was

Fig. 3.56. Three specimens deformed at various temperatures, × 1,7.
a-t = 800°C, n = 14 rev; b-t = 950°C, n = 23 rev.
c-t = 1150°C, n = 93 rev.

(Specimen a and b were made from steel 1 and specimen c from steel 2.)

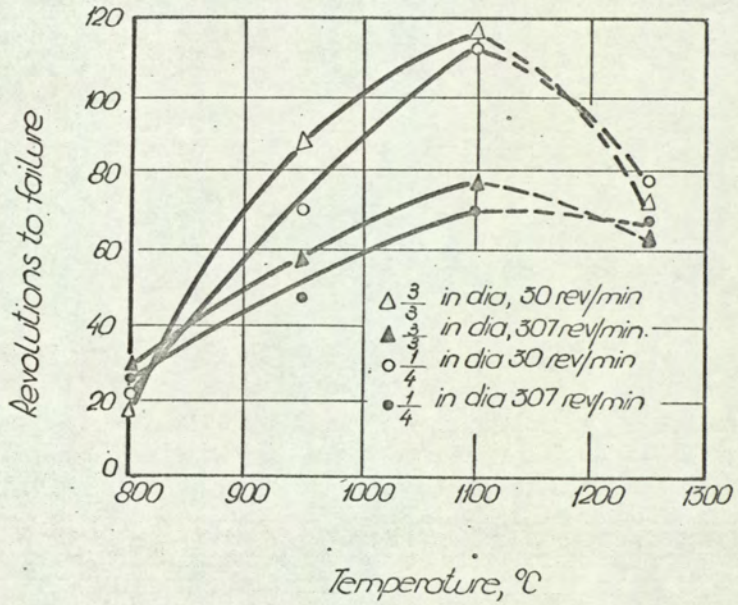

Fig. 3.57. Effect of temperature on the number of revolutions to failure for specimens made from steel 2.

deformed at 950°C, the deformation being quite uniform, and fracture started in several places. The lower specimen (Fig. 3.56,c) was deformed at 1150°C, producing in a change in its shape and fracture starting near the shoulder. The first two specimens illustrated were made from steel 1 and third from steel 2.

CONCLUSIONS

1) The cracks which appear outside are due to shear strain as a normal consequence of deformation when the maximum ductility is attained. When they appear in a helical form it means that there are layers with different contents in certain elements which give them a lower ductility compared with the rest of the material. This reduction in ductility is particularly apparent at lower temperatures (below 1150°C). At higher temperatures the difference in ductility between various layers outside seems to be much less. Cracks starting from outside are not associated directly with manganese, silicon, sulphur and phosphorus rich regions or phases.

2) The cracks which form inside at temperatures over 1150°C are associated with manganese and slicon inclusions and tend to lie along the reorientated fibre structure. These cracks are opened up by tensile stresses which may cause them to develop into large cavities. The fact that the cracks appear at about the mid-radius shows that these specimens made from rolled bar were richer in the above elements towards their axis, and the manganese and silicon rich inclusions are weaker and less ductile than the matrix in this range

of temperature. The cracks appear usually in both sides of specimen axis due to two main reasons:

(a) at the specimen axis tensile stress has a smaller value than at the mid-radius, hence this place is less susceptible to crack initiation and development;

(b) the original fibre structure is less reorientated at the specimen axis compared with the outside, hence axial stress does not act perpendicular to the fibre structure as it does nearer the outside.

3) In the temperature range where transformation $\alpha \rightarrow \gamma$ occurs and near it and also between approximately 1100 - 1250°C the fracture often starts near the shoulder. This kind of fracture is due to a difference in temperature between the mid-gauge and near shoulder. In and near the transformation range the fracture appears near shoulder because a small variation in temperature results in a big difference in resistance to deformation or in ductility between the two places. In the temperature range 1100 - 1250°C the fracture starts near the shoulder due to variation in axial stress distribution and also due to difference in ductility between the two places.

In order to create a smaller difference in temperature along the specimen gauge during deformation the ratio of shoulder diameter to gauge diameter of the specimen should be as small as practicable.

3.4 The Influence of the Specimen Size on the Hot Workability Measurement

Introduction

Many investigators have studied the influence of specimen size on hot-working characteristics of their materials, notably Hughes (45), Reynolds and Tegart (50).

Hughes tested specimens of $\frac{1}{2}$" and $\frac{1}{4}$" diameter having the same length and deformed them at various speeds, at various temperatures, his results being shown in Fig. 2.28. From this figure if the ratio $\frac{\pi n d}{l}$ is used (d being the specimen diameter, l - its length and n - the number of revolutions to failure) it appears that by increasing the specimen diameter the ductility increases. On the basis of experiments with a steel which exhibited higher ductility on increasing the strain rate up to a certain temperature, he connected the increment in ductility due to increase in specimen diameter with the rise in strain rate which was valid for the same number of rev/min).

Reynolds and Tegart used specimens of various diameters but the same ratio l/d, and also with the same diameters and various ratios l/d. Their results for specimens with the same diameter and different ratios deformed at various temperatures are given in Table 2.VI. From their results it appears that there is no proportion between the ratio l/d and the number of revolutions to failure.

Because Hughes did not maintain the same strain rate when he varied the specimen diameter, the increment

in ductility could be attributed to the increment in strain rate. Reynolds and Tegart did not specify whether or not they kept the strain rate constant by varying the ratio ℓ/d but they claimed that strain rate and specimen size affect the ductility. Hence, the influence of specimen size on the hot-workability measurement is not known for conditions of the same strain rate. Therefore this aspect was studied in the present work taking account of the previously obtained results.

EXPERIMENTS AND RESULTS

To study the influence of specimen diameter on the hot workability measurement two sizes of specimens were used; of $\frac{1}{4}$" and $\frac{3}{8}$" diameter. Both of them had the ratio $\ell/d = 4$. In this way for a given number of revolutions per minute the strain rate had the same value for both sizes. The specimens were machined from steel 2 and deformation was carried out at both 30 and 307 rev/min. The number of revolutions to failure against temperature are given in Fig. 3.57. It is to be noticed that at 1250°C all specimens with $\frac{3}{8}$" diameter broke near the shoulder whereas those of $\frac{1}{4}$" diameter did not.

For studying the influence of the ratio ℓ/d on the hot workability measurement specimens made from steel 1 were used. Dimensions ~~Diameters~~ were $\frac{3}{8}$" with 1", 1.6" and 2.5" length. Their length was chosen corresponding to the number of revolutions available on the torsion machine gearbox at speeds of 30,48 and 75 rev/min in such a manner that $\frac{\ell_1}{n_1} = \frac{\ell_2}{n_2} = \frac{\ell_3}{n_3}$ respectively $\frac{1}{30} = \frac{1.6}{48} = \frac{2.5}{75}$, thus maintaining a constant strain rate during

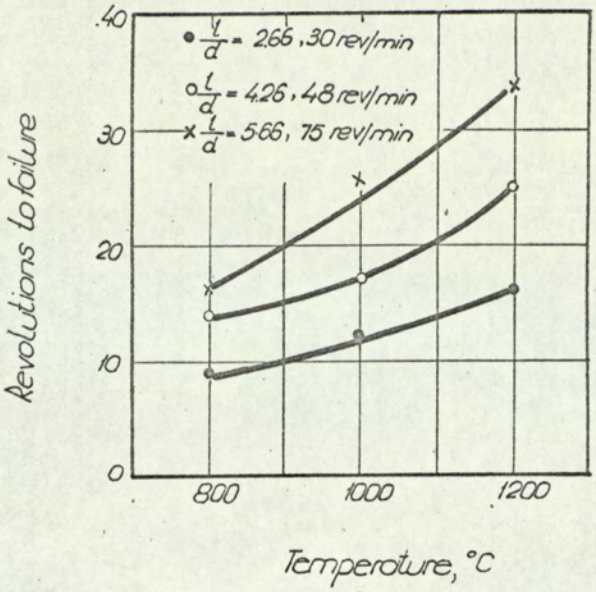

Fig. 3.58. Effect of temperature on the number of revolutions to failure for specimens made from steel 1.

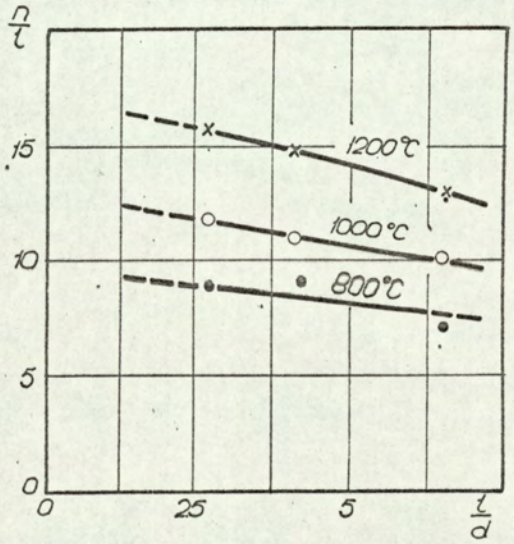

Fig. 3.59. Variation of the ratio $\frac{n}{l}$ with the ratio $\frac{l}{d}$ for specimens made from steel 1.

deformation. The number of revolutions to failure against temperature are shown in Fig. 3.58. In Fig. 3.59 the variation of the ratio $\frac{n}{e}$ against the ratio ℓ/d is shown for 800, 1000 and 1200°C.

DISCUSSION OF RESULTS

Looking at the Fig. 3.58 we see that although the strain rate was the same for both sizes, corresponding to a given number of revolutions per minute, the ductility is greater for the specimens with larger diameter, at temperatures corresponding to the peak of ductility. It can also be seen that by increasing the strain rate from 30 to 307 rev/min the ductility decreased. Thus:-

1) Comparing the variation of the ductility with temperature for both sizes of specimens and also for both strain rates suggests that the main factor which causes different values to be obtained for hot - workability for specimens with various diameters may be the true temperature of deformation and during deformation the temperature increases more in specimens with larger diameter. Hence, if two specimens start deformation from a given temperature, at the end of deformation the temperature will be higher in specimens with bigger diameter. This conclusion is reached by analysing the heat development and its loss during deformation.

The heat Q1 which develops into specimen in a given time as a function of specimen diameter is

$$Q1 = C1 \frac{\pi C_2 d^3}{4} \qquad 3.33$$

where C1 is a coefficent which connects the heat with the energy;

C2 - the value of the ratio ℓ/d

l - the length and d - the diameter of specimen gauge.

The heat Q2 which is lost in the same time as a function of

specimen diameter is

$$Q_2 = C_1^1 \pi C_2 d^2 + C_1^{11} \frac{\pi d^2}{2} \qquad 3.34$$

where C_1^1 is the coefficent of heat loss by radiation in a given time from specimen gauge to external medium;

C_1^{11} - the coefficent of heat loss by conduction in the same time from specimen gauge to its shoulder.

From the above equations:-

$$\frac{Q_1}{Q_2} = Cx\, d \qquad 3.35$$

i.e. the greater the specimen diameter the bigger is the ratio $\frac{Q_1}{Q_2}$, hence the higher will be the real temperature of the specimen during twisting for a given strain rate.

2) Although the ratio $\varepsilon/\dot{\varepsilon}$ decreases slightly by increasing strain rate from 30 to 307 rev/min (Fig. 3.16) and the true testing temperature is higher for greater strain rates, both of which contribute to the increase of ductility up to about 1100°C, the ductility actually decreased. It means that restoration processes occur at a lower rate in this steel compared with steels of lower carbon content, for which in the above conditions of testing the ductility usually increases. In this way the strain rate effect on hot workability has to be taken into consideration from three points of view:

(a) its effect on the increase in temperature;

(b) its effect on the grain boundary sliding;

(c) its effect on the competition between strain hardening and restoration process.

3) The fact that all specimens of $\frac{3}{8}$" dia. failed near shoulder shows that at this size the temperature increased more and a steeper gradient was created along the specimen gauge during deformation than in those of $\frac{1}{4}$" dia. This fracture also indicates that specimens with $\frac{3}{8}$" dia. failured prematurely and their number of revolutions to failure should be greater than of those with $\frac{1}{4}$" dia. even at 1250°C.

It is known that rolled bars tend to be richer in impurities inside with consequent lower ductility; furthermore, in specimens made from rolled bars the fracture starts sometimes from inside and develops towards outside at high temperatures. From this point of view it may be argued that the smaller the specimen diameter the faster will the fracture occur . Hence, a rise in ductility by increasing the specimen diameter may also be due to this reason.

From Fig. 3.59 it can be seen that there is no great variation of the ratio n/e with the ratio l/d . Taking as a basis the specimen which had 1" gauge length it appears that by increasing the ratio l/d the ratio n/e decreases slightly. The most likely reason responsible for this reduction in ductility is nonuniformity in deformation along the specimen gauge. This nonuniform seems to increase with increasing in the ratio l/d and may be due to the following reasons:-

(a) In any conditions of heating, by increasing the ratio l/d the possibility of producing a bigger difference in temperature along the specimen gauge is also bound to increase.

(b) By increasing the ratio ℓ/d the possibility of including portions along the specimen gauge which are weaker or have lower ductility than the rest of material, or even portions containing defects also increases.

(c) In the place where fracture occurs the deformation is a little greater than in any other place. This will contribute slightly to an increase in the number of revolutions to failure per the unit length more for specimens with smaller value of ℓ/d and less for those with greater value for this ratio. However, the change in the number of revolutions to failure by changing the ratio ℓ/d is quite small. Some greater differences amy appear in the transformation range of temperatures where the results cannot always be so easily reproduced.

CONCLUSIONS

1) Keeping the strain rate constant, increasing the specimen diameter usually resulted in an increase in the number of revolutions to failure. The main factors contributing to this increment in ductility seems to be the following:-

(a) rise in the true testing temperature during deformation more for specimens with bigger diameter and less for those with smaller diameter;

(b) ductility in the outer part of the specimens

machined from rolled bars is greater if the specimen diameter is greater, especially at higher testing temperatures.

2) Keeping the strain rate constant, and also the specimen diameter, no major difference in the ratio $\frac{n}{\ell}$ occurs by varying the ratio ℓ/d. However, due to nonuniformity in deformation along the specimen gauge, the ratio $\frac{n}{\ell}$ slightly decreases by measuring the ratio ℓ/d.

Near the transformation range of temperature where the fracture usually occurs near shoulder bigger differences in the ratio $\frac{n}{\ell}$ may sometimes be obtained by varying the ratio ℓ/d.

CHAPTER IV

Hot-workability Measurement of Mild Steel & Nodular Cast Iron

4.1 Hot-workability Measurement of Mild Steel

There are many data connected with hot-workability of steels in cast state and rolled or forged but they are not always in good agreement with each other. For instance Nicholson (82) who analysed various aspects of hot-workability, using many data obtained by many investigators, said that Conrad (private communication) showed that by increasing the degree of forging the ductility increased in the line of forging but it had a minimum in the transverse direction. Some data determined by United Steel Companies indicate that the forging temperature for low alloy steel as cast is the same as for wrought but its ductility is generally lower. Nippes, Savage and Grotke (83) showed that the peak of ductility for highly alloyed steel as cast is about 150°C below that when it has been previously rolled. Kubodera et al (84) said that the ductility of specimens taken from the bottom of the ingot is lower than of those from the top.

The main purpose of this study was to discover how axial force and hot-workability are affected by prior deformation compared with the same material as-cast. The first aspect has already been analysed, so that only the second will be discussed here.

EXPERIMENTS AND RESULTS

An ingot slice 6" x 6" x 20" was used for all experiments, cut from the centre section of the base of a 20" square ingot. Its composition is shown in Table 3.11 (steel 3). From this ingot three pieces were cut, from both ends and from the middle (A,B,C, Fig. 4.1) which were used for making specimens in the cast state. The pieces F and G were forged, one with 30% reduction in area and other with 75%, maintaining the same width and extending in only one direction. After forging all were heated at 930°C for 30 minutes then furnace cooled.

The specimens were cut in two directions, as for cast state and forged, as shown in Figure 4.1. Their dimensions were $\frac{3}{8}$" dia. and $1\frac{1}{2}$" gauge length. The specimens were deformed in the order of increasing number with increase in testing temperature (for instance FT1 was deformed at 800°C, FT2 at 900°C and so on). For testing a speed of 75 rev/min was used.

The variation of the number of revolutions to failure against temperature is shown in Fig. 4.2. All specimens made from slice B were deformed at 900°C to establish what variation could be expected across the ingot slice. The variation of the number of revolutions to failure against specimen number is shown in Fig. 4.3.

DISCUSSION OF RESULTS

Figure 4.3 reveals nonuniformity in ductility among the specimens cut across the ingot. This indicates that it is

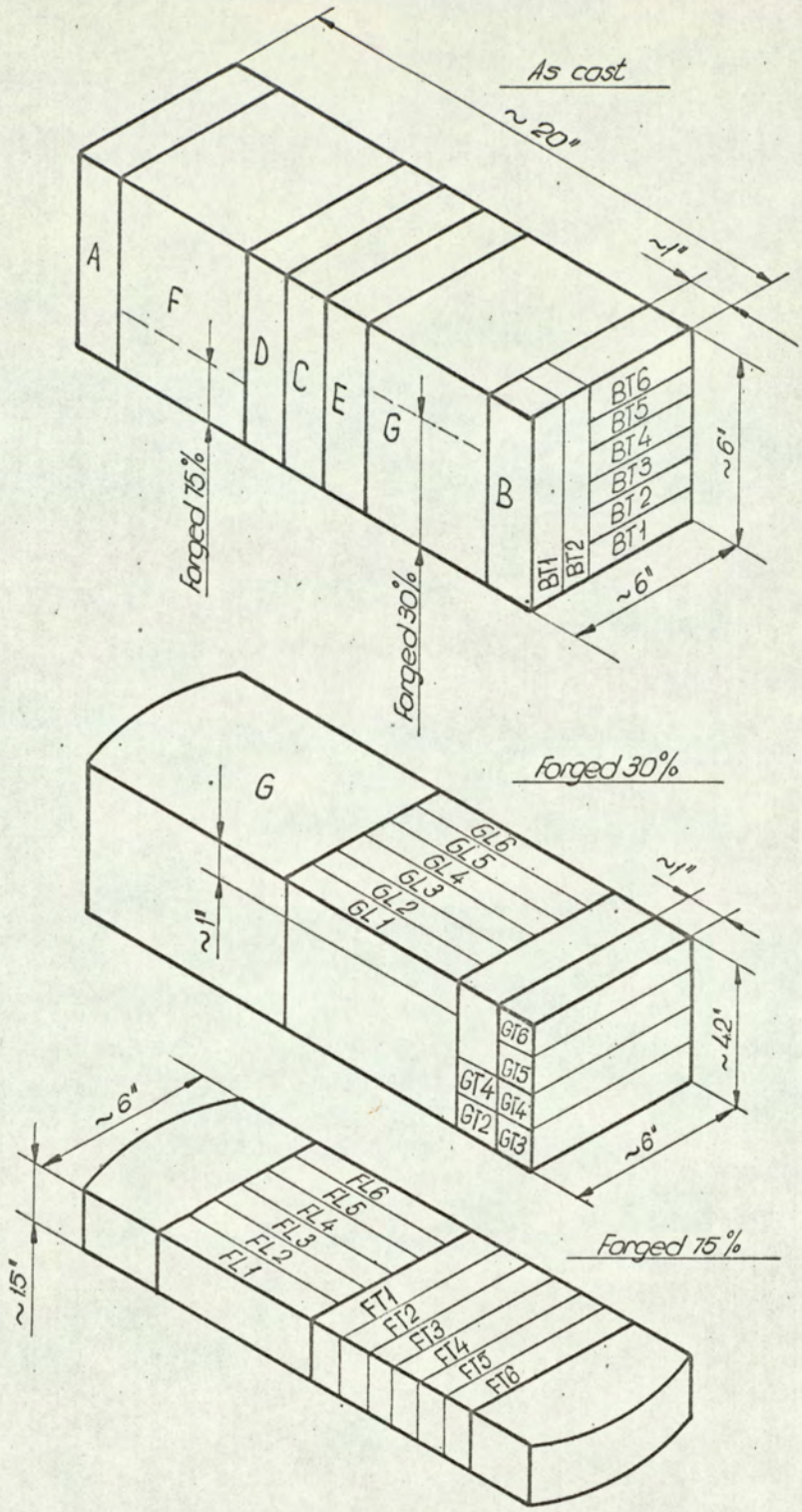

Fig. 4.1. Diagram showing specimen location from as cast and forged material of steel 3.

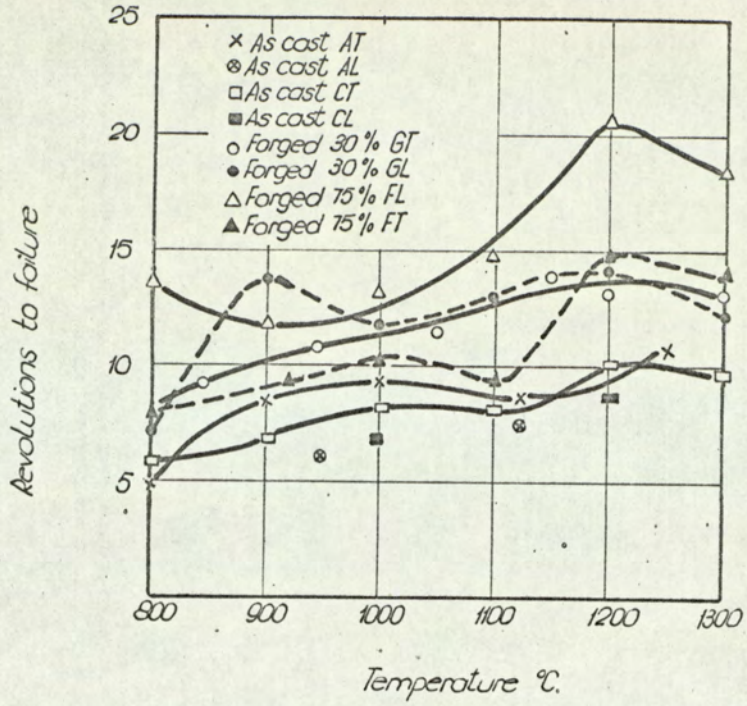

Fig. 4.2. Effect of temperature on the revolutions to failure for specimens deformed at 75 rev/min.

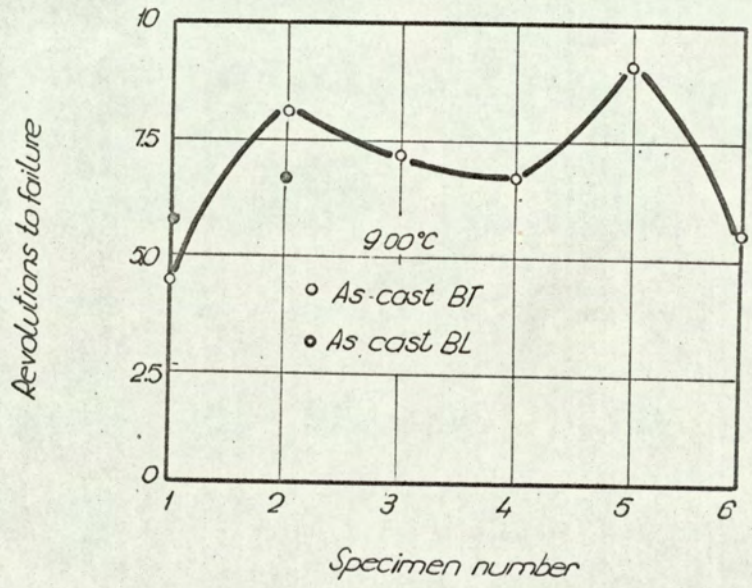

Fig. 4.3. Variation of revolutions to failure with specimen number.

quite difficult to draw conclusions on specimens made from cast material, and it is not suprising that the results given by different investigators are not always in ~~those~~ close agreement with each other. However, Fig. 4.2 shows that all specimens made from as-cast material had a lower ductility than those made from forged material, the maximum number of revolutions to failure being 11 for the cast state and 21 for that forged 75%.

The ductility increased in both directions after forging with a reduction in area of 30%. and there was no significant difference between specimens cut longitudinally and transversely to the direction of forging. For material forged 75% the ductility increased more in the direction of forging and decreased transversely compared with the material forged 30%.

The peak of ductility appeared around 1200°C for all specimens, showing that there is no difference in peak position along the temperature axis between as-cast and forged material. Axial force did not vary greatly from one specimen to another, again indicating that there is no real difference in behaviour of the material in the conditions studied. The main difference between the as-cast and forged states appears to be the number of revolutions to failure, being much greater for the wrought material.

Although only a few specimens were tested, the above results are in good agreement with the data obtained by Conrad and United Steel Company, and also confirm that results on cast material tend to be conflicting.

CONCLUSIONS

1) The ductility of as cast material is much lower than of wrought and is nonuniform.

2) By forging 30% reduction in area the ductility increased in both directions: longitudinally & transversely compared with material in the cast state. By forging 75% reduction in area the ductility increased in the forging direction and decreased in transversely direction compared with forging 30%. However, the ductility in the transverse direction of specimens made from the material forged 75% is still higher than of material in the 'as cast' state.

3) For all specimens tested the peak in ductility appeared around 1200°C which shows that the degree of forging has no or very little effect on it in the steel tested.

4.2. Hot-workability Measurement of Nodular Cast Iron

Due to its improved mechanical properties over common flake graphite irons, nodular cast iron has become established as a useful material in the building of machines, and consequently many studies has been carried out, a few of them concerned with its hot-workability.

Chang et al (85) showed that the best range of temperature for hot-working of spheroidal graphite cast iron is between 700 - 1100°C. However, even in this range the rate of deformation cannot be high. They also showed that this material can be deformed more by compression than by tension. Vetiska (86) studying spheroidal cast iron and mild steel found that nodular cast iron

had a lower ductility than mild steel.

The aim of the present work was to determine the ductility of nodular cast iron in both cast and annealed state, and how this material behaves from axial force point of view compared with steels.

EXPERIMENTS AND RESULTS

The material was supplied by B.C.I.R.A. in blocks 2" x 2" x 9" having the following content:
Carbon 3.39%, 1.92% Si, 0.049% Mg, 0.93% Ni, 0.07% Cr, 0.015% Ti, 0.05% Cu, 0.018% S, 0.022% P, less than 0.01% Al, 0.03% Co, 0.02% Mo, 0.01% V, 0.01% Sn, 0.01% As, 0.001% B, 0.0002% Pb, 0.003% Ce. Some of the blocks were annealed before testing by heating at 900°C, for 7 hours and then furnace cooled. Four specimens were machined from each block, the size being 5/16" dia. and 1¼" gauge length. For deformation a speed of 75 rev/min was used.

The number of revolutions to failure against temperature for both as cast and annealed conditions are shown in Fig. 4.4. The shape of the torque/revolutions curves was about the same for both states at any particular temperature, but it differed from lower temperature to higher. Axial force was also roughly the same. Two typical shapes of torque and axial force (for material in annealed state deformed at 720 and 960°C) are shown in Fig. 4.5 However, their absolute values were different. In Fig. 4.6 is shown the variation of shear stress (corresponding to the maximum value of torque) with temperature and in Fig. 4.7 the

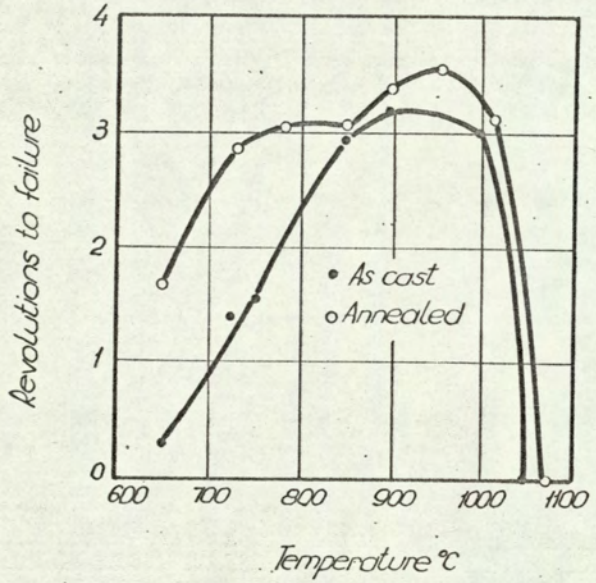

Fig. 4.4. Effect of temperature on the number of revolutions to failure for specimens deformed at 75 rev/min.

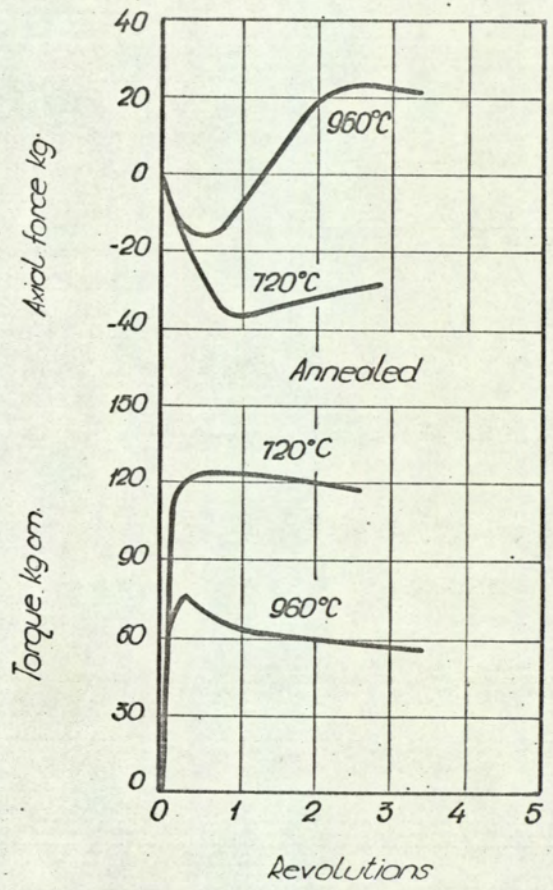

Fig. 4.5. Variation of torque and axial force during deformation.

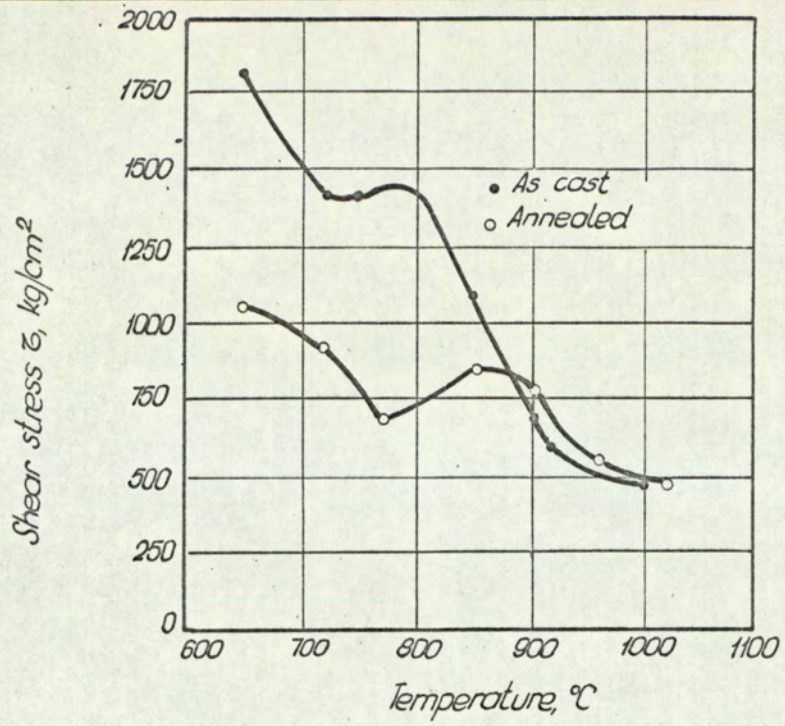

Fig. 4.6. Effect of temperature on the shear stress.

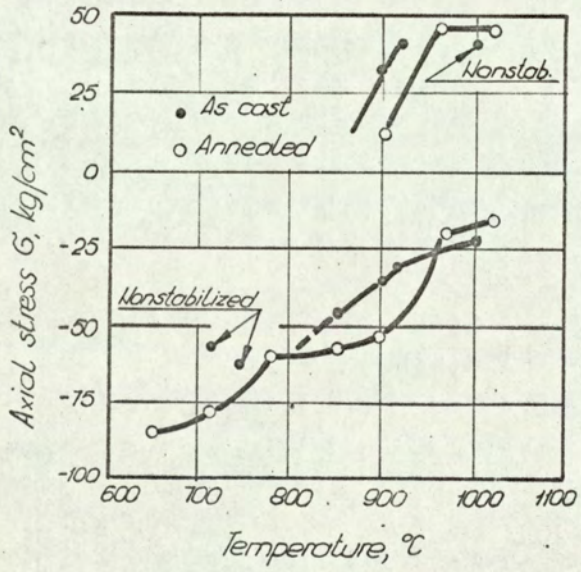

Fig. 4.7. Effect of temperature on the axial stress.

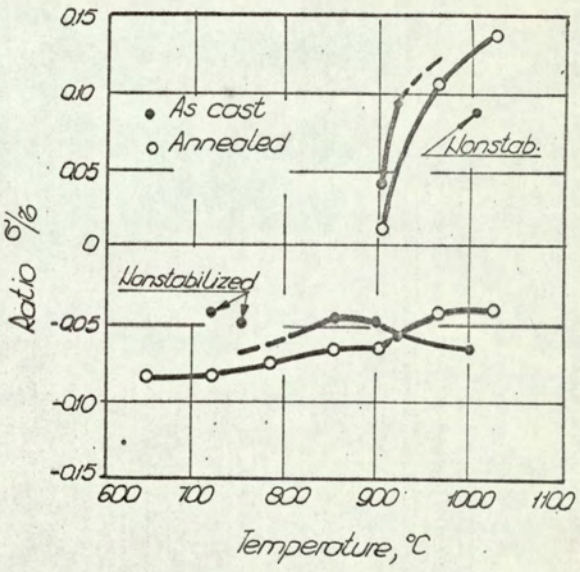

Fig. 4.8. Effect of temperature on the ratio G/σ.

variation of maximum tensile stress and minimum compression stress (corresponding to maximum and minimum axial force) with the same parameter. Because there is quite a big difference between the values of shear stress for the two states expecially below 850°C, the variation of the ratio σ/τ with temperature is also shown in Fig. 4.8.

In order to see how this material behaves in conditions of torsion combined with tension and compression respectively a few specimens made from as cast material were deformed without restraint by the grips and also with various values of applied axial force. The variation of the number of revolutions to failure and elongation with the ratio σ/τ is shown in Fig. 4.9.

DISCUSSION OF RESULTS

After annealing the ductility of spheroidal cast iron increased in the temperature range of 650 - 850°C compared with the cast state, but no big difference was observed between 850 and 1000°C. In the annealed state the ductility appears to be slightly better than the as-cast even in the higher temperature range.

The present results are in agreement with those of Chang for the annealed state only up to 1020°C. At 1060°C specimens made from annealed material broke straight away, showing no ductility. It was the same for specimens made from cast material and deformed at 1050°C. The ductility of nodular cast iron 'as-cast' appears therefore to be high over a narrower range of

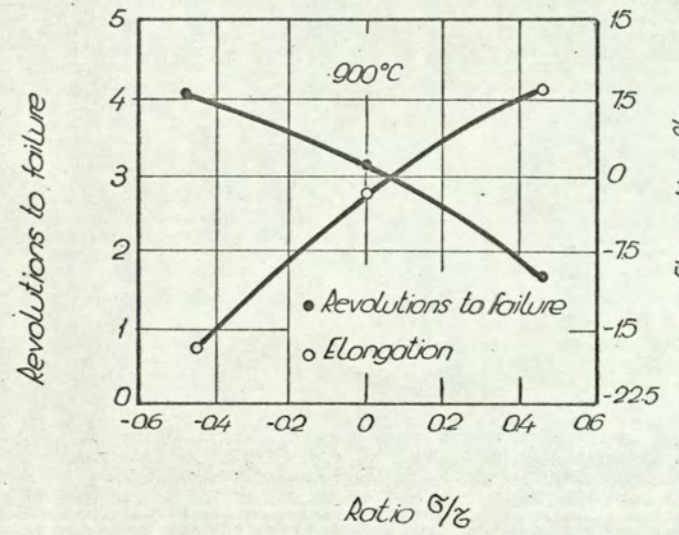

Fig. 4.9. Variation of the revolutions to failure and elongation with the ratio σ/z, for as cast material.

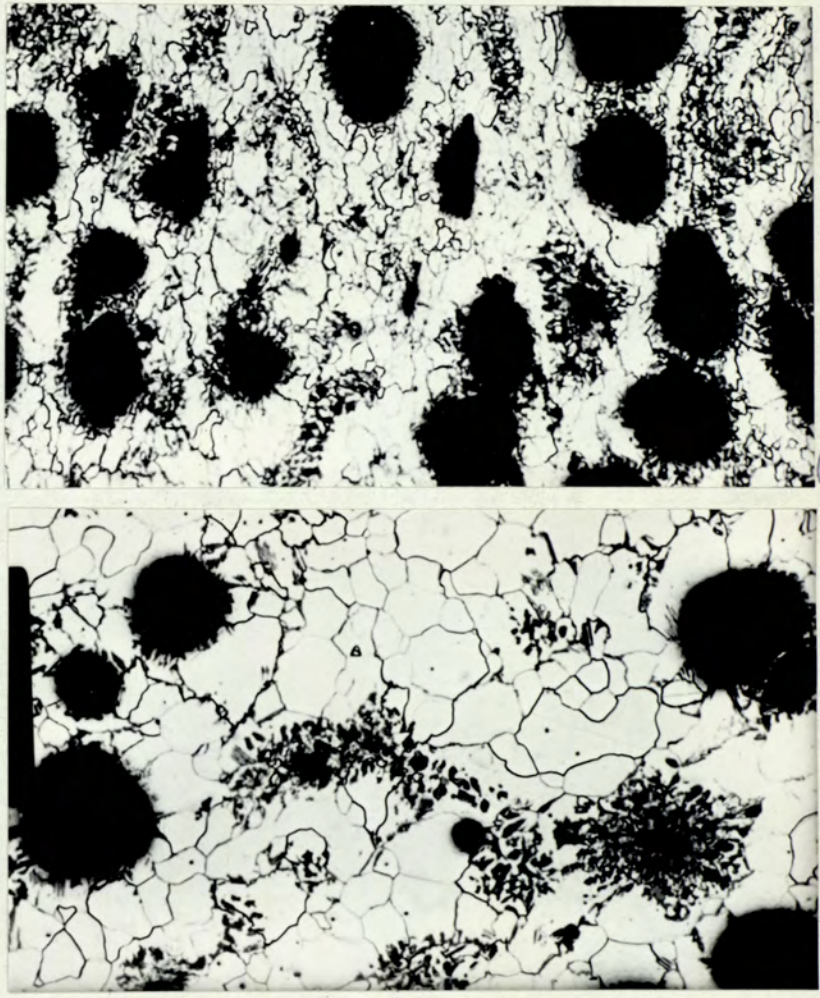

Fig. 4.10. Structures from outside (a) and from axis (b) for a specimen deformed at 780°C and cooled in air, ×200.

temperature than in the annealed state, being workable between approximately 850 and 1000°C, while in annealed state between 720 and 1020°C.

Comparing the ductility of nodular cast iron with that of as cast mild steel shows that, for the former, the number of revolutions to failure is about half than for the latter. Hence, although nodular cast iron permits plastic deformation in the above range of temperatures, only a limited amount of working is possible.

From point of view of resistance to deformation it appears that the best range of temperature is over 900°C for the material in the cast state and in a much wider range (750 - 1000°C) for annealed state.

From Fig. 4.7 it can be seen that although nodular cast iron has a melting temperature much below that of mild steel, axial compression force appears during deformation at higher temperature and the ratio σ_1/σ_2 (Fig. 4.8), which characterises the magnitude of tensile stress, has a much smaller value than for steel. Thus it seems that in nodular cast iron subgrains form more readily and grain boundary sliding occurs to a lesser degree than with steel at a given temperature. Indeed, from Fig. 4.10, where the structure from the axis and outside is shown for a specimen made from annealed cast iron and deformed at 780°C, a pronounced substructure can be seen although the specimen was cooled in free air after deformation. (Such a pronounced substructure was not observed in steel deformed and cooled under similar conditions).

Fig. 4.9 shows that nodular cast iron is affected markedly by superimposed tensile stress, ductility decreasing quite steeply by increasing the ratio σ/ε. Thus nodular cast iron needs to be deformed in conditions where tensile stresses are minimised as much as possible; or alternatively the rate of deformation in the presence of tensile stresses must be low.

Deformation of nodular cast iron seems to occur quite uniformly. No marked change in shape of nodules occured during deformation when the ends of the specimen were fixed. (Fig. 4.11,a.) However, by using superimposed compression force the nodules deformed very much near the outside and to a lesser extent nearer the axis (Fig. 4.11,b and c).

CONCLUSIONS

1) The tested nodular cast iron has greatest ductility between 850°C and 1000°C in cast state and between 720 and 1020°C in the annealed state. Apart from the fact in the annealed state the ductility is greater over a much wider range of temperature than in the as cast state, in the range of temperature 850 - 1000°C there is very little difference in behaviour.

2) The resistance to deformation is much higher in the as cast state up to about 870°C. Around 880°C and above the resistance to deformation is virtually the same in both conditions.

3) The ductility of nodular cast iron decreases sharply if tensile stress acts, but improves with compressive stress. Therefore during deformation it is necessary to adjust conditions so that compression stress is acting or to restrict deformation in the

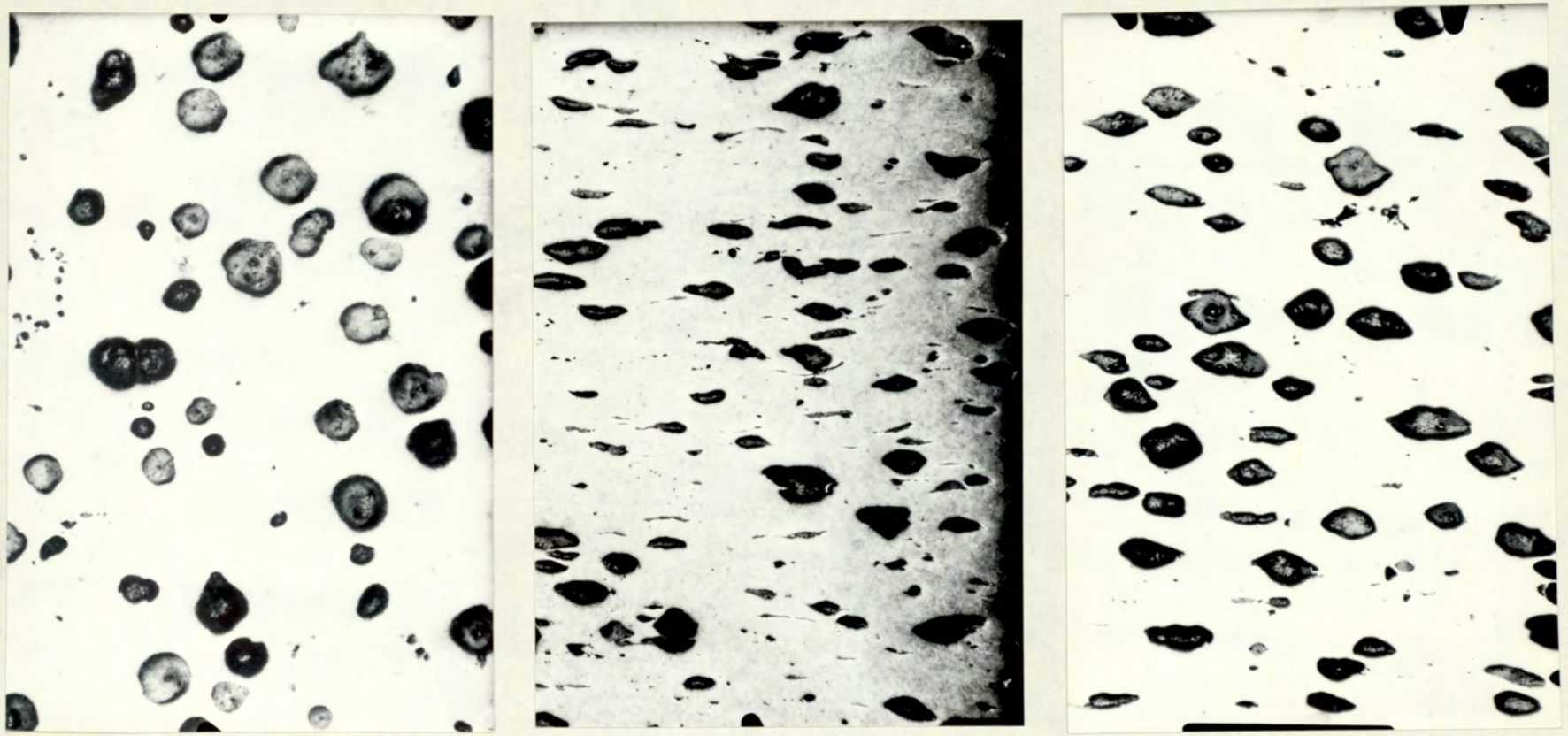

Fig. 4.11. Nodule deformation under various conditions, x 100
a - specimen kept fixed; b and c - specimen was shortend.
a - from mid-radius; b - from outside; c - from axis

presence of tensile stresses.

4) During deformation under conditions of torsion combined with compression the nodules deform. However, when the specimen is kept fixed the shape of nodules changes less, showing that in spite of the presence of nodules the material deforms quite uniformly.

5) The substructure developed in nodular cast iron appears to be more pronounced than for steel and less grain boundary sliding occurs at a given temperature.

REFERENCES

1. N.J. Korneev and I.G. Skugarev, Osnovi fizicohimiceskoi teorii obrabotki metallov davleniem, Masqiz, 1960

2. F.T. Sisco, Alloys of Iron and Carbon, vol. 2, McGraw-Hill, 1937, p. 95.

3. E.J. Balahanov, . Forjarea si matritarea la cald, Transl. IDT, Bucuresti, 1955.

4. P.A. Lane, Drop Forging Research, Metal Treatment and Drop Forging, 237, Aug. 1964

5. H.J. Henning and F.W. Boulger, Tests for Hot Workability, J. of Met. May 1963

6. S.J. Gubkin, Plasticeskaia deformatia metallov, Metalurghizdat, 1960

7. D. McLean, Mechanical Properties of Metals, John Wiley 2nd Edition.

8. D. Kirk, The Hot-working of Metals, Ph.D. Thesis, Univ. of Birmingham 1958.

9. T. Martin, The Tensile Properties of Aluminium at High Temperatures, J. Inst. Met. vol. 31, 192h, p.121

10. A. Portevin and P.G. Bastien, Study of the Forgeability of Various Light and Ultralight Alloys, J. Inst. Met. vol. 59, 1936, p.83

11. D.S. Klark and G. Dätwyler, Stress-Strain Relations Under Tension Impact Loading, ASTM, Vol. 38, part II, 1938 p.98

12. H.C. Mann, High Velocity Tension Impact Tests, ASTM Vol. 36 part II, 1936, p.85

13. C.W. MacGregor, The Tension Test, ASTM, vol. 40, 1940, p. 508

14. M. Manjoine and A. Nadai, High Speed Tension Test at Elevated Temperature, ASTM, vol. 40, 1940, p. 822

15. M. Manjoine and A. Nadai, High Speed Tension Test at Elevated Temperature, AJME, vol. 63, 1941 p.A.77

16. J.N. Greenwood, D.R. Miller and I.W. Suiter, Intergranular Cavitation in strained metals, Acta Met. vol. 2, 1954, p.250

17. R. Nordheim, T.B. King and N.I. Grant, The effect of phosphorus on the deformation and fracture characteristics of iron from 1600 to 2200°F, AIME, vol. 218, 1960, p. 1029

18. R. Castro and R. Poussardin, C.I.T. Pub. No. 2, 1962, p.505

19. E.A. Leech, P. Gregory and R. Eborall, A Hot Impact Tensile Test and its Relation to Hot-working Properties, J. Inst. Met. vol. 83, 1954-55, p.1602

20. P.W. Bridgman, Studies in Large Plastic Flow and Fracture, McGraw-Hill, 1952.

21. N.N. Davidenkov and N.S. Spiridinova, Analysis of Tensile Stress in the Neck of an Elongated Test Specimen, Sc. Res. Inst. Av. Moskow, 1945

22. E.R. Parker, H.R. Davis and A.E. Flanigan, ASTM, vol. 46, 1946, p.228

23. K. Puttick, Phil. Mag. vol. 4, 1959, p.964

24. T. Williams and H.F. Hall, The Effect of Specimen Size on Tensile Properties of Course Grained Medium Carbon Steel at Low Temperature, JISI, vol. 193, 1959, p.56.

25. P. Shahanian and J.R. Lane, Effect of Specimen Dimensions on High Temperature Mechanical Properties, ASTM, vol. 55, 1955, p.724.

26. E.P. Unksov, Injenernaia Feoria Plasticinosty, Masgiz, 1959

27. F. Robin, Resistance of Steels to Cracking at High Temperatures, I.S.I. Carnegie Scholarship Mem. 1910, vol. 2. p.70.

28. O.W. Ellis, An Investigation into the Effect of Constitution on the Malleability of Steel at High Temperatures, I.S.I. Carnegie Scholarship Mem. vol. 13, 1924, p. 47

29. W.L. Kent, The behaviour of Metals and Alloys During Hot Forging, J. Inst. Met. vol. 39, 1928, p. 209

30. M. Cook and E.C. Larke, Resistance of Copper and Copper Alloys to Homogenious Deformation in Compression, J. Inst. Met. vol. 71, 1945, p.371

31. J.F. Alder and V.A. Philips, The Effect of Strain Rate and Temperature on the Resistance of Aluminium, Copper and Steel to Compression, J. Inst. Met. vol. 83, 1954-55 p.80

32. C.W. McGregor and J.C. Fisher, J. Appl. Mech. 1946, vol.13 p.11.

33. M. Cook, Proceding of a Conference on Properties of Materials at High Rate of Strain, London, 1957, p.86.

34. R.R. Arnold and R.J. Parker, Resistance to Deformation of Aluminium and some Aluminium Alloys, J. Inst. Met. vol. 88, 1959-60, p. 255.

35. J.A. Bailey and E. Singer, Effect of Strain Rate and Temperature on the Resistance to Deformation of Aluminium, Aluminium Alloys and Lead, J. Inst. Met. Aug. 1964, p.404

36. V. Schroder, AIME, 1952, vol. 52 p. 3-4

37. V. Sacks, Limits of Forging, Modern Ind. Press, vol. 3, 1941, p.9

38. A. Tomilson and J.D. Stringer, The Closing of Internal Cavities in Forging by Upsetting, JISI, 1958, vol. 188, p.209

39. A. Zeerleder, R. Irmann and E. Burg, The Hot-working of Aluminium Alloys Through Forging and Upsetting, Schweizer Archiv and Annaler Suisses, Vol. 1, 1935, p.49

40. A. Sauver, Steel at Elevated Temperatures, ASTM, vol. 17, 1930 p.410

41. M. Itikara, Tohoku Imp. Univ. Tech. Rep. 1936-38, vol. 12, p.63

42. H.C. Thring, A. Quantitative Hot-workability Test for Metals, Iron Age, vol. 153, 1944 p.86

43. C.L. Clark and J. Russ, Hot-working Characteristics of Metals, Met. Techn. vol.12, 1945

44. F.K. Bloom, W.C. Clarke and P.A. Jennings, Relation of Structure of Stainless steel to Hot-ductility, Met. Progr. vol. 59, 1951, p.250

45. D.E.R. Hughes, The Hot-Torsion Test for Assessing Hot-working Properties of Metals, JISI, vol. 170, 1952, p.214

46. A. Nadai, Theory of Flow and Fracture of Solids, McGraw-Hill, 1931

47. A. Guenssier and R. Castro, Hot-workability of Alloy Steels, Met. Treat and Drop Forg. July-Aug. Sept. Oct. 1959

48. P. Bastien and A. Portevin, Sur une methode d'evaluation de la vitesse de recristallisation des metaux en cours de deformation a chaud, Ac.Sc. Paris, Comtes Rendus, vol. 254, Mars, p.2331.

49. J.L. Robins, O. Cutner and D. Sherby, Role of Crystal Structure on the Ductility of Pure Iron at Elevated Temperature, JISI, vol. 199, 1961, p. 175

50. R.A. Reynolds and W.J. McG. Tegart, The Deformation of some Pure Irons by High Speed Torsion over the Temperature Range 700-1200°C, JISI, vol. 200, 1962, p.2044.

51. D. Hardwick and W.J. McG. Tegart, La deformation des metaux et alliages par torsion a haute temperature, Mem. Sc. Rev. Met. vol. 58, 1961, p.869

52. H. Hardwick and W.J. McG. Tegart, Structural Change During the Deformation of Copper, Aluminium and Nickel at High Temperature and High Strain rates, J. Inst. Met. vol. 90 1961-62, p.17.

53. C. Rossard et. P. Blain, Premiers resultates de rechearches sur la deformation des aciers a chaud, Rev. Met. No.6 1958, p.573

54. C. Rossard et. P. Blain, Evolution de la structure de l'acier sur l'effect de la deformation plastique a chaud, Mem, Sc. Rev. Met. No. 56, 1959, p.285

55. H. Ormerod and W.J. McG. Tegart, Resistance to Deformation of Superpure Aluminium at High Temperature and Strain rates, J. Inst. Met. vol. 89, 1960-61, p.94.

56. D. Bunting, The Brittle Ranges in Brass as shown by the Izod Impact Test, J. Inst. Met. vol. 31, 1924, p.47

57. A.R. Bailey, McDonald and L.E. Samuels, The Effect of High and Low Temperatures on the Notched-bar Characteristics, of a Cast High Tensile Beta-Brass, J.Inst. Met. vol. 85, 1956, p.25

58. H.F. Moore, H.B. Wishart and S.W. Lyon, Slow Bend and Impact Test of Notched-bar at Low Temperatures, ASTM, vol.36, part II, 1936, p.110.

59. C. Crussard et al, A Study of Impact Test and the Mechanism of Brittle Fracture, JISI vol.183, 1956, p.146.

60. A.P. Green and B.B. Hundy, Initial Plastic Yielding in Notch Bend Test, J. Mech. Phys of Solids, vol. 4, 1956, p.128

61. L.H. Martin and L.O. Bieber, Methods of Evaluating Hot-malleability of Nickel and High Nickel Alloys, AJME, 1948, p.15

62. ATosefsson et al, The Influence of Sulphur and Oxygen in Causing Red-shortness in Steel, JISI, vol. 191, 1959, p.240

63. Chizikov, Translation.

64. J. Hanning and W. Boulger, Tests for Hot-workability, J. of Met May, 1963.

65. Discussion on the Working Properties of Metals, J. Inst. Met. No. 83, 1954-55, p.548

66. A Guenssier and R. Castro, Relations entre les fragilites a chaud et a froid dans les aciers austenitigues du type 18.8, Rev. Met. No. 2, 1958, p.107

67. H.W. Swift, Tensional Effect of Torsional ~~Observation~~ Overstrain in Mild Steel, J S , vol. 140, 1939

68. R.L'Hermite, Etude theoretique et experimentale cur la torsion compuse, Comte Rendu, 1947, p141

69. Th. von Iferson, Plasticity in Engineering,

70. A Nadai, Theory of Flow and Fracture of Solids, McGraw-Hill, 1950

71. C. Crussard and R. Tomhankar, High Temperature Deformation of Steel, AIME, vol. 212, 1958, p. 718.

72. J.E. Dorn, Mechanical Behaviour of Materials at Elevated Temperatures, McGraw-Hill, 1961

73. P.N. Randal, Creep-rupture Proporties of a Carbon Steel and a Low Alloy Steel at 1200 to 1800°F.

74. J.A. Martin, M. Herman, and N. Brown, Grain Boundary Displacement Vs Grain Deformation, AIME, vol. 209, 1957, p.78

75. B. Fazan, D. Sherby and E. Dorn, Some Observations on Grain Boundary Shearing During Creep, AIME, vol. 200, 1954, p.919

76. D. McLean and M.H. Farmer, The relation During Creep Between Grain Boundary Sliding, Subcrystal Size and Extension, J. Inst. Met. vol. 85, 1956-57, p.41

77. D.L. Martin and E.R. Parker, AIME, vol. 156, 1944, p.126

78. R. Hill, The Mathematical Theory of Plasticity, Oxford, 1960

79. E.A. Dewis, Combined Tension and Torsion Test with Fixed Principal Directions, J. Appl. Mech. vol.22, 1955

80. B. Crossland and R. Hill, On the Plastic Behaviour of Thick Tubes Under Conbined Torsion and Internal Pressure, J. Mech. Phys. Solid vol. 1-2, 1952-54

81. D. Hardwick, Ph.S. Thesis, Univ. of Sheffield.

82. A Nicholson, Hot-workability Testing of Steels, Iron & Steel, June and July, 1964

83. E.F. Nippes, W.F. Savage and G. Grotke, Welding Res. Council, No. 33, Feb. 1957

84. J. Kubodera et al. Tetsu - to - Hagane, vol. 44, 1958, p.1053

85. Chang-Tso-mey et al, The Working Capacity of Spheroidal graphite cast iron, Freiberger Forschungsh, 1957 (B.16) p.82.

86. A. Vetiska, Contribution to the Study of the Deformation of Spheroidal Graphite Cast Iron and of Mild Steel, Rev. Met. Mem. Sc. 1960, V.57

87. F.B. Pickering, some Effects of Mechanical Working on the Deformation of Non-metallic Inclusions, J.S.J, vol.189 1958, p.148

88. T. Malkievic and S. Rudnik, Deformation of Non-metallic Inclusions During rolling of Steel, J.I.S.I, vol. 201, 1963, p.33

89. I. Dragan, Some problems connected with the stamping of cast semifinished products, Metalurgia, No. 10. 1963